

# Optimal and Feedback Control for Hyperbolic Conservation Laws

Pushkin Kachroo

Dissertation submitted to the Faculty of the  
Virginia Polytechnic Institute and State University  
in partial fulfillment of the requirements for the degree of

Doctor of Philosophy

in

Mathematics

Joseph A. Ball, Chair

Slimane Adjerid

John A Burns

Martin Klaus

May 10, 2007

Blacksburg, Virginia

Keywords: Hyperbolic PDE, Evacuation, Feedback, Optimal, Control, Entropy

Copyright 2007, Pushkin Kachroo

# Optimal and Feedback Control for Hyperbolic Conservation Laws

Pushkin Kachroo

(ABSTRACT)

This dissertation studies hyperbolic partial differential equations for Conservation Laws motivated by traffic control problems. New traffic models for multi-directional flow in two dimensions are derived and their properties studied. Control models are proposed where the control variable is a multiplicative term in the flux function. Control models are also proposed for relaxation type systems of hyperbolic PDEs. Existence of optimal control for the case of constant controls is presented. Unbounded and bounded feedback control designs are proposed. These include advective, diffusive, and advective-diffusive controls. Existence result for the bounded advective control is derived. Performance of the relaxation model using bounded advective control is analyzed. Finally simulations using Godunov scheme are performed on unbounded and bounded feedback advective controls.

# Dedication

*To the Pure Joy of Mathematics.*

# Acknowledgments

I would like to express my sincere thanks and gratitude to my advisor Prof. Joseph A. Ball.

I am also grateful to the committee members, Prof. Adjerid, Prof. Burns and Prof. Klaus for their helpful remarks.

I am greatly indebted to my wife Anjala Krishen and my daughters Axenya Kachen and Sheen Kachen for their understanding, patience and support during the entire period of my study.

I am also very appreciative of the love and support that my parents, Ms. Sadhna Kachroo and Dr. P. L. Kachroo, my brother, Dhananjaya, and his son, Myshkin have provided. My *other* parents Dr. Kumar Krishen and Ms. Vijay Krishen have been very helpful throughout my work.

This research is supported in part from the National Science Foundation through grant no. CMS-0428196 with Dr. S. C. Liu as the Program Director. This support is gratefully acknowledged. Any opinion, findings, and conclusions or recommendations expressed in this study are those of the writer and do not necessarily reflect the views of the National Science Foundation.

# Contents

<b>1</b>	<b>Introduction</b>	<b>1</b>
1.1	Motivation and Research Goal . . . . .	1
1.1.1	Vehicular Traffic Control . . . . .	1
1.1.2	Pedestrian Traffic Control . . . . .	2
1.1.3	Evacuation Problems . . . . .	2
1.2	Literature Survey . . . . .	5
1.2.1	Traffic Models . . . . .	5
1.2.2	Traffic Control . . . . .	6
1.2.3	Mathematical Theory of Hyperbolic Conservation Laws . . . . .	6
1.3	Contributions . . . . .	7
1.4	Outline of the Dissertation . . . . .	8
<b>2</b>	<b>Derivation of Conservation Laws</b>	<b>10</b>
2.1	Mass Conservation . . . . .	10
2.1.1	Mass Conservation in One Dimension . . . . .	11
2.1.2	Mass Conservation in Two Dimensions . . . . .	13

2.1.3	Mass Conservation in n Dimensions . . . . .	17
2.2	Momentum Conservation . . . . .	17
2.2.1	Momentum Conservation in One Dimension . . . . .	17
2.2.2	Momentum Conservation in Two Dimensions . . . . .	18
2.2.3	Momentum Equation with Viscosity . . . . .	19
2.3	Energy Conservation . . . . .	22
2.4	Combined Equations . . . . .	22
2.4.1	Equation of State . . . . .	24
2.5	General Conservation . . . . .	27
<b>3</b>	<b>Traffic Models: One Dimensional Case</b>	<b>30</b>
3.1	Lighthill-Whitham-Richards Model . . . . .	30
3.1.1	Greenshield's Model . . . . .	31
3.1.2	Greenberg Model . . . . .	31
3.1.3	Underwood Model . . . . .	34
3.1.4	Diffusion Model . . . . .	35
3.1.5	Other Models . . . . .	35
3.1.6	LWR Models . . . . .	36
3.2	Payne-Whitham Model . . . . .	39
3.2.1	Characteristic Variables . . . . .	41
3.2.2	Characteristic Variables for Payne-Whitham Model . . . . .	42
3.3	Aw-Rascle Model . . . . .	44

3.3.1	Characteristic Variables for Aw-Rascle Model . . . . .	46
3.4	Zhang Model . . . . .	48
3.4.1	Characteristic Variables for Zhang Model . . . . .	49
3.5	Pedestrian and Control Models in One Dimension . . . . .	51
3.5.1	LWR Pedestrian Model with Greenshields Flow . . . . .	52
3.5.2	Payne-Whitham Pedestrian Model with Greenshields Flow . . . . .	52
3.5.3	Aw-Rascle Pedestrian Model with Greenshields Flow . . . . .	53
3.5.4	Zhang Pedestrian Model with Greenshields Flow . . . . .	53
<b>4</b>	<b>Traffic Models: Two-Dimensional Case</b>	<b>55</b>
4.1	Two-Dimensional LWR Model . . . . .	55
4.1.1	Eigenvalues . . . . .	57
4.2	Two-Dimensional Payne-Whitham Model . . . . .	57
4.2.1	Eigenvalues and Eigenvectors . . . . .	58
4.2.2	Eigenvalues and Eigenvectors in an Arbitrary Direction . . . . .	60
4.3	Two-Dimensional Aw-Rascle Model . . . . .	61
4.4	Two-Dimensional Zhang Model . . . . .	62
<b>5</b>	<b>Conservation Law Solutions</b>	<b>64</b>
5.1	Method of Characteristics . . . . .	64
5.1.1	Characteristics in Two Dimensions . . . . .	66
5.1.2	Characteristics for a System . . . . .	67

5.2	Classical or Strong Solutions . . . . .	67
5.3	Weak Solutions . . . . .	68
5.3.1	Blowup of Solutions . . . . .	69
5.3.2	Generalized Solutions . . . . .	73
5.3.3	Generalized Solution Property . . . . .	74
5.3.4	Weak Solution Property . . . . .	75
5.3.5	Trace Operator for Functions of Bounded Variation . . . . .	77
5.4	Scalar Riemann Problem . . . . .	80
5.4.1	Shock Solution . . . . .	80
5.4.2	Rarefaction Solution . . . . .	82
5.5	Admissibility Conditions . . . . .	84
5.5.1	Vanishing Viscosity Solution . . . . .	84
5.5.2	Entropy Admissible Solution . . . . .	84
5.5.3	Lax Admissibility Condition . . . . .	88
5.6	Kruzkov's Entropy Function . . . . .	89
5.7	Well-posedness . . . . .	90
5.7.1	Solution Properties for Scalar Cauchy Problem . . . . .	90
5.8	Oleinik Entropy Condition . . . . .	91
5.8.1	Sup-norm Decay of the Solution . . . . .	92
5.9	Scalar Initial-Boundary Problem . . . . .	92
<b>6</b>	<b>Traffic Control</b>	<b>95</b>

6.1	Scalar Conservation Law Solution . . . . .	95
6.2	Optimal Flux Control for Scalar Conservation Law . . . . .	97
6.2.1	Optimal Control in Space of Constant Controls . . . . .	99
6.3	Feedback Control for Scalar Law . . . . .	101
6.3.1	Advection Control . . . . .	102
6.3.2	Diffusion Control . . . . .	106
6.3.3	Advective-Diffusion Control . . . . .	112
6.4	Advective Feedback Control for Relaxation Systems . . . . .	115
6.4.1	Unbounded Advection for Relaxation Systems . . . . .	119
6.4.2	Bounded Advection for Relaxation Systems . . . . .	121
6.5	Wellposedness for Bounded Advection Control . . . . .	122
6.5.1	Riemann Problems . . . . .	125
6.5.2	Existence of Solution . . . . .	135
<b>7</b>	<b>Simulations for Advective Control</b>	<b>144</b>
7.1	Godunov's Method . . . . .	144
7.1.1	Matlab Code . . . . .	146
7.2	Simulation Results for Advective Control . . . . .	151
7.2.1	Unbounded Control Results . . . . .	151
7.2.2	Bounded Control Results . . . . .	151
<b>8</b>	<b>Conclusions</b>	<b>163</b>

8.1	Summary . . . . .	163
8.2	Contributions . . . . .	164
8.3	Future Work . . . . .	165
	Bibliography . . . . .	166

# List of Figures

1.1	Static Evacuation Map . . . . .	3
1.2	Evacuation Digraph . . . . .	4
2.1	Conservation of Mass . . . . .	11
2.2	Conservation of Mass in 2D . . . . .	13
2.3	Conservation of Momentum . . . . .	18
2.4	Conservation of Momentum in the x-Direction . . . . .	19
2.5	Stresses on a Planar Fluid . . . . .	20
2.6	Conservation in General Setting . . . . .	28
3.1	Fundamental Diagram using Greenshield Model . . . . .	32
3.2	Fundamental Diagram using Greenberg Model . . . . .	33
3.3	Fundamental Diagram using Underwood Model . . . . .	34
3.4	Fundamental Diagram using Multi-regime Model . . . . .	37
4.1	Pedestrian Traffic in 2D . . . . .	56
4.2	Propagation in an Arbitrary Direction . . . . .	60

5.1	Initial Data . . . . .	65
5.2	Characteristic Slopes . . . . .	66
5.3	Solution after some time . . . . .	66
5.4	Characteristic Speed . . . . .	70
5.5	Initial Conditions . . . . .	70
5.6	Characteristics . . . . .	71
5.7	Initial Conditions Propagating . . . . .	72
5.8	Domain to Illustrate Trace Property . . . . .	76
5.9	Domain with $\phi$ . . . . .	77
5.10	Dominated Convergence Relationships . . . . .	78
5.11	General Convergence Relationships . . . . .	79
5.12	Finite Measure Space Convergence Relationships . . . . .	79
5.13	Shockwave Solution to Riemann Problem . . . . .	81
5.14	Shockwave Speed Derivation . . . . .	81
5.15	Blank Region in $x - t$ Space . . . . .	82
5.16	Entropy Violating (Rejected) Solution . . . . .	83
5.17	Rarefaction Solution . . . . .	83
5.18	Boundary Data . . . . .	93
6.1	Advection Control in 1D . . . . .	103
6.2	Advection Control in 2D . . . . .	105
6.3	Diffusion Control in 1D . . . . .	107

6.4	Diffusion Control in 2D . . . . .	110
6.5	Advective-Diffusion Control in 1D . . . . .	112
6.6	Advective-Diffusion Control in 2D . . . . .	114
6.7	Feedback Bounded Advective Flux . . . . .	124
6.8	Case 1: Fundamental Diagram . . . . .	127
6.9	Case 1 Characteristics . . . . .	128
6.10	Case 2: Fundamental Diagram . . . . .	129
6.11	Case 2 and Case 3 Characteristics . . . . .	130
6.12	Case 3: Fundamental Diagram . . . . .	131
6.13	Case 4: Fundamental Diagram . . . . .	131
6.14	Case 4 Characteristics . . . . .	132
6.15	Case 5: Fundamental Diagram . . . . .	133
6.16	Case 5 Characteristics . . . . .	134
6.17	Case 6: Fundamental Diagram . . . . .	135
6.18	Case 6 Characteristics . . . . .	136
6.19	Piecewise Affine Flux Approximation . . . . .	139
6.20	Case 1 Shock . . . . .	140
6.21	Case 2 Shocks . . . . .	141
6.22	Wave Front Tracking . . . . .	142
7.1	Characteristics for Computing Flux . . . . .	145
7.2	File Dependencies for Matlab Simulation Code . . . . .	147

7.3	Traffic Flow with Constant Free Flow Speed . . . . .	150
7.4	Unbounded Feedback Advective Control . . . . .	152
7.5	Bounded Feedback Advective Control . . . . .	153
7.6	Bounded Feedback Advective Control: Case1 . . . . .	155
7.7	Bounded Feedback Advective Control: Case2 . . . . .	157
7.8	Bounded Feedback Advective Control: Case3 . . . . .	158
7.9	Bounded Feedback Advective Control: Case4 . . . . .	160
7.10	Bounded Feedback Advective Control: Case5 . . . . .	161
7.11	Bounded Feedback Advective Control: Case6 . . . . .	162

# List of Tables

3.1	Payne-Whitham Model Terms . . . . .	39
6.1	Riemann Problems for Bounded Advective Control . . . . .	126
7.1	Simulation Parameters for Constant Free Flow Speed . . . . .	149
7.2	Riemann Problems for Bounded Advective Control Simulations . . . . .	154

# Chapter 1

## Introduction

### 1.1 Motivation and Research Goal

Traffic congestion is a major problem in most big cities in the world. In U.S.A. every year there are about 40,000 to 50,000 fatalities on highway related accidents. About a billion dollars worth of productivity is lost in traffic jams every year. With the advances in microelectronics technology, sensors and microprocessors have become available for very low cost. Intelligent Transportation Systems (I.T.S.) is an area that deals with using technology to help solve the traffic problem using sensor, actuators and other electronics technology. By controlling the flow of traffic, it is hoped that many accidents can be prevented and also smooth flow can help avoid congestions.

#### 1.1.1 Vehicular Traffic Control

There are many ways to control vehicular traffic. Some of these are:

1. Ramp Metering Control: Ramp metering allows controlling the inflow rate into a highway from a street. The control is influenced by controlling the green cycle for a

traffic light. The control can be performed in an open loop setting. It can also be performed by using sensors to measure the traffic density on the highway in real time and then controlling the inflow rate based on the measured density.

2. **Signalized Intersection Control:** Traffic lights can be controlled either in an open loop manner based on the time of the day etc., or in a feedback loop based on measurements made to measure the traffic queues.
3. **Speed Control:** Speed Control can be performed by placing speed signs that can be changed dynamically based on speed measurements or can be fixed at different values at different time of the day, or also based on special events.
4. **Point Diversion:** Imagine a highway bifurcating into two and the two highways meeting again at some point. Traffic reaching the bifurcation point can take either of the two routes. Point diversion is traffic control that attempts to satisfy some criterion such as equal travel time in alternate routes etc. by choosing an appropriate split ratio at the diversion point.

### **1.1.2 Pedestrian Traffic Control**

There is also a great need for control of pedestrian traffic. This can also be performed using the microelectronics technology. Various sensors can be used to monitor real time traffic density and/or traffic velocity, so that different real-time instructions can be given to people to change their speed or direction for smooth flow of traffic.

### **1.1.3 Evacuation Problems**

Many lives can be saved by designing effective evacuation strategies during emergencies. In general, evacuation can be performed for any area, such as a parking area, city, or even larger area. Efficient evacuation is very important especially in the case of buildings, or an area of

a building. This becomes even more evident when one contemplates situations like 9-11, or a natural or a human made disaster affecting a building, such as a fire, earthquake, etc.

In most buildings, there is a static evacuation plan (see Figure 1.1) that shows people the route to the exit.

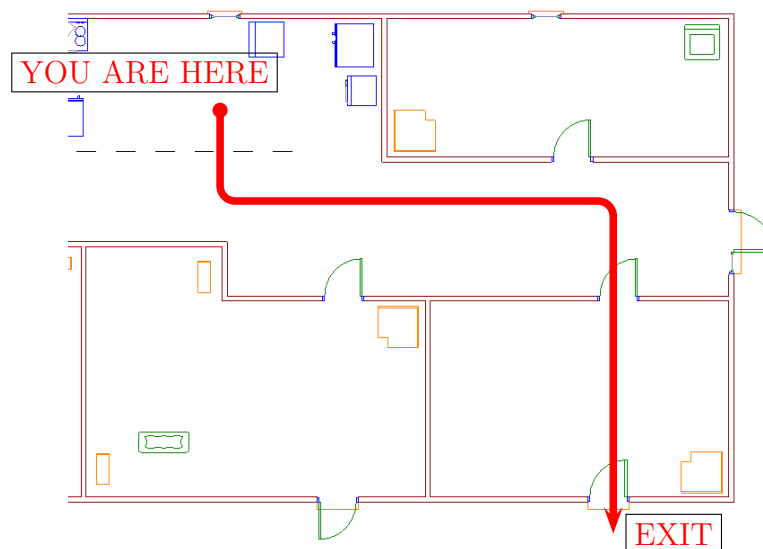


Figure 1.1: Static Evacuation Map

However, this map is static and tells people to take the same route no matter what the current traffic conditions are. In order to evacuate people effectively, the directions should be made dynamic depending on the current traffic situations. For instance, if there are multiple routes available to the exit and one of the routes is congested, then people can be told to take the other route. The speed of the people can be also controlled by informing them how fast to move so that they don't move too quickly to a place and cause congestion. There could be many ways that the information about speed can be conveyed to people. One way would be to have a light matrix whose blinking could be related to the desired speed. The exact design would depend on human factors research that would be needed in this case.

Sensors like cameras and infrared based sensors can be used to get real-time measurements of traffic density distribution that can be used by feedback controllers for efficient evacuation of people. In general, it is possible that we can make the people move as fast as possible to achieve time-optimal control. However, due to human factors issues that could possibly lead to undesired behavior. For instance, stampedes could be caused if people simply moved as fast as possible toward the exit. This dissertation is based on the philosophy that evacuation should involve a smooth following of some desired traffic patterns that lead to orderly removal of people from the area.

Now, the evacuation problem we are studying can be viewed as a digraph, where each room or an area is represented by a node, and each corridor or path from one node to another is represented by an arc as shown in Figure 1.2.

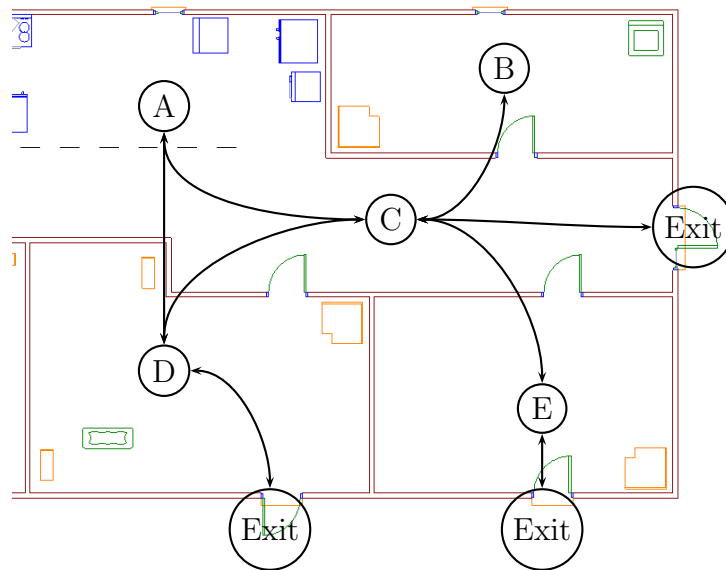


Figure 1.2: Evacuation Digraph

The flow of people from one node to another becomes a one-dimensional traffic control problem. If the evacuation has to be done from a big hall, then the evacuation problem

becomes a two-dimensional problem. The main motivation for the work presented in this dissertation comes from these one and two-dimensional traffic control problems.

## 1.2 Literature Survey

### 1.2.1 Traffic Models

There are essentially three types of traffic models: microscopic, mesoscopic and macroscopic. Microscopic ones model each vehicle as an individual entity and are car-following models in literature ([12], [18], [19], [26], [59], [72]), whereas macroscopic ones ([16], [52]) model traffic as a continuum. The mesoscopic ones are in between, such as the kinetic theory based models ([66], [39]). Cellular automata based models also exist ([55], [54]) that come under the microscopic modeling, since in those models, the cells can either be empty or contain a vehicle.

Macroscopic traffic models use some relationship between density and (equilibrium) speed. Many models for this relationship have been proposed such as Greenshield model ([30]), Greenberg model ([29]), Underwood model ([85]), Northwestern University model ([34]), Pipes-Munjal model ([64]) and multi-regime models ([52]). The macroscopic models can be based on a single partial differential equation (PDE), such as the Lighthill-Whitham-Richards model ([49], [70]), or a system of multiple PDEs such as the Payne-Whitham model ([63], [91]), Aw-Rascle model ([4], [68]) and Zhang model ([92], [93]). Macroscopic models for networks have also been proposed ([65]).

Pedestrian dynamics especially in the context of evacuation dynamics is a relatively new area ([75], [57]). These models also can be microscopic or macroscopic. Cellular automata based models also have been proposed ([89]). Simulation models have also been developed ([90]).

## 1.2.2 Traffic Control

The use of automatic control theory for traffic problems was started by Papageorgiou ([62]) and followed up by Kachroo for dynamic traffic assignment problems ([38]), dynamic routing ([67]), ramp metering problems ([37]), and by Ball for signalized intersection control([6]). Some preliminary models as well as linearized and Lyapunov based controls for pedestrian evacuations are given in [2], [88] and [87].

## 1.2.3 Mathematical Theory of Hyperbolic Conservation Laws

Some of the classical work on hyperbolic theory of PDEs with application in mathematical physics and gas dynamics is presented in [13] and [91]. A recent book on the mathematical physics aspects of hyperbolic conservation laws is written by Dafermos ([15]). Mathematical theory of hyperbolic systems of conservation laws has recently received great attention and many books have been published in this area ([10], [9], [32]) [42], [44], [76], [77].

### Control of Hyperbolic Conservation Laws

Control of hyperbolic conservation laws has been done using various techniques. Theory for infinite dimensional optimization and control theory is developed by Fattorini ([24]) and Lions ([50]). Optimal control of distributed systems especially in the context of viscous incompressible fluids is presented in ([25]). Optimization theory in a more abstract setting is presented in [58]. In [82], [83], and [84] Ulbrich studies control problems where the control comes in through the source term and the initial conditions. He also develops sensitivity and adjoint calculus for conservation laws based on shift variations. He also shows the convergence of optimal controls for discretized problems to the optimal control for the original problem. In the present work, we consider problems where the control enters through the flux term. Hence, we work in the framework of distributed controls. We study feedback control solutions where the aim is not optimization, but some desired closed-loop behavior

of traffic flow.

## 1.3 Contributions

The specific contributions of this dissertation work are listed below.

1. The two dimensional models of traffic that use magnitude and angle vector fields to drive pedestrian movement allowing for multi-directional flow are proposed in this dissertation. Their analysis has also been performed. These models include two-dimensional LWR, two-dimensional Payne-Whitham model, two-dimensional Aw-Rascle model, and two-dimensional Zhang model. Eigenvalues and eigenvectors in arbitrary directions are obtained. All this work is presented in Chapter 4.
2. Section 6.2 presents the  $L^1$  contraction property of the solution with respect to the controls. Subsection 6.2.1 presents existence results for optimal control in the space of constant controls.
3. Section 6.3 presents some specific designs for feedback control for scalar conservation law. Subsection 6.3.1 presents the control design that provides feedback advection. Subsection 6.3.2 presents the control design to produce feedback diffusion. Similarly, subsection 6.3.3 presents the corresponding control design that provides feedback advective-diffusion. All these feedback controls are presented for unbounded and bounded cases as well as for one and two-dimensional problems. The bounds are to be understood in the sense of the values the control variables can take. Section 6.4 presents the results for advective feedback control for relaxation systems. Subsection 6.4.1 presents unbounded advection for relaxation systems, where corollary 6.4.1 presents the main result. Subsection 6.4.2 presents bounded advection for relaxation systems. Section 6.5 presents wellposedness for bounded advection control. In this section, the proof involves substituting the bounded control into the dynamics to obtain

the closed loop that has a modified flux. The modified flux is Lipschitz, and hence standard existence results would apply. We go through the steps of the proof to show that at each step the density remains in  $[0, \rho_m]$ . Subsection 6.5.1 presents all different types of Riemann problems for bounded feedback advective control. Subsection 6.5.2 presents the main existence results (see theorem 6.5.2) for bounded advective control using front tracking method.

4. Chapter 7 presents numerical simulation results for unbounded and bounded feedback advective control using Godunov scheme. These results validate the analysis presented in Chapter 6.

## 1.4 Outline of the Dissertation

This dissertation is divided into the following chapters.

1. Chapter 1 presents the motivation, background and contributions of the dissertation.
2. Chapter 2 presents the derivation of conservation laws for mass, momentum and energy. This chapter is a review chapter and presents standard material on these derivations.
3. Chapter 3 presents one dimensional macroscopic traffic models. The chapter presents the scalar traffic model, as well as some systems of relaxation PDE models of traffic that also use momentum terms in the models. This chapter is also a review chapter and presents these models that have been proposed previously by other researchers.
4. Chapter 4 presents the new traffic models that this dissertation proposes. These models allow for distributed control via the traffic flux term, and also allows for modeling of one and two dimensional traffic. A relaxation system of PDE traffic models is also proposed in this chapter, and their corresponding eigenvalues and eigenvectors are also calculated.

5. Chapter 5 presents the necessary background mathematical theory for scalar conservation laws and relaxation models. This material is essential for developing the existence of optimal control results and for feedback control theory for the traffic models. The material in this chapter is a collection of results from relevant literature that lays the mathematical foundation for the main contributions of this dissertation.
6. Chapter 6 is the most important chapter of this dissertation as it presents most of the main contributions of this dissertation. It presents the existence results for optimal controls for traffic control problems as well as tabulating (without any optimization considerations) closed-loop behaviors of physical interest arising from various specific choices of feedback control laws.
7. Chapter 7 presents the numerical simulations using Godunov's method for advective control problems for initial-boundary data problems. The simulations are performed to clearly show the validity of results from Chapter 6.

# Chapter 2

## Derivation of Conservation Laws

In this chapter we review the derivation of the scalar and vector conservation laws. There are many references that give derivations for conservation laws, such as [91], [13], [45] and [81].

### 2.1 Mass Conservation

Let us consider a section from distance  $x_1$  to distance  $x_2$  from some reference point on the  $x$ -axis (see Figure 2.1). Let this section contain a fluid with a scalar density field  $\rho(t, x)$ . Fluid enters this section from its left edge given by the flux (or flow)  $q(x_1, t)$  and it leaves this section at its right edge at  $x_2$  where the flux is given by  $q(x_2, t)$ . Flux is the product of density and speed of flow as shown in equation (2.1). For conservation of mass, the change in density in a section can happen only due to the fluxes at the boundary, which in this one dimensional case is at  $x_1$  and  $x_2$ . Mathematically this statement can be written in integral or differential forms.

$$q(t, x) = \rho(t, x)v(t, x) \tag{2.1}$$

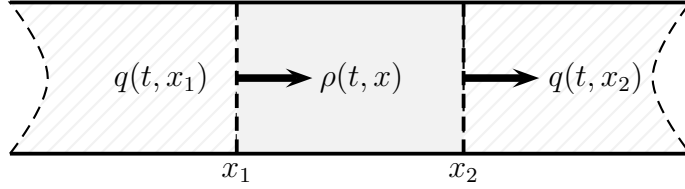


Figure 2.1: Conservation of Mass

### 2.1.1 Mass Conservation in One Dimension

The mass in the section from  $x = x_1$  to  $x = x_2$  at time  $t$  is given by

$$\text{mass in } [x_1, x_2] \text{ at time } t = \int_{x_1}^{x_2} \rho(t, x) dx \quad (2.2)$$

The total mass that enters the section from the edge at  $x = x_1$  is given by

$$\text{Inflow at } x_1 \text{ from time } t_1 \text{ to } t_2 = \int_{t_1}^{t_2} \rho(t, x_1) v(t, x_1) dt \quad (2.3)$$

Similarly, the total mass that leaves the section from the edge at  $x = x_2$  is given by

$$\text{Outflow at } x_2 \text{ from time } t_1 \text{ to } t_2 = \int_{t_1}^{t_2} \rho(t, x_2) v(t, x_2) dt \quad (2.4)$$

The conservation law states that the change in mass in the section  $[x_1, x_2]$  from time  $[t_1, t_2]$  is equal to the mass that enters through the flux at  $x_1$  from which the mass that exits through the flux at  $x_2$  has been subtracted. This is stated below as the conservation law in the *first integral form*.

$$\int_{x_1}^{x_2} \rho(t_2, x) dx - \int_{x_1}^{x_2} \rho(t_1, x) dx = \int_{t_1}^{t_2} \rho(t, x_1) v(t, x_1) dt - \int_{t_1}^{t_2} \rho(t, x_2) v(t, x_2) dt \quad (2.5)$$

Alternately, this can also be written in the *second integral form* as:

$$\frac{d}{dt} \int_{x_1}^{x_2} \rho(t, x) dx = \rho(t, x_1) v(t, x_1) - \rho(t, x_2) v(t, x_2) \quad (2.6)$$

Equation (2.5) can be written as

$$\int_{x_1}^{x_2} [\rho(t_2, x) - \rho(t_1, x)] dx = \int_{t_1}^{t_2} [\rho(t, x_1) v(t, x_1) - \rho(t, x_2) v(t, x_2)] dx \quad (2.7)$$

If  $\rho(t, x)$  and  $v(t, x)$  are differentiable functions then we get

$$\rho(t_2, x) - \rho(t_1, x) = \int_{t_1}^{t_2} \frac{\partial}{\partial t} \rho(t, x) dt \quad (2.8)$$

and

$$\rho(t, x_2) v(t, x_2) - \rho(t, x_1) v(t, x_1) = \int_{x_1}^{x_2} \frac{\partial}{\partial x} (\rho(t, x) v(t, x)) dx \quad (2.9)$$

Using equations (2.8) and (2.9) in (2.7) gives the following equation.

$$\int_{x_1}^{x_2} \int_{t_1}^{t_2} \left\{ \frac{\partial}{\partial t} \rho(t, x) + \frac{\partial}{\partial x} [\rho(t, x) v(t, x)] \right\} dt dx = 0 \quad (2.10)$$

Since this must be satisfied for all intervals of time and  $x$  then it must be true that the following *differential form of the conservation law* is satisfied.

$$\frac{\partial}{\partial t} \rho(t, x) + \frac{\partial}{\partial x} [\rho(t, x) v(t, x)] = 0 \quad (2.11)$$

In terms of the mass flux, this equation can be written as

$$\frac{\partial}{\partial t}\rho(t, x) + \frac{\partial}{\partial x}q(t, x) = 0 \quad (2.12)$$

### 2.1.2 Mass Conservation in Two Dimensions

Consider the conservation law in two dimensions as shown in Figure 2.2. Here, the flow in the  $x$ -direction is  $q_1$  and the flow in the  $y$ -direction is given by  $q_2$ . If  $u(t, x, y)$  is the speed of the fluid in the  $x$ -direction at time  $(t, x, y)$ , and  $v(t, x, y)$  is the speed of the fluid in the  $y$ -direction at time  $(t, x, y)$ , then we have the following two relationships for corresponding flows and speeds.

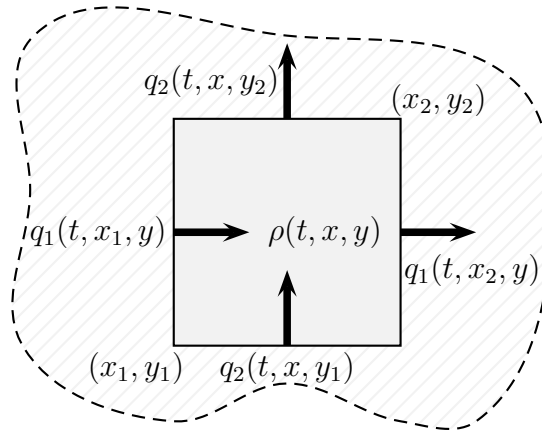


Figure 2.2: Conservation of Mass in 2D

$$q_1(t, x) = \rho(t, x)u(t, x) \quad (2.13)$$

$$q_2(t, x) = \rho(t, x)v(t, x) \quad (2.14)$$

The development of conservation of mass in two dimensions follows along the same lines as

the case of single dimension. The mass in the section from  $(x_1, y_1)$  to  $(x_2, y_2)$  at time  $t$  is given by

$$\text{mass in region}[(x_1, y_1)(x_2, y_2)] \text{ at time } t = \int_{x_1}^{x_2} \int_{y_1}^{y_2} \rho(t, x, y) dx dy \quad (2.15)$$

The total mass that enters the section from the edge at  $x = x_1$  is given by

$$\text{Inflow at } x_1 \text{ from time } t_1 \text{ to } t_2 = \int_{y_1}^{y_2} \int_{t_1}^{t_2} \rho(t, x_1, y) u(t, x_1, y) dt dy \quad (2.16)$$

Similarly, the total mass that leaves the section from the edge at  $x = x_2$  is given by

$$\text{Outflow at } x_2 \text{ from time } t_1 \text{ to } t_2 = \int_{y_1}^{y_2} \int_{t_1}^{t_2} \rho(t, x_2, y) u(t, x_2, y) dt dy \quad (2.17)$$

The total mass that enters the section from the edge at  $y = y_1$  is given by

$$\text{Inflow at } y_1 \text{ from time } t_1 \text{ to } t_2 = \int_{x_1}^{x_2} \int_{t_1}^{t_2} \rho(t, x, y_1) v(t, x, y_1) dt dx \quad (2.18)$$

Similarly, the total mass that leaves the section from the edge at  $y = y_2$  is given by

$$\text{Outflow at } y_2 \text{ from time } t_1 \text{ to } t_2 = \int_{x_1}^{x_2} \int_{t_1}^{t_2} \rho(t, x, y_2) v(t, x, y_2) dt dx \quad (2.19)$$

The conservation law states that the change in mass in the section from time  $[t_1, t_2]$  is equal to the exchange that takes place at the boundary of the section. This is stated below as the conservation law in the *first integral form* for two dimensions.

$$\begin{aligned}
& \int_{x_1}^{x_2} \int_{y_1}^{y_2} \rho(t_2, x, y) dx dy - \int_{x_1}^{x_2} \int_{y_1}^{y_2} \rho(t_1, x, y) dx dy \\
&= \int_{y_1}^{y_2} \int_{t_1}^{t_2} \rho(t, x_1, y) u(t, x_1, y) dy dt + \int_{x_1}^{x_2} \int_{t_1}^{t_2} \rho(t, x, y_1) v(t, x, y_1) dx dt \\
&- \int_{y_1}^{y_2} \int_{t_1}^{t_2} \rho(t, x_2, y) u(t, x_2, y) dy dt - \int_{x_1}^{x_2} \int_{t_1}^{t_2} \rho(t, x, y_2) v(t, x, y_2) dx dt \quad (2.20)
\end{aligned}$$

Alternately, this can also be written in the *second integral form* as:

$$\begin{aligned}
& \frac{d}{dt} \int_{x_1}^{x_2} \int_{y_1}^{y_2} \rho(t_2, x, y) dx dy \\
&= \int_{y_1}^{y_2} \rho(t, x_1, y) u(t, x_1, y) dy + \int_{x_1}^{x_2} \rho(t, x, y_1) v(t, x, y_1) dx \\
&- \int_{y_1}^{y_2} \rho(t, x_2, y) u(t, x_2, y) dy - \int_{x_1}^{x_2} \rho(t, x, y_2) v(t, x, y_2) dx \quad (2.21)
\end{aligned}$$

Equation (2.20) can be written as

$$\begin{aligned}
& \int_{x_1}^{x_2} \int_{y_1}^{y_2} [\rho(t_2, x, y) dx dy - \rho(t_1, x, y)] dx dy \\
&= \int_{y_1}^{y_2} \int_{t_1}^{t_2} [\rho(t, x_1, y) u(t, x_1, y) - \rho(t, x_2, y) u(t, x_2, y)] dy dt \\
&+ \int_{x_1}^{x_2} \int_{t_1}^{t_2} [\rho(t, x, y_2) v(t, x, y_2) - \rho(t, x, y_1) v(t, x, y_1)] dx dt \quad (2.22)
\end{aligned}$$

If  $\rho(t, x, y)$ ,  $u(t, x, y)$  and  $v(t, x, y)$  are differentiable functions then we get

$$\rho(t_2, x, y) - \rho(t_1, x, y) = \int_{t_1}^{t_2} \frac{\partial}{\partial t} \rho(t, x, y) dt \quad (2.23)$$

$$\rho(t, x_2, y) u(t, x_2, y) - \rho(t, x_1, y) u(t, x_1, y) = \int_{x_1}^{x_2} \frac{\partial}{\partial x} (\rho(t, x, y) u(t, x, y)) dx \quad (2.24)$$

and

$$\rho(t, x, y_2)v(t, x, y_2) - \rho(t, x, y_1)v(t, x, y_1) = \int_{y_1}^{y_2} \frac{\partial}{\partial y}(\rho(t, x, y)v(t, x, y))dy \quad (2.25)$$

Using equations (2.23), (2.24) and (2.25) in (2.20) gives the following equation.

$$\int_{y_1}^{y_2} \int_{x_1}^{x_2} \int_{t_1}^{t_2} \left\{ \frac{\partial}{\partial t}\rho(t, x, y) + \frac{\partial}{\partial x}[\rho(t, x, y)u(t, x, y)] + \frac{\partial}{\partial y}[\rho(t, x, y)v(t, x, y)] \right\} dt dx dy = 0 \quad (2.26)$$

Since this must be satisfied for all intervals of time,  $x$  and  $y$  then it must be true that the following *differential form of the conservation law* is satisfied.

$$\frac{\partial}{\partial t}\rho(t, x, y) + \frac{\partial}{\partial x}[\rho(t, x, y)u(t, x, y)] + \frac{\partial}{\partial y}[\rho(t, x, y)v(t, x, y)] = 0 \quad (2.27)$$

or

$$\frac{\partial}{\partial t}\rho(t, x, y) + \nabla \cdot [\rho(t, x, y)v(t, x, y)] = 0 \quad (2.28)$$

In terms of the mass flux, this equation can be written as

$$\frac{\partial}{\partial t}\rho(t, x, y) + \frac{\partial}{\partial x}q_1(t, x, y) + \frac{\partial}{\partial y}q_2(t, x, y) = 0 \quad (2.29)$$

or

$$\frac{\partial}{\partial t}\rho(t, x, y) + \nabla \cdot q(t, x, y) = 0 \quad (2.30)$$

### 2.1.3 Mass Conservation in n Dimensions

For the n-dimensional case, density is given by  $\rho(t, x)$ , velocity by  $v(t, x) \in R^n$  and flux by  $q(t, x) \in R^n$  where  $x \in R^n$ . The flux is given by

$$q(t, x) = \rho(t, x)v(t, x) \quad (2.31)$$

and the conservation law is given by

$$\frac{\partial}{\partial t}\rho(t, x) + \nabla \cdot q(t, x) = 0 \quad (2.32)$$

## 2.2 Momentum Conservation

First we will study momentum conservation in one dimension, then followed by two dimensional and viscous cases.

### 2.2.1 Momentum Conservation in One Dimension

Let us consider a section in one dimension (see Figure 2.3). The momentum of the fluid in the section is given by the product of the density  $\rho(t, x)$  and the velocity  $v(t, x)$ . Just as in the case of conservation of mass, the flux for momentum is given by the product of momentum and the velocity, i.e.  $\rho(t, x)v^2(t, x)$ . Now, according to Newton's second law (see [17]), the change of momentum should be equal to the force applied. Force is equal to the product of pressure and area. Taking area to be of unit measurement in our problem, we get force to be  $p(t, x_1)$  on the left edge, and  $p(t, x_2)$  on the right.

Applying Newton's law to the section, we obtain

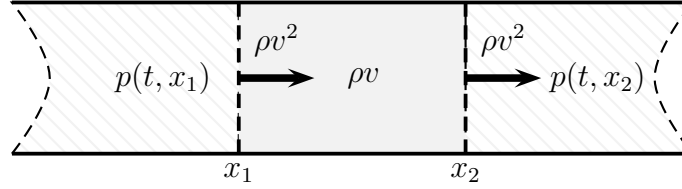


Figure 2.3: Conservation of Momentum

$$\frac{\partial}{\partial t}[\rho(t, x)v(t, x)] + \frac{\partial}{\partial x}[\rho(t, x)v^2(t, x) + p(t, x)] = 0 \quad (2.33)$$

### 2.2.2 Momentum Conservation in Two Dimensions

There are two momentum fields in two dimensions. One is the momentum in the  $x$  direction (considered in 2.4) given by  $\rho(t, x, y)u(t, x, y)$  and the other in the  $y$  direction given by  $\rho(t, x, y)v(t, x, y)$ , where  $u(t, x, y)$  is the velocity in the  $x$  direction and  $v(t, x, y)$  is the same in the  $y$  direction. We can derive the conservation of momentum in the  $x$ -direction as follows.

Momentum in the  $x$ -direction in the section is given by  $\rho(t, x, y)u(t, x, y)$ . The flux in the  $x$  direction is due to the velocity in  $x$ -direction given by  $u(t, x, y)$  and is equal to the product of this velocity with the momentum. The flux is equal to  $\rho(t, x, y)u^2(t, x, y)$ . The flux in the  $y$  direction is due to the velocity in  $y$ -direction given by  $v(t, x, y)$  and is equal to the product of this velocity with the momentum. The flux is equal to  $\rho(t, x, y)u(t, x, y)v(t, x, y)$ .

According to Newton's law, total change in the linear momentum in the  $x$ -direction is equal to the force in the  $x$ -direction. The force comes from the pressure as in the one dimension case and we obtain

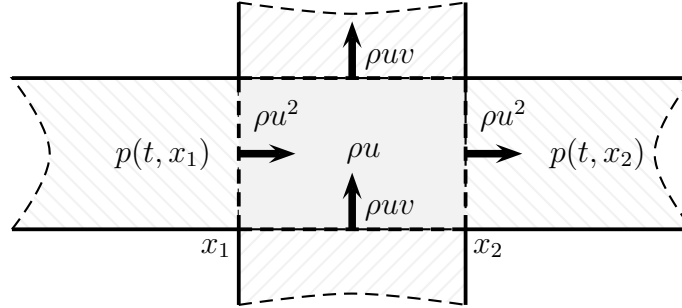


Figure 2.4: Conservation of Momentum in the x-Direction

$$\frac{\partial}{\partial t}[\rho(t, x, y)u(t, x, y)] + \frac{\partial}{\partial x}[\rho(t, x, y)u^2(t, x, y) + p(t, x, y)] + \frac{\partial}{\partial y}\rho(t, x, y)u(t, x, y)v(t, x, y) = 0 \quad (2.34)$$

Ignoring the dependencies on  $(t, x, y)$  we can write the momentum equation in the  $x$ - and  $y$  directions as follows.

$$\begin{aligned} \frac{\partial}{\partial t}[\rho u] + \frac{\partial}{\partial x}[\rho u^2 + p] + \frac{\partial}{\partial y}\rho u v &= 0 \\ \frac{\partial}{\partial t}[\rho v] + \frac{\partial}{\partial x}\rho u v + \frac{\partial}{\partial y}[\rho v^2 + p] &= 0 \end{aligned} \quad (2.35)$$

### 2.2.3 Momentum Equation with Viscosity

Let us study the two dimensional flow again where the fluid has shear and normal stresses including pressure (see Figure 2.5).

The total change in linear momentum in the  $x$ -direction is given by

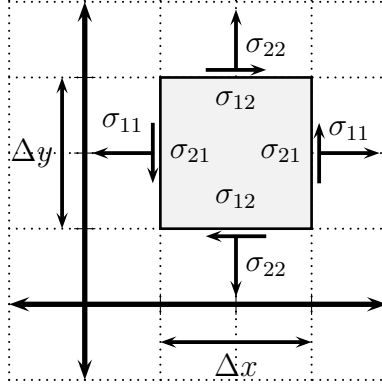


Figure 2.5: Stresses on a Planar Fluid

$$\begin{aligned}
 \text{Change in Momentum in } x \text{ direction} &= \frac{\partial}{\partial t}[\rho(t, x, y)u(t, x, y)] + \frac{\partial}{\partial x}\rho(t, x, y)u^2(t, x, y) \\
 &+ \frac{\partial}{\partial y}\rho(t, x, y)u(t, x, y)v(t, x, y)
 \end{aligned} \tag{2.36}$$

This should equal the force in  $x$  direction. The force is due to the normal and shear stresses in the same direction. The change in stress in  $x$  direction is

$$\begin{aligned}
 \text{Stress in } x \text{ direction} &= \sigma_{11}(t, x + \Delta x, y) - \sigma_{11}(t, x, y) + \\
 &\sigma_{12}(t, x, y + \Delta y) - \sigma_{21}(t, x, y)
 \end{aligned} \tag{2.37}$$

Taking appropriate limits as  $\Delta x \rightarrow 0$ ,  $\Delta y \rightarrow 0$  and matching with equation (2.36), we get

$$\begin{aligned}
 \frac{\partial}{\partial t}\rho u + \frac{\partial}{\partial x}\rho u^2 + \frac{\partial}{\partial y}\rho uv &= \frac{\partial}{\partial x}\sigma_{11} + \frac{\partial}{\partial y}\sigma_{12} \\
 \frac{\partial}{\partial t}\rho v + \frac{\partial}{\partial x}\rho uv + \frac{\partial}{\partial y}\rho v^2 &= \frac{\partial}{\partial x}\sigma_{21} + \frac{\partial}{\partial y}\sigma_{22}
 \end{aligned} \tag{2.38}$$

Now, pressure is the stress which is same in all directions. Hence, we can remove the pressure from the principle component of stresses as follows.

$$\begin{aligned}\sigma_{11} &= -p + \overline{\sigma_{11}} \\ \sigma_{22} &= -p + \overline{\sigma_{22}}\end{aligned}\tag{2.39}$$

Using (2.39) in (2.38), we get

$$\begin{aligned}\frac{\partial}{\partial t}\rho u + \frac{\partial}{\partial x}(\rho u^2 + p) + \frac{\partial}{\partial y}\rho uv &= \frac{\partial}{\partial x}\overline{\sigma_{11}} + \frac{\partial}{\partial y}\sigma_{12} \\ \frac{\partial}{\partial t}\rho v + \frac{\partial}{\partial x}\rho uv + \frac{\partial}{\partial y}(\rho v^2 + p) &= \frac{\partial}{\partial x}\sigma_{21} + \frac{\partial}{\partial y}\overline{\sigma_{22}}\end{aligned}\tag{2.40}$$

Let us assume the following relationship between stress and strain

$$\begin{aligned}\overline{\sigma_{11}} &= \mu \frac{\partial}{\partial x}u \\ \sigma_{12} &= \mu \frac{\partial}{\partial y}u \\ \sigma_{21} &= \mu \frac{\partial}{\partial x}v \\ \overline{\sigma_{22}} &= \mu \frac{\partial}{\partial y}v\end{aligned}\tag{2.41}$$

In (2.41) we have taken  $\mu$  to be the constant coefficient of viscosity. Now substituting (2.41) in (2.40), we obtain

$$\begin{aligned}\frac{\partial}{\partial t}\rho u + \frac{\partial}{\partial x}(\rho u^2 + p) + \frac{\partial}{\partial y}\rho uv &= \mu\left(\frac{\partial^2 u}{\partial x^2} + \frac{\partial^2 u}{\partial y^2}\right) \\ \frac{\partial}{\partial t}\rho v + \frac{\partial}{\partial x}\rho uv + \frac{\partial}{\partial y}(\rho v^2 + p) &= \mu\left(\frac{\partial^2 v}{\partial x^2} + \frac{\partial^2 v}{\partial y^2}\right)\end{aligned}\tag{2.42}$$

Equation (2.42) can also be written as

$$\frac{\partial}{\partial t} \begin{bmatrix} \rho u \\ \rho v \end{bmatrix} + \frac{\partial}{\partial x} \begin{bmatrix} \rho u^2 \\ \rho uv \end{bmatrix} + \frac{\partial}{\partial y} \begin{bmatrix} \rho uv \\ \rho v^2 \end{bmatrix} + \nabla p = \mu \Delta \begin{bmatrix} u \\ v \end{bmatrix} \quad (2.43)$$

In equation (2.43), if we take  $\mu$  to be zero, we obtain the non-viscous equation (2.35).

## 2.3 Energy Conservation

The derivation of energy conservation laws follows the same steps as the ones followed by conservation of mass and momentum. Energy flux in the  $x$ -direction is given by  $uE$  and in the  $y$ -direction by  $vE$ . Change of energy in unit time in a given direction is obtained from the power in that direction. Power is work done per unit time. Work is the inner-product (or dot product) of force and distance covered in that direction. Since force per unit area is pressure, power is given as a product of pressure and speed in the direction of interest. Hence, the conservation of energy in the two dimensional case is given as

$$\frac{\partial}{\partial t} E + \frac{\partial}{\partial x} [u(E + p)] + \frac{\partial}{\partial y} [v(E + p)] = 0 \quad (2.44)$$

## 2.4 Combined Equations

Combining the equations (2.27), (2.35) and (2.44), we get the following equation.

$$\frac{\partial}{\partial t} \begin{bmatrix} \rho \\ \rho u \\ \rho v \\ E \end{bmatrix} + \frac{\partial}{\partial x} \begin{bmatrix} \rho u \\ \rho u^2 + p \\ \rho uv \\ u(E + p) \end{bmatrix} + \frac{\partial}{\partial y} \begin{bmatrix} \rho v \\ \rho uv \\ \rho v^2 + p \\ v(E + p) \end{bmatrix} = 0 \quad (2.45)$$

If we define the vector

$$U = \begin{bmatrix} \rho \\ \rho u \\ \rho v \\ E \end{bmatrix} \quad (2.46)$$

and the corresponding vector flux in  $x$ -direction as

$$F_1 = \begin{bmatrix} \rho u \\ \rho u^2 + p \\ \rho uv \\ u(E + p) \end{bmatrix} \quad (2.47)$$

in the  $y$ -direction as

$$F_2 = \begin{bmatrix} \rho v \\ \rho uv \\ \rho v^2 + p \\ v(E + p) \end{bmatrix} \quad (2.48)$$

then we can show the vector conservation law as

$$\frac{\partial U}{\partial t} + \nabla \cdot F = 0 \quad (2.49)$$

$F$  is the vector flux, whose component in the  $x$ -direction is  $F_1$  and whose component in the  $y$ -direction is  $F_2$ .

### 2.4.1 Equation of State

Notice that in (2.45) there are four equations but five unknowns ( $\rho$ ,  $u$ ,  $v$ ,  $E$ , and  $p$ ). Hence we need another equation for solvability of the system. For gases energy is the sum of kinetic energy and internal energy ( $e$ ) as shown below.

$$E = \frac{1}{2}\rho(u_2^2 + v_2^2) + \rho e \quad (2.50)$$

The equation of state gives the formula for the internal energy in terms of pressure and density assuming chemical and thermodynamic equilibrium. The equation to be used depends on what type of gas it is.

#### Polytropic Gas

For an ideal gas with specific heat at constant volume given by  $c_v$ , the internal energy  $e$  is the following function of temperature.

$$e = c_v T \quad (2.51)$$

Temperature  $T$  is related to density  $\rho$  and pressure  $p$  by

$$p = R\rho T \quad (2.52)$$

where  $R$  is called the gas constant.

If a gas is kept at a constant volume as energy is added to it, the change in internal energy is given by

$$de = c_v dT \quad (2.53)$$

On the other hand if a gas is kept at a constant pressure as energy is added to it, some work is also done in increasing the volume. The change in internal energy is give by

$$d\left(e + \frac{p}{\rho}\right) = c_p dT \quad (2.54)$$

Enthalpy  $h$  is defined as

$$h = e + \frac{p}{\rho} \quad (2.55)$$

so that

$$h = c_p T \quad (2.56)$$

Using equations (2.56) and (2.51) in (2.52) gives

$$c_p - c_v = R \quad (2.57)$$

Using (2.51) and substituting  $T$  from (2.52), we get the following for the internal energy.

$$e = \frac{c_v P}{R\rho} \quad (2.58)$$

Using ratio of specific heats  $\gamma = c_p/c_v$  and (2.57), we get

$$e = \frac{p}{(\gamma - 1)\rho} \quad (2.59)$$

Finally, substituting (2.59) into (2.50) gives the additional equation for the polytropic gas.

$$E = \frac{1}{2}\rho(u_2 + v_2) + \frac{p}{(\gamma - 1)} \quad (2.60)$$

### Isothermal Flow

In the situation where the temperature of the gas is kept at a constant temperature  $T$ , energy is not conserved, and we can use the mass and momentum conservation equations only. Energy is not constant since external energy is required to keep the constant temperature. Since temperature is kept constant, because of equation (2.52) we obtain a linear relationship between pressure and density as

$$p = a^2 \rho \quad (2.61)$$

where  $a = \sqrt{RT}$ ,  $T$  being the constant temperature. It can also be shown that  $a$  is the speed of sound (sound speed is given as the partial derivative of pressure with respect to density since sound travels as small disturbances in pressure). Using this, the system for isothermal flow for a two-dimensional flow becomes

$$\frac{\partial}{\partial t} \begin{bmatrix} \rho \\ \rho u \\ \rho v \end{bmatrix} + \frac{\partial}{\partial x} \begin{bmatrix} \rho u \\ \rho u^2 + a^2 \rho \\ \rho uv \end{bmatrix} + \frac{\partial}{\partial y} \begin{bmatrix} \rho v \\ \rho uv \\ \rho v^2 + a^2 \rho \end{bmatrix} = 0 \quad (2.62)$$

### Isentropic Flow

Entropy (a measure of disorder in a system) is defined as

$$S = c_v \log(p/\rho^\gamma) + k \quad (2.63)$$

where  $k$  is a constant. Using equation (2.63) we can find an expression for pressure in terms of entropy and density as

$$p = \kappa \exp^{S/c_v} \rho^\gamma \quad (2.64)$$

where  $\kappa$  is a constant.

Clearly, if entropy is constant, the equation of state is given by

$$p = \bar{\kappa} \rho^\gamma \quad (2.65)$$

where

$$\bar{\kappa} = \kappa \exp^{S/c_v} \quad (2.66)$$

Hence using equation (2.65) in the two dimensional system becomes

$$\frac{\partial}{\partial t} \begin{bmatrix} \rho \\ \rho u \\ \rho v \end{bmatrix} + \frac{\partial}{\partial x} \begin{bmatrix} \rho u \\ \rho u^2 + \bar{\kappa} \rho^\gamma \\ \rho u v \end{bmatrix} + \frac{\partial}{\partial y} \begin{bmatrix} \rho v \\ \rho u v \\ \rho v^2 + \bar{\kappa} \rho^\gamma \end{bmatrix} = 0 \quad (2.67)$$

It can also be shown by using the definition of entropy in equation (2.63) in conservation laws in the differential form that in the regions of smooth flow entropy is conserved, i.e.

$$S(t, x, y)_t + u(t, x, y)S(t, x, y)_x + v(t, x, y)S(t, x, y)_y = 0 \quad (2.68)$$

## 2.5 General Conservation

This section derives the conservation law in more general setting as presented in [35]. This general setting is illustrated in Figure 2.6.

The conservation law in general setting is given by

$$\frac{\partial u}{\partial t} + \nabla \cdot f = 0 \quad (2.69)$$

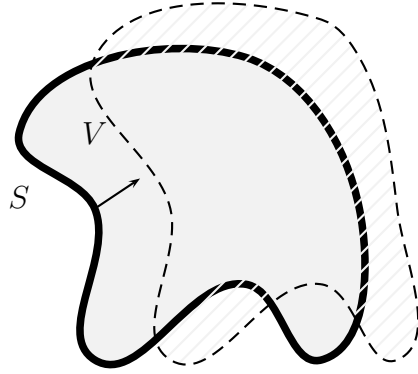


Figure 2.6: Conservation in General Setting

Consider a cell of volume  $V$  that has a boundary  $S$ . The volume contains material  $\int u dV$  that changes over time because of flux  $f$  that flows only through the boundary. In time  $\Delta t$  the boundary moves to a new location changing the volume from  $V$  to  $(V + \Delta V)$ . The material inside the volume  $(V + \Delta V)$  is  $(u + \Delta u)$ . To obtain the total change in  $u$  we get

$$\begin{aligned}
 \int_{V+\Delta V} (u + \Delta u) dV - \int_V u dV &= \int_V (u + \Delta u) dV + \int_{\Delta V} (u + \Delta u) dV - \int_V u dV \\
 &= \int_V u dV + \int_V \Delta u dV + \int_{\Delta V} u dV + \int_{\Delta V} \Delta u dV - \int_V u dV \\
 &= \int_V \Delta u dV + \int_{\Delta V} u dV + \int_{\Delta V} \Delta u dV \tag{2.70}
 \end{aligned}$$

We neglect the last term on the right hand side since it involves second order differential terms. The second term shows the material that is in the differential volume. The new volume can be written in terms of the surface as  $dV = S \Delta t$  and therefore, the second term can be written as

$$\int_{\Delta V} u dV = \oint_S uv_n d(S\Delta t) \quad (2.71)$$

Here  $v_n$  is the outward normal component of the velocity at the surface. We can write equation (2.70) as

$$\int_{V+\Delta V} (u + \Delta u) dV - \int_V u dV = \int_V \Delta u dV + \oint_S uv_n d(S\Delta t) \quad (2.72)$$

Dividing both sides by  $\Delta t$  and taking  $\Delta t \rightarrow 0$  we get

$$\frac{\partial}{\partial t} \int_V u dV = \int_V \frac{\partial u}{\partial t} dV + \oint_S uv_n dS \quad (2.73)$$

Using the divergence theorem ([51]) and applying equation (2.69) in (2.73) we get the integral form of the conservation law for the moving boundary case as

$$\frac{\partial}{\partial t} \int_V u dV = \oint_S (f_n + uv_n) dS \quad (2.74)$$

Here  $f_n$  is the normal component of the flux. If the cell is stationary, then we get the following integral form of the conservation law.

$$\frac{\partial}{\partial t} \int_V u dV = \oint_S f_n dS \quad (2.75)$$

# Chapter 3

## Traffic Models: One Dimensional Case

In this chapter we review macroscopic traffic models and how they relate to conservation equations. We consider one-dimensional and two-dimensional vehicular and pedestrian traffic models. Traffic models can be microscopic (see [12]), mesoscopic or macroscopic (see [16], [52]). Macroscopic models treat traffic as a continuum and these are the models of interest to this dissertation. Microscopic models treat each vehicle or pedestrian as an individual entity and treats acceleration as the control variable that depends on inter-vehicular or inter-pedestrian density (see [7], [12], [38]). Mesoscopic models use kinetic models for traffic using Boltzmann equation from statistical mechanics (see [66]).

### 3.1 Lighthill-Whitham-Richards Model

The LWR model, named after the authors in [49] and [70], is a macroscopic one-dimensional traffic model. The conservation law for traffic in one dimension is given by

$$\frac{\partial}{\partial t}\rho(t, x) + \frac{\partial}{\partial x}f(t, x) = 0 \tag{3.1}$$

In this equation  $\rho$  is the traffic density (vehicles or pedestrians) and  $f$  is the flux which is

the product of traffic density and the traffic speed  $v$ , i.e.  $f = \rho v$ . There are many models researchers have proposed for how the flux should be dependent on traffic conditions. This relationship is given by the *fundamental diagram*.

### 3.1.1 Greenshield's Model

Greenshield's model (see [30]) uses a linear relationship between traffic density and traffic speed.

$$v(\rho) = v_f \left(1 - \frac{\rho}{\rho_m}\right) \quad (3.2)$$

where  $v_f$  is the free flow speed and  $\rho_m$  is the maximum density. Free flow speed is the speed of traffic when the density is zero. This is the maximum speed. The maximum density is the density at which there is a traffic jam and the speed is equal to zero. The flux function is concave as can be confirmed by noting the negative sign of the second derivative of flow with respect to density, i.e.  $\partial^2 f / \partial \rho^2 < 0$ . The fundamental diagram refers to the relationship that the traffic density  $\rho$ , traffic speed  $v$  and traffic flow  $f$  have with each other. These relationships are shown in Figure 3.1.

### 3.1.2 Greenberg Model

In this model (see [29]) the speed-density function is given by

$$V(\rho) = v_f \ln\left(\frac{\rho_m}{\rho}\right) \quad (3.3)$$

Greenberg fundamental diagram is shown in Figure 3.2.

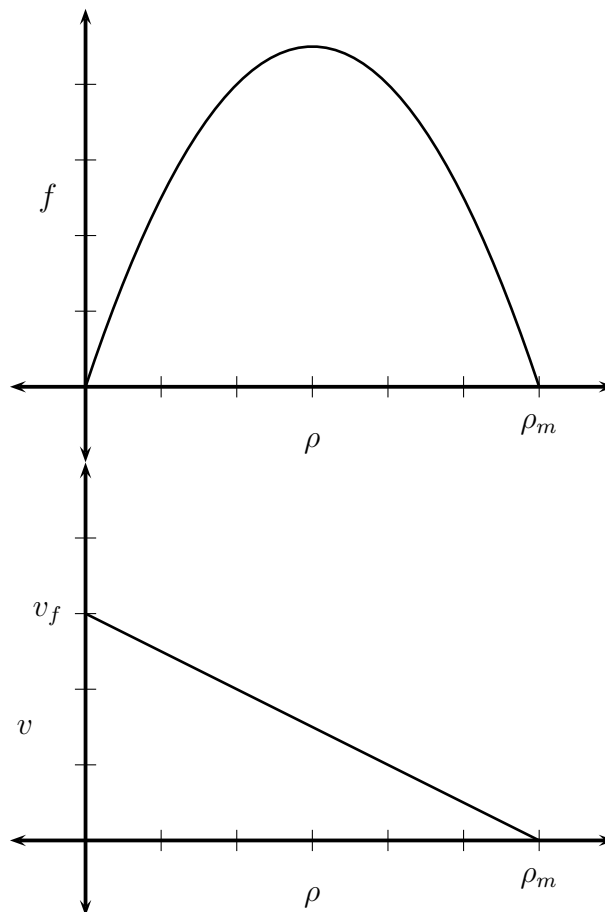


Figure 3.1: Fundamental Diagram using Greenshield Model

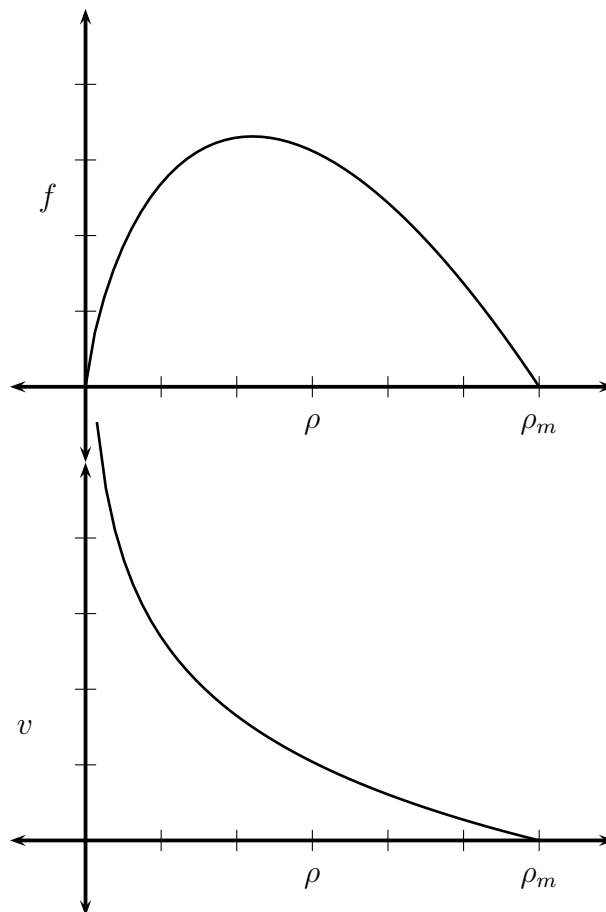


Figure 3.2: Fundamental Diagram using Greenberg Model

### 3.1.3 Underwood Model

In the Underwood model (see [85]) the velocity-density function is represented by

$$V(\rho) = v_f \exp\left(\frac{-\rho}{\rho_m}\right) \quad (3.4)$$

Underwood fundamental diagram is shown in Figure 3.3.

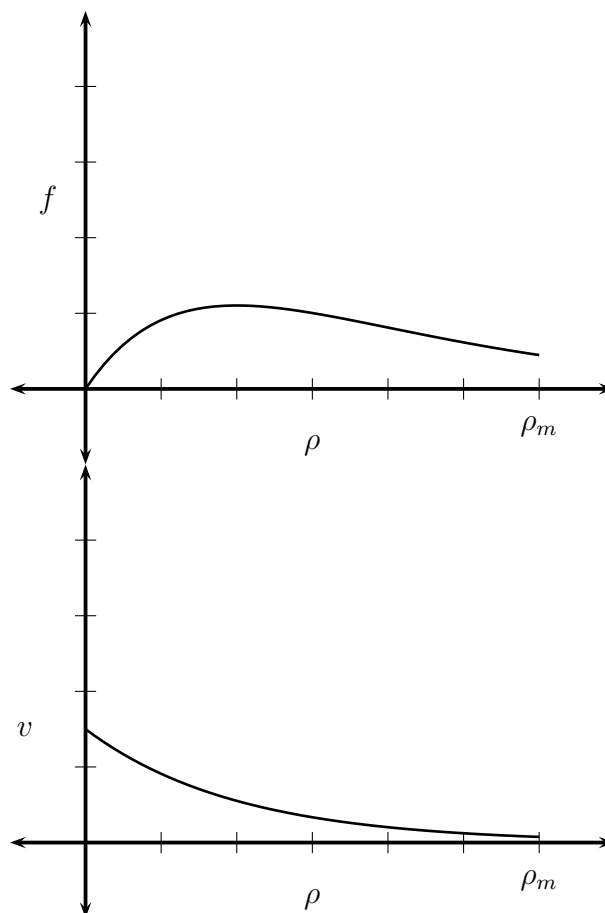


Figure 3.3: Fundamental Diagram using Underwood Model

### 3.1.4 Diffusion Model

Diffusion model is an extension of the Greenshield's model where the traffic speed depends not only on the traffic density but also on the density gradient. This models the driver behavior where changes in traffic density in the  $x$ -direction affect the traffic speed. The model is given by

$$V(\rho) = v_f \left(1 - \frac{\rho}{\rho_m}\right) - \frac{D}{\rho} \left(\frac{\partial \rho}{\partial x}\right) \quad (3.5)$$

where  $D$  is a diffusion coefficient given by  $D = \tau v_r^2$ ,  $v_r$  is a random velocity, and  $\tau$  is a relaxation parameter.

### 3.1.5 Other Models

There do exist other models such as Northwestern University model, Drew model, Pipes-Munjal model, and multi-regime models. The speed-density relationships for these models are given below:

#### Northwestern University model

The speed-density relationship for this model [34] is given by

$$V(\rho) = v_f \exp\left(-0.5 \left(\frac{\rho}{\rho_0}\right)^2\right) \quad (3.6)$$

#### Drew model

The speed-density relationship for this model [22] is given by

$$V(\rho) = v_f \left( 1 - \left( \frac{\rho}{\rho_m} \right)^{(n+1)/2} \right) \quad (3.7)$$

Drew model is a generalization of other models such that taking different values for  $n$  in his model results in other models.

### Pipes-Munjal Model

The speed-density relationship for this model [64] is given by

$$V(\rho) = v_f \left( 1 - \left( \frac{\rho}{\rho_m} \right)^n \right) \quad (3.8)$$

This model is also a generalization of other models such that taking different values for  $n$  in this model results in other models.

### Multi-regime Model

The speed-density relationship for this model can use different expressions in different regions [52]. For instance it can use a constant speed in uncongested region and linear speed in the congested region.

$$V(\rho) = \begin{cases} v_f & \text{if } \rho < \frac{\rho_m}{2} \\ v_f \left( 1 - \frac{\rho}{\rho_m} \right) & \text{otherwise} \end{cases} \quad (3.9)$$

The fundamental diagram for this model is shown in Figure 3.4.

### 3.1.6 LWR Models

Here we combine different fundamental relationships with the scalar conservation law.

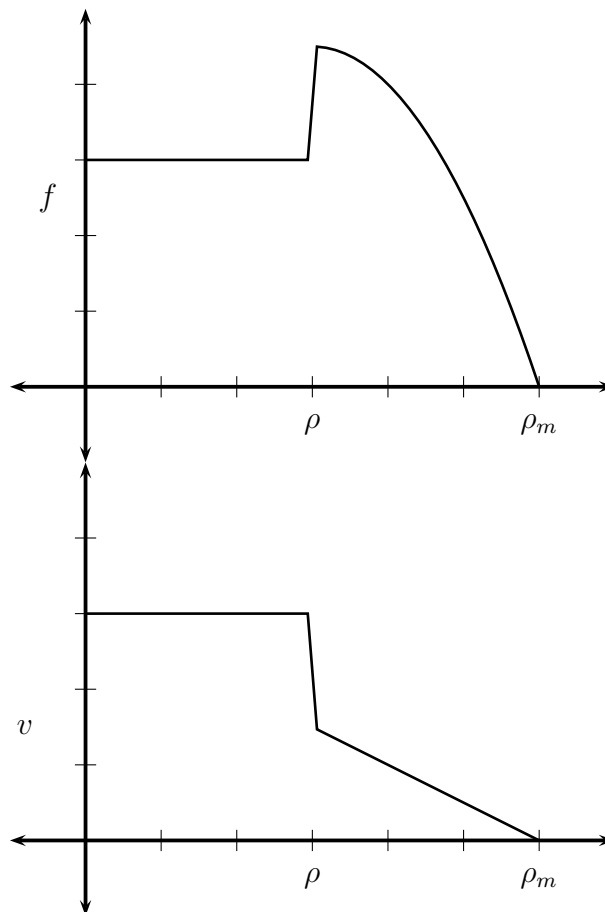


Figure 3.4: Fundamental Diagram using Multi-regime Model

**LWR Model with Greenshields Flow**

LWR model with Greenshields flow becomes

$$\frac{\partial}{\partial t}\rho + \frac{\partial}{\partial x}v_f\rho\left(1 - \frac{\rho}{\rho_m}\right) = 0 \quad (3.10)$$

**LWR Model with Greenberg Flow**

LWR model with Greenwood flow becomes

$$\frac{\partial}{\partial t}\rho + \frac{\partial}{\partial x}v_f\rho\ln\left(\frac{\rho_m}{\rho}\right) = 0 \quad (3.11)$$

**LWR Model with Underwood Flow**

LWR model with Underwood flow becomes

$$\frac{\partial}{\partial t}\rho + \frac{\partial}{\partial x}v_f\rho\exp\left(\frac{-\rho}{\rho_m}\right) = 0 \quad (3.12)$$

**LWR Model with Diffusion**

LWR model with diffusive flow becomes the following viscous scalar conservation law.

$$\frac{\partial}{\partial t}\rho + \frac{\partial}{\partial x}\left[v_f\left(1 - \frac{\rho}{\rho_m}\right) - \frac{D}{\rho}\left(\frac{\partial\rho}{\partial x}\right)\right] = 0 \quad (3.13)$$

Term	Meaning
$V(\rho)$	Equilibrium Speed
$\tau$	Relaxation Time
$(V(\rho) - v)/\tau$	Relaxation
$(A(\rho))_x / \rho$	Anticipation
$\mu v_{xx} / \rho$	Viscosity

Table 3.1: Payne-Whitham Model Terms

## 3.2 Payne-Whitham Model

PW model or the Payne-Whitham model was proposed in the 1970s independently in [63] and [91]. It uses two PDEs to represent the traffic dynamics. In its most general form, the model takes the following form [65].

$$\begin{aligned}
 \rho_t + (\rho v)_x &= 0 \\
 v_t + v v_x &= \frac{V(\rho) - v}{\tau} - \frac{(A(\rho))_x}{\rho} + \mu \frac{v_{xx}}{\rho}
 \end{aligned} \tag{3.14}$$

Table 3.1 shows the different terms in this model. The first PDE is the conservation of traffic “mass” and the second tries to emulate the fluid momentum equation.

The anticipation term is similar to the pressure term in fluids. In some specific models the term is taken as

$$A(\rho) = c_0^2 \rho \tag{3.15}$$

for some constant  $c_0$ . The relaxation term is there so that in equilibrium the speed follows the value  $V(\rho)$ . This could be chosen to be given by Greenshields formula or some other chosen formula. If we ignore the viscosity and use equation 3.15 then we get the PW model similar to isothermal flow as

$$\begin{aligned} \rho_t + (\rho v)_x &= 0 \\ v_t + v v_x &= \frac{V(\rho) - v}{\tau} - \frac{(c_0^2 \rho)_x}{\rho} \end{aligned} \quad (3.16)$$

Equation (3.14) can be written in a conservation form by using the conservation of mass in the second equation to obtain

$$\begin{aligned} \rho_t + (\rho v)_x &= 0 \\ (\rho v)_t + (\rho v^2 + c_0^2 \rho)_x &= \rho \frac{V(\rho) - v}{\tau} + \mu v_{xx} \end{aligned} \quad (3.17)$$

In the vector form this model becomes

$$u_t + f(u)_x = S \quad (3.18)$$

where

$$u = \begin{pmatrix} \rho \\ \rho v \end{pmatrix}, f(u) = \begin{pmatrix} \rho v \\ v^2 + c_0^2 \rho \end{pmatrix} \text{ and } S = \begin{pmatrix} 0 \\ \rho \frac{V(\rho) - v}{\tau} + \mu v_{xx} \end{pmatrix} \quad (3.19)$$

We can write this in quasi-linear form as (see [53])

$$u_t + A(u)u_x = S \quad (3.20)$$

where

$$A(u) = \frac{\partial f}{\partial u} = \begin{pmatrix} 0 & 1 \\ c_0^2 - v^2 & 2v \end{pmatrix} \quad (3.21)$$

The two eigenvalues of this matrix are

$$\lambda_1 = v + c_0 \text{ and } \lambda_2 = v - c_0 \quad (3.22)$$

The corresponding eigenvectors are

$$v_1 = \begin{pmatrix} 1 \\ v + c_0 \end{pmatrix} \text{ and } v_2 = \begin{pmatrix} 1 \\ v - c_0 \end{pmatrix} \quad (3.23)$$

There has been some criticism of PW model, since it mimics the fluid behavior too closely especially the fact that it shows isotropic behavior, whereas the traffic behavior should be anisotropic. Isotropic models like the fluid models show that disturbances can travel in all directions the same way. However, for vehicular traffic that is moving forward the driver behavior should be affected by what happens in the front and not in the back. This deficiency has been overcome by other models, such as the AR and Zhang models presented next.

### 3.2.1 Characteristic Variables

Using the eigenvectors from the quasilinear form the system of PDEs can be diagonalized if the system is strictly hyperbolic, so that the system of PDEs transforms into two scalar PDEs. To perform these steps, we start with the quasilinear form where any source terms have been ignored. The analysis on characteristic variables for various macroscopic traffic models is adapted from [53].

$$u_t + A(u)u_x = 0 \quad (3.24)$$

Let  $\lambda_1$  and  $\lambda_2$  be two distinct real eigenvalues and  $v_1$  and  $v_2$  be their corresponding *independent right* eigenvectors. Construct a square matrix whose columns are these eigenvectors (see any linear algebra textbook such as [79] and [43]).

$$X_R = [v_1 | v_2] \quad (3.25)$$

From linear algebra  $X_R X_R^{-1} = I$  and also  $X_R^{-1} A X_R = \Gamma$ , where  $\Gamma$  is the diagonal matrix consisting of the eigenvalues as the diagonal terms. Pre-multiplying equation (3.24) with  $X_R^{-1}$  and using  $X_R X_R^{-1} = I$ , we obtain

$$X_R^{-1} u_t + \Gamma X_R^{-1} u_x = 0 \quad (3.26)$$

Now, if we define

$$R_t = X^{-1} u_t \text{ and } R_x = X^{-1} u_x, \quad (3.27)$$

we can write the quasilinear system 3.24 as

$$R_t + \Gamma R_x = 0 \quad (3.28)$$

The characteristic variables  $r_1$  and  $r_2$  are constant along the characteristics  $dx/dt = \lambda_1, \lambda_2$  respectively, where

$$R = \begin{pmatrix} r_1 \\ r_2 \end{pmatrix} \quad (3.29)$$

### 3.2.2 Characteristic Variables for Payne-Whitham Model

For the Payne-Whitham model from equations (3.23) and (3.22) we get

$$X_R = \begin{pmatrix} 1 & 1 \\ v + c_0 & v - c_0 \end{pmatrix} \quad (3.30)$$

and

$$\Gamma = \begin{pmatrix} v + c_0 & 0 \\ 0 & v - c_0 \end{pmatrix} \quad (3.31)$$

For equation (3.27) here we obtain

$$R_t = \begin{pmatrix} \frac{\rho}{2c_0}(v_t + c_0(\ln \rho)_t) \\ -\frac{\rho}{2c_0}(v_t - c_0(\ln \rho)_t) \end{pmatrix} \quad (3.32)$$

Similarly,

$$R_x = \begin{pmatrix} \frac{\rho}{2c_0}(v_x + c_0(\ln \rho)_x) \\ -\frac{\rho}{2c_0}(v_x - c_0(\ln \rho)_x) \end{pmatrix} \quad (3.33)$$

We can define a matrix  $M$  such that  $R_t = M\bar{R}_t$ . Consequently,  $R_x = M\bar{R}_x$ . Then

$$M = \frac{\rho}{2c_0} \begin{pmatrix} 1 & 0 \\ 0 & -1 \end{pmatrix} \quad (3.34)$$

and

$$\bar{R} = \begin{pmatrix} v_t + c_0 \ln \rho \\ v_t - c_0 \ln \rho \end{pmatrix} \quad (3.35)$$

Now, equation (3.28) becomes

$$M(\bar{R}_t + \Gamma\bar{R}_x) = 0 \quad (3.36)$$

When  $\rho \neq 0$   $M$  is invertible and so we can solve

$$\bar{R}_t + \Gamma \bar{R}_x = 0 \quad (3.37)$$

Using notation

$$\bar{R} = \begin{pmatrix} \bar{r}_1 \\ \bar{r}_2 \end{pmatrix} \quad (3.38)$$

we can obtain the following by inverting equation 3.35.

$$\begin{pmatrix} v \\ \rho \end{pmatrix} = \begin{pmatrix} \frac{1}{2}(\bar{r}_1 + \bar{r}_2) \\ \exp\left(\frac{\bar{r}_1 - \bar{r}_2}{2c_0}\right) \end{pmatrix} \quad (3.39)$$

### 3.3 Aw-Rascle Model

A new model in [4] and improved in [68] is designed to model the anisotropic traffic behavior. The following is the Aw-Rascle or AR model where we have added the relaxation term.

$$\begin{aligned} \rho_t + (\rho v)_x &= 0 \\ [v + p(\rho)]_t + v [(v + p(\rho))]_x &= \frac{V(\rho) - v}{\tau} \end{aligned} \quad (3.40)$$

where  $V(\rho)$  is the equilibrium speed generally taken as Greenshields relationship. The pressure term is usually taken as

$$p(\rho) = c_0^2 \rho^\gamma \quad (3.41)$$

where  $\gamma > 0$  and  $c_0 = 1$ .

For further analysis, we will ignore the relaxation term. For smooth solutions system (3.40) is equivalent to the following system that is obtained by multiplying the first equation by  $p'(\rho)$  in (3.40) and then adding that to the second equation. That operation leads to the model in the following form.

$$\begin{aligned}\rho_t + (\rho v)_x &= 0 \\ v_t + [v - \rho p'(\rho)] v_x &= 0\end{aligned}\tag{3.42}$$

The AR model in conservation form is given below.

$$\begin{aligned}\rho_t + (\rho v)_x &= 0 \\ [\rho(v + p(\rho))]_t + [\rho v(v + p(\rho))]_x &= 0\end{aligned}\tag{3.43}$$

Now, we define a new variable  $m = \rho(v + p(\rho))$ , so that the model can be written as

$$\begin{aligned}\rho_t + (m - \rho p)_x &= 0 \\ m_t + \left[ \frac{m^2}{\rho} - mp \right]_x &= 0\end{aligned}\tag{3.44}$$

In the vector form this model becomes

$$u_t + f(u)_x = 0\tag{3.45}$$

where

$$u = \begin{pmatrix} \rho \\ m \end{pmatrix}, \text{ and } f(u) = \begin{pmatrix} m - \rho p \\ \frac{m^2}{\rho} - mp \end{pmatrix}\tag{3.46}$$

We can write this vector form in the quasi-linear form and obtain the eigenvalues and eigenvectors for the system. The quasilinear form is

$$u_t + A(u)u_x = 0 \quad (3.47)$$

where

$$A(u) = \frac{\partial f}{\partial u} = \begin{pmatrix} -(\gamma + 1)p & 1 \\ -\frac{m^2}{\rho^2} - \frac{\gamma pm}{\rho} & \frac{2m}{\rho} - p \end{pmatrix} \quad (3.48)$$

The two eigenvalues of this matrix are

$$\lambda_1 = v \text{ and } \lambda_2 = v - \gamma p \quad (3.49)$$

The corresponding eigenvectors are

$$v_1 = \begin{pmatrix} 1 \\ v + (\gamma + 1)p \end{pmatrix} \text{ and } v_2 = \begin{pmatrix} 1 \\ v + p \end{pmatrix} \quad (3.50)$$

### 3.3.1 Characteristic Variables for Aw-Rascle Model

For the Aw-Rascle model we get

$$X_R = \begin{pmatrix} 1 & 1 \\ v + (\gamma + 1)p & v + p \end{pmatrix} \quad (3.51)$$

and

$$\Gamma = \begin{pmatrix} v & 0 \\ 0 & v - \gamma p \end{pmatrix} \quad (3.52)$$

For equation 3.27 here we obtain

$$R_t = \begin{pmatrix} \frac{\rho}{\gamma p}(v_t + p_t) \\ -\frac{\rho}{\gamma p}v_t \end{pmatrix} \quad (3.53)$$

Similarly,

$$R_x = \begin{pmatrix} \frac{\rho}{\gamma p}(v_x + p_x) \\ -\frac{\rho}{\gamma p}v_x \end{pmatrix} \quad (3.54)$$

We can define matrix  $M$  such that  $R_t = M\bar{R}_t$ . Consequently,  $R_x = M\bar{R}_x$ . Then

$$M = \frac{\rho}{\gamma p} \begin{pmatrix} 1 & 0 \\ 0 & -1 \end{pmatrix} \quad (3.55)$$

and

$$\bar{R} = \begin{pmatrix} v + p \\ v \end{pmatrix} \quad (3.56)$$

Now, equation 3.28 becomes

$$M(\bar{R}_t + \Gamma\bar{R}_x) = 0 \quad (3.57)$$

When  $\frac{\rho}{\gamma p} \neq 0$   $M$  is invertible and so we can solve

$$\bar{R}_t + \Gamma\bar{R}_x = 0 \quad (3.58)$$

Using notation

$$\bar{R} = \begin{pmatrix} \bar{r}_1 \\ \bar{r}_2 \end{pmatrix} \quad (3.59)$$

we can obtain the following by inverting equation 3.56.

$$\begin{pmatrix} v \\ \rho \end{pmatrix} = \begin{pmatrix} \bar{r}_2 \\ (\bar{r}_1 - \bar{r}_2)^{1/\gamma} \end{pmatrix} \quad (3.60)$$

### 3.4 Zhang Model

We present here another model [92], [93] that retains the anisotropic traffic property, because its momentum equation is derived from a microscopic *car-following* model. The Zhang model is given by the following set of PDEs.

$$\begin{aligned} \rho_t + (\rho v)_x &= 0 \\ v_t + [v + \rho V'(\rho)] v_x &= \frac{V(\rho) - v}{\tau} \end{aligned} \quad (3.61)$$

Ignoring the relaxation term, the conservation form of this model becomes

$$\begin{aligned} \rho_t + (\rho v)_x &= 0 \\ [\rho(v - V(\rho))]_t + [\rho v(v - V(\rho))]_x &= 0 \end{aligned} \quad (3.62)$$

Now, we define a new variable  $m = \rho(v - V(\rho))$ , so that the model can be written as

$$\begin{aligned} \rho_t + (m - \rho P)_x &= 0 \\ m_t + \left[ \frac{m^2}{\rho} - mP \right]_x &= 0 \end{aligned} \quad (3.63)$$

In the vector form this model becomes

$$u_t + f(u)_x = 0 \quad (3.64)$$

where

$$u = \begin{pmatrix} \rho \\ m \end{pmatrix}, \text{ and } f(u) = \begin{pmatrix} m + \rho V(\rho) \\ \frac{m^2}{\rho} + mV(\rho) \end{pmatrix} \quad (3.65)$$

We can write this vector form in the quasi-linear form and obtain the eigenvalues and eigenvectors for the system. The quasilinear form is

$$u_t + A(u)u_x = 0 \quad (3.66)$$

where

$$A(u) = \frac{\partial f}{\partial u} = \begin{pmatrix} \rho V'(\rho) + V(\rho) & 1 \\ -\frac{m^2}{\rho^2} + mV'(\rho) & \frac{2m}{\rho} + V(\rho) \end{pmatrix} \quad (3.67)$$

The two eigenvalues of this matrix are

$$\lambda_1 = v \text{ and } \lambda_2 = v + \rho V'(\rho) \quad (3.68)$$

The corresponding eigenvectors are

$$v_1 = \begin{pmatrix} 1 \\ v - V(\rho) - \rho V'(\rho) \end{pmatrix} \text{ and } v_2 = \begin{pmatrix} 1 \\ v - V(\rho) \end{pmatrix} \quad (3.69)$$

### 3.4.1 Characteristic Variables for Zhang Model

For the Zhang model we get

$$X_R = \begin{pmatrix} 1 & 1 \\ v - V(\rho) - \rho V'(\rho) & v - V(\rho) \end{pmatrix} \quad (3.70)$$

and

$$\Gamma = \begin{pmatrix} v & 0 \\ 0 & v + \rho V'(\rho) \end{pmatrix} \quad (3.71)$$

For equation (3.27) here we obtain

$$R_t = \begin{pmatrix} \frac{-1}{V'(\rho)} \left( \frac{m}{\rho} \right)_t \\ \frac{1}{V'(\rho)} \left( \frac{m}{\rho} + V(\rho) \right)_t \end{pmatrix} \quad (3.72)$$

Similarly,

$$R_x = \begin{pmatrix} \frac{-1}{V'(\rho)} \left( \frac{m}{\rho} \right)_x \\ \frac{1}{V'(\rho)} \left( \frac{m}{\rho} + V(\rho) \right)_x \end{pmatrix} \quad (3.73)$$

We can define matrix  $M$  such that  $R_t = M\bar{R}_t$ . Consequently,  $R_x = M\bar{R}_x$ . Then

$$M = \frac{1}{V'(\rho)} \begin{pmatrix} -1 & 0 \\ 0 & 1 \end{pmatrix} \quad (3.74)$$

and

$$\bar{R} = \begin{pmatrix} \frac{m}{\rho} \\ \frac{m}{\rho} + V(\rho) \end{pmatrix} \quad (3.75)$$

Now, equation (3.28) becomes

$$M(\bar{R}_t + \Gamma \bar{R}_x) = 0 \quad (3.76)$$

When  $\rho \neq 0$   $M$  is invertible and so we can solve

$$\bar{R}_t + \Gamma \bar{R}_x = 0 \quad (3.77)$$

Using notation

$$\bar{R} = \begin{pmatrix} \bar{r}_1 \\ \bar{r}_2 \end{pmatrix} \quad (3.78)$$

we can obtain the following by inverting equation 3.75.

$$\begin{pmatrix} V(\rho) \\ m \end{pmatrix} = \begin{pmatrix} \bar{r}_2 - \bar{r}_1 \\ \rho \bar{r}_1 \end{pmatrix} \quad (3.79)$$

### 3.5 Pedestrian and Control Models in One Dimension

There is one major difference between vehicular traffic and pedestrian traffic. In vehicular traffic if we use the LWR model, traffic density fixes the value of traffic speed. However, in pedestrian flow, just knowing the traffic density does not fix the pedestrian speed. The actual speed depends on the function that the pedestrians are performing. For example, if pedestrians are inside a museum or in a school their movement is dependent on the activity that is taking place. If however, the pedestrians are all trying to exit from a corridor, then their speed becomes a function of density just like the vehicular traffic. Notice that even in a single corridor, people could be moving in both directions at different places, but vehicular traffic on a highway or street lane is unidirectional. The models (such as Greenshields) only have to provide the speed based on density, since the direction of travel

is fixed. If we introduce a time-varying scalar field that abstracts the activity that is taking place for pedestrians we can modify the vehicular traffic model to get pedestrian models. For distributed traffic control problems, this field will be used as the control variable.

### 3.5.1 LWR Pedestrian Model with Greenshields Flow

In order to convert the LWR model with Greenshields flow into a pedestrian model, we can make the free-flow speed to be the scalar control field. This is a very natural choice, since if we consider the case when there is only a single pedestrian, then according to Greenshields model, the speed would be the constant free-flow speed. A pedestrian could be going in the positive or negative direction and the magnitude would be in the closed interval  $[0, v_m]$  where  $v_m$  is a constant maximum possible speed. The model then becomes

$$\frac{\partial}{\partial t}\rho + \frac{\partial}{\partial x}v_f(t, x)\rho\left(1 - \frac{\rho}{\rho_m}\right) = 0 \quad (3.80)$$

where  $v_f(t, x) \in [-v_m, v_m]$ .

### 3.5.2 Payne-Whitham Pedestrian Model with Greenshields Flow

We can convert the Payne Whitham model by making the  $V(\rho)$  term change with time and space. We can use Greenshields relationship combined with this to produce the time-dependent scalar field. The model then becomes

$$v_t + v v_x = \frac{V(t, x, \rho) - v}{\tau} - \frac{\rho_t + (\rho v)_x}{\rho} + \mu \frac{v_{xx}}{\rho} \quad (3.81)$$

where

$$V(t, x, \rho) = v_f(t, x)\rho\left(1 - \frac{\rho}{\rho_m}\right) \quad (3.82)$$

The control scalar field for the movement becomes  $v_f(t, x)$ .

### 3.5.3 Aw-Rascle Pedestrian Model with Greenshields Flow

The Aw-Rascle model with the relaxation term can be used for controlled traffic. The model with the control term is presented below.

$$\begin{aligned} \rho_t + (\rho v)_x &= 0 \\ [v + p(\rho)]_t + v [(v + p(\rho))]_x &= \frac{V(t, x, \rho) - v}{\tau} \end{aligned} \quad (3.83)$$

The control variable is the equilibrium velocity term, which combined with Greenshields model can be taken as

$$V(t, x, \rho) = v_f(t, x)\rho\left(1 - \frac{\rho}{\rho_m}\right) \quad (3.84)$$

### 3.5.4 Zhang Pedestrian Model with Greenshields Flow

Zhang model with the relaxation term can be also used similarly for controlled traffic. The model with the control term is presented below.

$$\begin{aligned} \rho_t + (\rho v)_x &= 0 \\ v_t + [v + \rho V'(\rho)] v_x &= \frac{V(\rho) - v}{\tau} \end{aligned} \quad (3.85)$$

The control variable is the equilibrium velocity term, which combined with Greenshields model can be taken as

$$V(t, x, \rho) = v_f(t, x) \rho \left( 1 - \frac{\rho}{\rho_m} \right) \quad (3.86)$$

# Chapter 4

## Traffic Models: Two-Dimensional Case

In this chapter we develop two dimensional versions of model we considered in chapter 4. The main addition in the models for two dimensional versions is a *desired* velocity vector field that makes the actual velocity to follow some movement profile. We propose two-dimensional extensions of the traffic models that can be used for pedestrian traffic modeling. Autonomous two-dimensional bi-directional traffic models have been proposed in [2]. Controls that require implementation in patches and sensors that make average measurements in patches are presented in [1]. Lyapunov based controllers for traffic are presented in [88], [88] and [86]. Apart from these, the author has not found literature in macroscopic traffic models in two dimensions.

### 4.1 Two-Dimensional LWR Model

Consider Figure 4.1 for the case of two dimensional traffic flow. We can take any of the fundamental relationships between traffic density and speed. For the sake of illustration

we choose the Greenshields model. Unlike the one-dimensional case however, we have an additional scalar field  $\theta(t, x, y)$  that has to be provided to dictate where people will move to. Moreover, even the free-flow speed will also be another scalar field,  $v_f(t, x, y)$ . This enables the modeling of pedestrians performing different tasks, such as being in a school, in an art gallery etc. The model with these fields included is provided below.

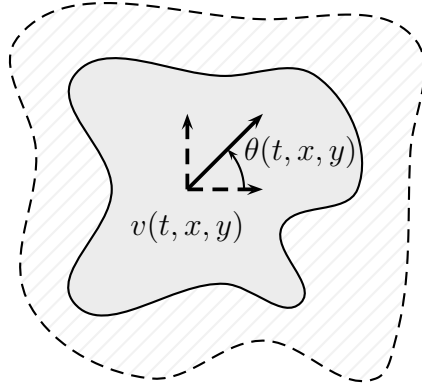


Figure 4.1: Pedestrian Traffic in 2D

$$\frac{\partial}{\partial t}\rho + \frac{\partial}{\partial x}v_f \cos \theta \left(1 - \frac{\rho}{\rho_m}\right)\rho + \frac{\partial}{\partial y}v_f \sin \theta \left(1 - \frac{\rho}{\rho_m}\right)\rho = 0 \quad (4.1)$$

Alternately, we can write this model in the divergence form

$$\frac{\partial}{\partial t}\rho(t, x, y) + \nabla \cdot q(t, x, y) = 0 \quad (4.2)$$

where

$$q = v_f \left(1 - \frac{\rho}{\rho_m}\right) \rho \begin{pmatrix} \cos \theta \\ \sin \theta \end{pmatrix} \quad (4.3)$$

### 4.1.1 Eigenvalues

In this scalar model, we obtain the two eigenvalues by writing the model in quasi-linear form as follows.

$$\frac{\partial}{\partial t}\rho + \frac{\partial[v_f \cos \theta(1 - \frac{\rho}{\rho_m})\rho]}{\partial x}\rho_x + \frac{\partial[v_f \sin \theta(1 - \frac{\rho}{\rho_m})\rho]}{\partial y}\rho_y = 0 \quad (4.4)$$

Therefore, the eigenvalues are

$$\lambda_1 = \frac{\partial[v_f \cos \theta(1 - \frac{\rho}{\rho_m})\rho]}{\partial x} = v_f \cos \theta \left(1 - \frac{2\rho}{\rho_m}\right) \quad (4.5)$$

and

$$\lambda_2 = \frac{\partial[v_f \sin \theta(1 - \frac{\rho}{\rho_m})\rho]}{\partial y} = v_f \sin \theta \left(1 - \frac{2\rho}{\rho_m}\right) \quad (4.6)$$

## 4.2 Two-Dimensional Payne-Whitham Model

A viscous two-dimensional version of the Payne-Whitham model suitable for pedestrian modeling is proposed below. We use  $v$  for the  $x$ -component and  $w$  for the  $y$ -component of velocity. We use the full derivative of velocity in two dimensions and also modify the relaxation and the viscosity term. The anticipation term remains the same as it represents traffic pressure which is isotropic. The modified model is shown in equation (4.7).

$$\begin{aligned} \rho_t + (\rho v)_x + (\rho w)_y &= 0 \\ v_t + vv_x + vv_y &= \frac{V_1(t, x, y, \rho) - v}{\tau} - \frac{(A(\rho))_x}{\rho} + \mu \left( \frac{v_{xx}}{\rho} + \frac{v_{yy}}{\rho} \right) \\ w_t + ww_x + ww_y &= \frac{V_2(t, x, y, \rho) - w}{\tau} - \frac{(A(\rho))_y}{\rho} + \mu \left( \frac{w_{xx}}{\rho} + \frac{w_{yy}}{\rho} \right) \end{aligned} \quad (4.7)$$

In this model, we have

$$V_1(t, x, y, \rho) = v_f \cos \theta \left(1 - \frac{\rho}{\rho_m}\right) \quad (4.8)$$

and

$$V_2(t, x, y, \rho) = v_f \sin \theta \left(1 - \frac{\rho}{\rho_m}\right) \quad (4.9)$$

Generally we take

$$A(\rho) = c_0^2 \rho \quad (4.10)$$

In conservation form this model becomes

$$\begin{aligned} \rho_t + (\rho v)_x + (\rho w)_y &= 0 \\ (\rho v)_t + (\rho v^2 + c_0^2)_x + (\rho v w)_y &= \rho \frac{V_1(\rho) - v}{\tau} + \mu v_{xx} + \mu v_{yy} \\ (\rho w)_t + (\rho w v)_x + (\rho w^2 + c_0^2)_y &= \rho \frac{V_2(\rho) - v}{\tau} + \mu w_{xx} + \mu w_{yy} \end{aligned} \quad (4.11)$$

### 4.2.1 Eigenvalues and Eigenvectors

To obtain the eigenvalues and eigenvectors we write the model in the vector form

$$u_t + f_1(u)_x + f_2(u)_y = R + V \quad (4.12)$$

where

$$u = \begin{bmatrix} \rho \\ \rho v \\ \rho w \end{bmatrix}, f_1(u) = \begin{bmatrix} \rho v \\ \rho v^2 + c_0^2 \rho \\ \rho w v \end{bmatrix} \text{ and } f_2(u) = \begin{bmatrix} \rho w \\ w v \\ \rho v^2 + c_0^2 \end{bmatrix} \quad (4.13)$$

We can write equation 4.12 in quasilinear form to get

$$u_t + A(u)u_x + B(u)u_y = R + V \quad (4.14)$$

where

$$A(u) = \frac{\partial f_1}{\partial u} = \begin{bmatrix} 0 & 1 & 0 \\ c_0^2 - v^2 & 2v & 0 \\ -vw & w & v \end{bmatrix} \text{ and } B(u) = \frac{\partial f_2}{\partial u} = \begin{bmatrix} 0 & 0 & 1 \\ -vw & w & v \\ c_0^2 - w^2 & 0 & 2w \end{bmatrix} \quad (4.15)$$

The eigenvalues for matrix  $f_1$  are

$$\lambda_1(f_1) = v - c_0, \lambda_2(f_1) = v \text{ and } \lambda_3(f_1) = v + c_0 \quad (4.16)$$

The corresponding eigenvectors are

$$e_1(f_1) = \begin{bmatrix} 1 \\ v - c_0 \\ w \end{bmatrix}, e_2(f_1) = \begin{bmatrix} 0 \\ 0 \\ 1 \end{bmatrix} \text{ and } e_3(f_1) = \begin{bmatrix} 1 \\ v + c_0 \\ w \end{bmatrix} \quad (4.17)$$

The eigenvalues for matrix  $f_2$  are

$$\lambda_1(f_2) = w - c_0, \lambda_2(f_2) = w \text{ and } \lambda_3(f_2) = w + c_0 \quad (4.18)$$

The corresponding eigenvectors are

$$e_1(f_2) = \begin{bmatrix} 1 \\ v \\ w - c_0 \end{bmatrix}, e_2(f_2) = \begin{bmatrix} 0 \\ 1 \\ 0 \end{bmatrix} \text{ and } e_3(f_2) = \begin{bmatrix} 1 \\ v \\ w + c_0 \end{bmatrix} \quad (4.19)$$

## 4.2.2 Eigenvalues and Eigenvectors in an Arbitrary Direction

As shown in [46], we consider initial data given of the following form.

$$u(0, x, y) = \psi(\vec{n} \cdot \vec{x}) = \psi(n^x x + n^y y) \quad (4.20)$$

This is illustrated in Figure 4.2.

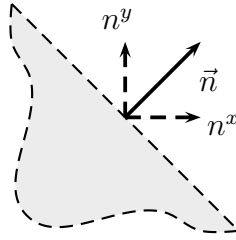


Figure 4.2: Propagation in an Arbitrary Direction

In the direction perpendicular to  $\vec{n}$  since the datum is constant no change will take place, and therefore, the solution will be a plane wave with speed  $s$ . The solution can be written as

$$u(t, x, y) = \bar{u}(\vec{n} \cdot \vec{x} - st) \quad (4.21)$$

Ignoring the relaxation and viscosity term in equation (4.12), we get

$$u_t + A(u)u_x + B(u)u_y = 0 \quad (4.22)$$

Now, by substituting the plane wave equation (4.21) in equation (4.22), we get

$$(\bar{A} - sI) \bar{u}'(\vec{n} \cdot \vec{x} - st) = 0 \quad (4.23)$$

where

$$\bar{A} = n^x A + n^y B \quad (4.24)$$

For strict hyperbolicity, this matrix should have real and distinct eigenvalues for arbitrary  $\vec{n}$ .

The eigenvalues for matrix  $\bar{A}$  are

$$\lambda_1(\bar{A}) = \vec{n} \cdot \vec{v} - c_0, \lambda_2(\bar{A}) = \vec{n} \cdot \vec{v} \text{ and } \lambda_3(\bar{A}) = \vec{n} \cdot \vec{v} + c_0 \quad (4.25)$$

where  $\vec{v} = [v \ w]'$ . The corresponding eigenvectors are

$$e_1(\bar{A}) = \begin{bmatrix} 1 \\ v - n^x c_0 \\ w - n^y c_0 \end{bmatrix}, e_2(\bar{A}) = \begin{bmatrix} 0 \\ -n^y \\ n^x \end{bmatrix} \text{ and } e_3(\bar{A}) = \begin{bmatrix} 1 \\ v + n^x c_0 \\ w + n^y c_0 \end{bmatrix} \quad (4.26)$$

### 4.3 Two-Dimensional Aw-Rascle Model

A two-dimensional version of the Aw-Rascle model with relaxation terms suitable for pedestrian modeling is proposed below. We modify the relaxation terms so that  $v_f(t, x, y)$  and  $\theta(t, x, y)$  scalar fields can enter the dynamics to affect the pedestrian movement. The modified model is shown in equation (4.27).

$$\begin{aligned}
\rho_t + (\rho v)_x + (\rho w)_y &= 0 \\
[v + p(\rho)]_t + v [v + p(\rho)]_x + w [(v + p(\rho))]_y &= \frac{V_1(t, x, y, \rho) - v}{\tau} \\
[w + p(\rho)]_t + v [(w + p(\rho))]_x + w [(w + p(\rho))]_y &= \frac{V_2(t, x, y, \rho) - w}{\tau}
\end{aligned} \tag{4.27}$$

where

$$V_1(t, x, y, \rho) = v_f \cos \theta \left(1 - \frac{\rho}{\rho_m}\right) \tag{4.28}$$

and

$$V_2(t, x, y, \rho) = v_f \sin \theta \left(1 - \frac{\rho}{\rho_m}\right) \tag{4.29}$$

## 4.4 Two-Dimensional Zhang Model

A two-dimensional version of the Zhang model suitable for pedestrian modeling is proposed below. We modify the  $V(\rho)$  term so that  $v_f(t, x, y)$  and  $\theta(t, x, y)$  scalar fields can enter the dynamics to affect the pedestrian movement. The modified model is shown in equation (4.30).

$$\begin{aligned}
\rho_t + (\rho v)_x + (\rho w)_y &= 0 \\
v_t + [v + \rho V_1'(\rho)] v_x + [v + \rho V_1'(\rho)] v_y &= \frac{V_1(t, x, y, \rho) - v}{\tau} \\
w_t + [w + \rho V_2'(\rho)] w_x + [w + \rho V_2'(\rho)] w_y &= \frac{V_2(t, x, y, \rho) - w}{\tau}
\end{aligned} \tag{4.30}$$

where

$$V_1(t, x, y, \rho) = v_f \cos\theta \left(1 - \frac{\rho}{\rho_m}\right) \quad (4.31)$$

and

$$V_2(t, x, y, \rho) = v_f \sin\theta \left(1 - \frac{\rho}{\rho_m}\right) \quad (4.32)$$

# Chapter 5

## Conservation Law Solutions

In this chapter we present various notions of solutions of conservation laws, such as classical or strong solutions, as well as distributional and weak solutions. We also review various admissibility conditions for solutions. Finally, we review the notion of solution for scalar initial-boundary value problem.

### 5.1 Method of Characteristics

We can use method of characteristics to solve quasilinear partial differential equations which allows us to convert the PDE into ordinary differential equations. As an example, consider

$$u_t + uu_x = 0 \tag{5.1}$$

If  $u = u(t, x)$  solves (5.1), let  $x = x(t)$  solve ODE

$$\dot{x}(t) = u(t, x(t)) \tag{5.2}$$

Set  $z(t) = u(t, x(t))$ . Then  $\dot{z}(t) = 0$ . Notice that

$$\frac{d}{dt}u(t, x(t)) = u_t + \frac{dx}{dt}u_x \quad (5.3)$$

Using equation (5.3) with equation (5.1) gives

$$\frac{du}{dt} = 0, \quad \frac{dx}{dt} = u \quad (5.4)$$

This shows that we can use the initial data  $u_0(x)$  to propagate the solution in the  $(t, x)$  plane.

In general, if we have

$$u_t + h(t, x, u)u_x = g(t, x, u) \quad (5.5)$$

The characteristics would give us

$$\frac{du}{dt} = g(t, x, u), \quad \frac{dx}{dt} = h(t, x, u) \quad (5.6)$$

As a solution of equation 5.1 consider the initial data given in Figure 5.1.

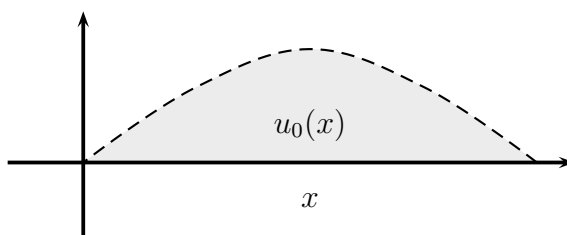


Figure 5.1: Initial Data

As we see in equation(5.4) the slope of the characteristics in the  $(x, t)$ -plane is equal to the

value of  $u$ . This value is transferred on the characteristic line on which this value is constant. The slopes are illustrated in Figure 5.2.

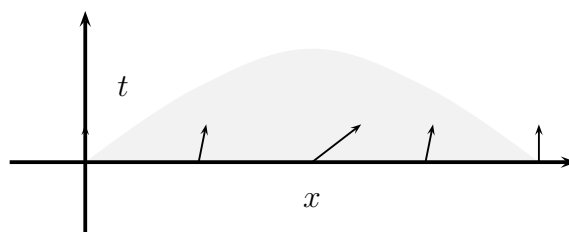


Figure 5.2: Characteristic Slopes

We can find the solution  $u(t, x)$  after some time by following the characteristics, as shown in Figure 5.3

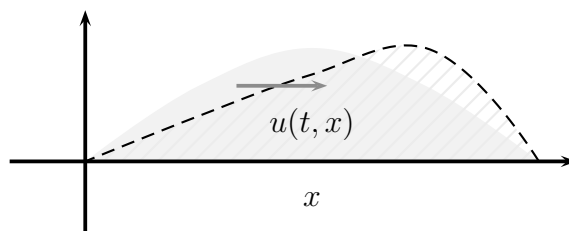


Figure 5.3: Solution after some time

### 5.1.1 Characteristics in Two Dimensions

We can use the method of characteristics to solve quasilinear partial differential equations in two (or more) dimensions as well which allows us to convert the PDE into a set of ordinary differential equations. As an example, consider

$$u_t + f_1(t, x, y)u_x + f_2(t, x, y)u_y = h(t, x, y) \quad (5.7)$$

The left hand side of this equation can be considered a directional derivative as before where in the two dimensional case now

$$\frac{Du(t, x(t), y(t))}{Dt} = u_t + \frac{dx}{dt}u_x + \frac{dy}{dt}u_y \quad (5.8)$$

Using equation (5.8) with equation (5.7) gives

$$\frac{du}{dt} = h(t, x, y), \quad \frac{dx}{dt} = f_1(t, x, y) \quad \text{and} \quad \frac{dy}{dt} = f_2(t, x, y) \quad (5.9)$$

### 5.1.2 Characteristics for a System

Consider the first-order quasilinear system of equations

$$u_t + f(u)_x = 0 \quad (5.10)$$

where  $u : R^+ \times R \rightarrow R^n$  and  $f : R^n \rightarrow R^n$  is smooth.

**Definition 5.1.1.** A curve  $t \mapsto x(t)$  is a characteristic curve for (5.10) whose solution is  $u(t, x)$  if the following matrix is singular.

$$\frac{dx}{dt}I - \nabla f(u(t, x)) \quad (5.11)$$

## 5.2 Classical or Strong Solutions

For a scalar conservation law

$$u_t + f'(u)u_x = 0 \quad (5.12)$$

with initial condition

$$u(x, 0) = u_0(x), \quad (5.13)$$

strong or classical solution is defined below for  $f : R \mapsto R$  smooth and continuous  $u_0(x)$ .

**Definition 5.2.1.** *We say that  $u(t, x) : (R^+ \times R) \mapsto R$  is a classical solution of the Cauchy problem if  $u(t, x) \in C^1(R^+ \times R)$  and (5.12) with (5.13) is satisfied.*

We have the following theorem for strong solutions for the scalar conservation law (5.12) (see [69]).

**Theorem 5.2.1.** *Any  $C^1$  solution of the single conservation law (5.12) for sufficiently smooth flux  $f(u)$  is constant along its characteristics that must satisfy*

$$\frac{dx}{dt} = f'(u(t, x(t))) \quad (5.14)$$

### 5.3 Weak Solutions

In this section we use method of characteristics to see that even for smooth initial conditions the strong solutions cannot be extended in time indefinitely. In fact, even smooth initial conditions can lead to discontinuous solutions in finite time. Therefore, we will need a notion of solutions that is more general than the notion of strong solutions. Let us illustrate this blowup of solutions next.

### 5.3.1 Blowup of Solutions

To see how smooth initial solutions blow up, let us consider the scalar traffic model.

$$\frac{\partial}{\partial t}\rho(t, x) + \frac{\partial}{\partial x}f(\rho) = 0 \quad (5.15)$$

where

$$f(\rho) = v(\rho)\rho \quad (5.16)$$

and

$$v(\rho) = v_f\left(1 - \frac{\rho}{\rho_m}\right) \quad (5.17)$$

In quasilinear form we write equation 5.15 as

$$\frac{\partial}{\partial t}\rho(t, x) + f'(\rho)\frac{\partial}{\partial x}\rho(t, x) = 0 \quad (5.18)$$

Combining equations (5.16) and (5.17), we get

$$f(\rho) = v_f\rho\left(1 - \frac{\rho}{\rho_m}\right) \quad (5.19)$$

From equation (5.19) we obtain the *characteristic speed* by differentiating.

$$f'(\rho) = v_f\left(1 - 2\frac{\rho}{\rho_m}\right) \quad (5.20)$$

The characteristic speed is the value obtained from the slope of the fundamental diagram at the given density as shown in Figure 5.4

Now, let us consider the initial traffic conditions that are shown in Figure 5.5.

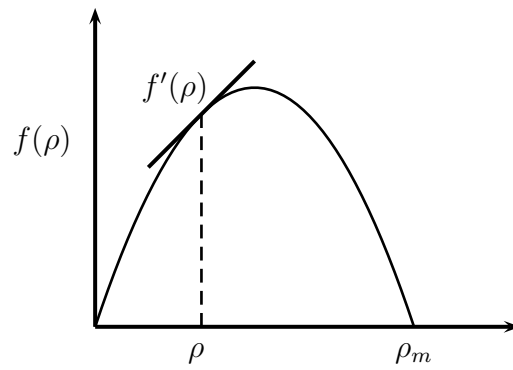


Figure 5.4: Characteristic Speed

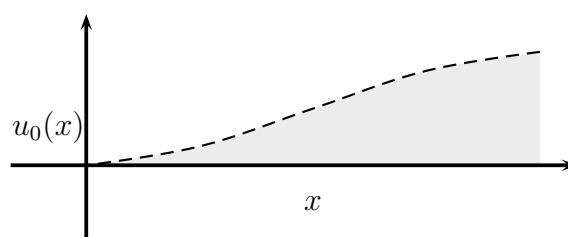


Figure 5.5: Initial Conditions

The characteristics in the  $(t, x)$ -plane starting at initial time are shown in Figure 5.6.

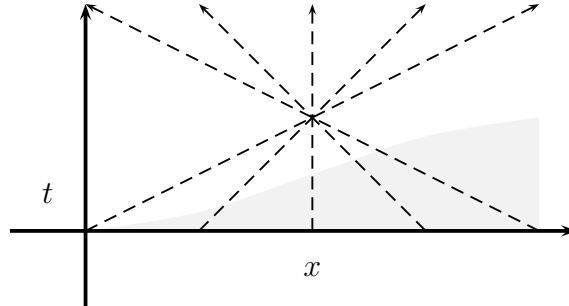


Figure 5.6: Characteristics

We can see that after some finite time the characteristics intersect. That would mean that at a single point  $(t, x)$  there are multiple possible values for  $\rho$ . If we propagate the initial curve, we can see that the traffic density gets a discontinuity as shown in Figure 5.7.

We need to allow solutions that can have discontinuities as shown in Figure 5.7. However the integral form the conservation law should still be satisfied. Hence, we define weak solutions for conservation laws.

### Implicit Solution

Another way to observe singularities in solutions of the conservation law (5.12) is to view the following implicit solution of the conservation law (see [78]). This solution comes from following characteristic back from  $(t, x)$  to a point when  $t = 0$ .

$$u(t, x) = u_0(x - tf'(u(t, x))) \quad (5.21)$$

where  $u(0, x) = u_0(x)$  is the initial smooth data.

Using the implicit function theorem (see [74]) and performing

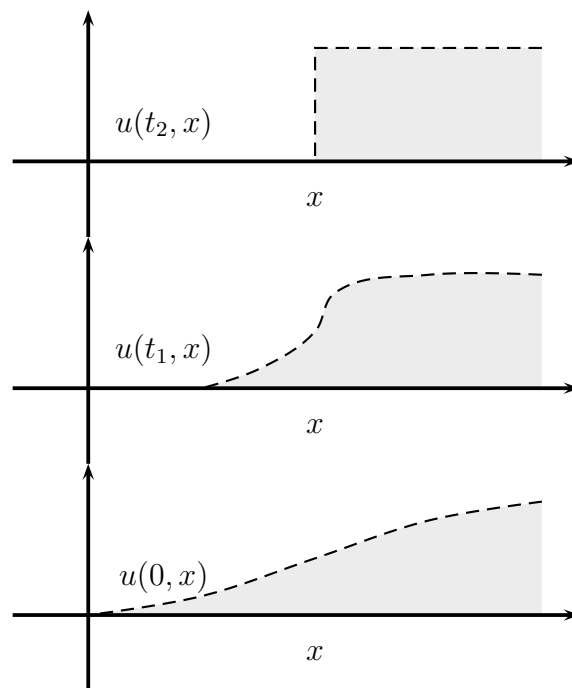


Figure 5.7: Initial Conditions Propagating

$$\frac{D}{Dt}[u(t, x) - u_0(x - tf'(u(t, x)))] = 0 \quad (5.22)$$

we get

$$u_t = -\frac{f'(u)u'_0}{1 + f''(u)u'_0t} \quad (5.23)$$

Performing

$$\frac{D}{Dx}[u(t, x) - u_0(x - tf'(u(t, x)))] = 0 \quad (5.24)$$

we get

$$u_x = \frac{u'_0}{1 + f''(u)u'_0t} \quad (5.25)$$

This shows that if  $u'_0 < 0$  at some point both  $u_t$  and  $u_x$  become unbounded when  $(1 + f''(u)u'_0t) \rightarrow 0$

### 5.3.2 Generalized Solutions

For a conservation law

$$u_t + f(u)_x = 0 \quad (5.26)$$

with initial condition

$$u(x, 0) = u_0(x), \quad (5.27)$$

where  $u_0(x) \in L^1_{loc}(R; R^n)$ , solution in the distributional sense is defined below for smooth vector field  $f : R^n \rightarrow R^n$  (see [10]).

**Definition 5.3.1.** *A measurable locally integrable function  $u(t, x)$  is a solution in the distributional sense of the Cauchy problem ((5.26)) if for every  $\phi \in C_0^\infty(R^+ \times R) \mapsto R^n$*

$$\iint_{R^+ \times R} [u(t, x) \phi_t(t, x) + f(u(t, x)) \phi_x(t, x)] dx dt + \int_R u_0(x) \phi(x, 0) dx = 0 \quad (5.28)$$

### Weak Solutions

A measurable locally integrable function  $u(t, x)$  is a weak solution in the distributional sense of the Cauchy problem ((5.26)) if it is a distributional solution in the open strip  $(0, T) \times \mathbb{R}$ , satisfies the initial condition (5.27) and if  $u$  is continuous as a function from  $[0, T]$  into  $L^1_{loc}$ . We require  $u(t, x) = u(t, x^+)$  and

$$\lim_{t \rightarrow 0} \int_R |u(t, x) - u_0(x)| dx = 0 \quad (5.29)$$

Every weak solution is also a generalized solution but a generalized solution is not necessarily a weak solution. To see this we can take a generalized solution and make the value of the solution zero at initial time (i.e. on a set of measure zero). This would still be a generalized solution to the problem, but would not be a weak solution.

### 5.3.3 Generalized Solution Property

Generalized solutions have a nice convergence property that is stated and proved here (see [10]).

**Lemma 5.3.1.** *If  $u_n$  is a sequence of distributional solutions to the conservation law (5.26), then*

1.  $(u_n \rightarrow u, f(u_n) \rightarrow f(u) \text{ in } L^1_{loc}) \Rightarrow u \text{ is a solution of the conservation law (5.26).}$

2. ( $u_n \rightarrow u$  in  $L^1_{loc}$  and if all  $u_n$  take values in a compact set)  $\Rightarrow u$  is a solution of the conservation law (5.26).

*Proof.* 1. Assume that  $u_n \rightarrow u$ , and  $f(u_n) \rightarrow f(u)$  in  $L^1_{loc}$  and that  $\phi \in C^1_0$  then we estimate

$$\begin{aligned} & \left| \iint_{\Omega} \{u_n \phi_t + f(u_n) \phi_x\} dt dx - \iint_{\Omega} \{u \phi_t + f(u) \phi_x\} dt dx \right| \\ & \leq \iint_{\Omega} \{|u_n - u| |\phi_t| + |f(u_n) - f(u)| |\phi_x|\} dt dx \quad (5.30) \\ & \leq \|u_n - u\|_{supp\phi,1} \|\phi_t\|_{\infty} + \|f(u_n) - f(u)\|_{supp\phi,1} \|\phi_x\|_{\infty} \rightarrow 0, \text{ as } n \rightarrow \infty \end{aligned}$$

2. The second part follows from the first part once we verify that  $f(u_n) \rightarrow f(u)$  in  $L^1_{loc}$  under the assumption that all the functions  $u_n$  take values in a fixed compact subset  $K$  of  $\Omega$ . As  $f$  is a smooth vector field,  $f$  is uniformly bounded on compact subsets. As the values of  $u_n$  stay inside  $K$ , it follows that  $f(u_n)$  is uniformly bounded, say  $\|f(u_n)\| \leq M$ . Then  $\|f(u_n(x)) - f(u(x))\| \leq 2M$  for all  $x$  in the support of  $\phi$  where the constant function  $2M$  is integrable over the support of  $\phi$ .

By dropping down to a subsequence if necessary, from the fact that  $u_n \rightarrow u$  in  $L^1_{loc}$  we can also assume that  $u_n \rightarrow u$  pointwise on the support of  $\phi$  and hence also  $f(u_n) \rightarrow f(u)$  on the support of  $\phi$ . We now can use the *Lebesgue Dominated Convergence Theorem* (see [73] or [20]) to see that  $f(u_n) \rightarrow f(u)$  in  $L^1_{supp\phi}$  (or, more generally, in  $L^1_{loc}$ ) as required.

□

### 5.3.4 Weak Solution Property

There is a very important property that weak solutions possess but general distributional solutions don't. The property is the continuity of the solution with respect to the initial data. For problems with boundary data, similar continuity is required for the data given on

the boundary. Generalized solutions are insensitive to data on a set of measure zero, but weak solutions have the continuity property that does not allow that. To understand the difference let us study a domain that is shown in Figure 5.8(see [10]). The domain is

$$\Omega = \{(t, x); t \in [t_1, t_2], \gamma_1(t) \leq x \leq \gamma_2(t)\} \quad (5.31)$$

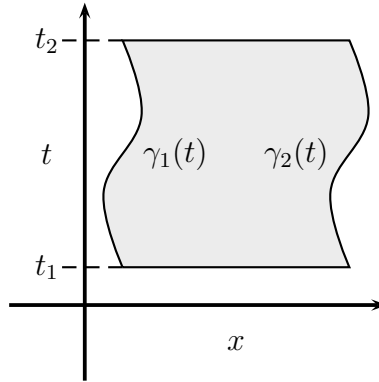


Figure 5.8: Domain to Illustrate Trace Property

A smooth solution, by the application of the *divergence theorem* (see [51]) should satisfy

$$\begin{aligned} 0 = & \iint_{\Omega} (u_t + f(u)_x) dt dx = \int_{\gamma_1(t_2)}^{\gamma_2(t_2)} f(u(t_2, x)) dx - \int_{\gamma_1(t_1)}^{\gamma_2(t_1)} f(u(t_1, x)) dx \\ & + \int_{t_1}^{t_2} [u(t, \gamma_1(t)) + f(u(t_1, \gamma_1(t)))\dot{\gamma}_1(t)] dt - \int_{t_1}^{t_2} [u(t_1, \gamma_2(t)) + f(u(t_1, \gamma_2(t)))\dot{\gamma}_2(t)] dt \end{aligned} \quad (5.32)$$

Arbitrary generalized solutions will not satisfy equation (5.32) because the curves have measure zero and the values of the solution on these curves can be chosen arbitrarily. However, weak solutions will satisfy this equation due to continuity from  $t \mapsto u(t, \cdot)$  when we consider point values satisfying  $u(t, x) = u(t, x^+)$ .

To see this, consider a smooth real-valued non-decreasing function  $\beta : R \rightarrow [0, 1]$ , such that  $\beta(r) = 0$  for  $r \leq 0$  and  $\beta = 1$  for  $r \geq 1$ . A scaled version of this function is  $\beta^\epsilon(r) = \beta(r/\epsilon)$ . We can use this scaled version to define a region surrounding  $\Omega$  where the following function is non-zero and is equal to zero on its boundary.

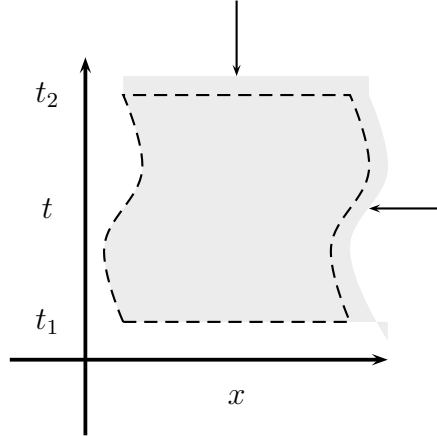


Figure 5.9: Domain with  $\phi$

$$\phi^\epsilon(t, x) = [\beta^\epsilon(x - \gamma_1(t)) - \beta^\epsilon(x - \gamma_2(t))] [\beta^\epsilon(t - t_1) - \beta^\epsilon(t - t_2)] \tag{5.33}$$

We obtain result from equation (5.32) here if we take the limit  $\epsilon \rightarrow 0$  in

$$\int_0^\infty \int_{-\infty}^\infty \{u\phi_t^\epsilon + f(u)\phi_x^\epsilon\} dxdt = 0 \tag{5.34}$$

### 5.3.5 Trace Operator for Functions of Bounded Variation

The conservation law solutions are obtained using the sequential compactness property of functions of bounded variation (BV) shown by Helly’s theorem (see [56] and theorem 5.3.1)

which is also implied by Alaoglu theorem (see [20]). The trace property of BV functions is very useful in fixing initial and boundary conditions for conservation laws.

For a scalar conservation law on  $(0, T) \times \Omega$  where  $\Omega$  is a bounded subset of  $R^n$  with a piecewise regular boundary  $\Gamma$ , we present the following lemma from [11] about the trace operator on BV functions.

**Lemma 5.3.2.** *For  $u \in BV((0, T) \times \Omega)$ , a trace  $\gamma u$  in  $L^\infty$  for  $t = 0$  and in  $L^\infty((0, T) \times \Omega)$  exists which is reached through  $L^1$  convergence. Specifically, there is a bounded operator  $\sigma : BV((0, T) \times \Omega) \rightarrow L^\infty(\Omega)$  such that  $\sigma\phi = \phi(0, \cdot)$  for  $\phi$  smooth on  $L^\infty((0, T) \times \Omega)$ .*

The proof depends on the fact that BV functions have right and left limits and the fact that for  $\Omega$  bounded, a.e. convergence for the dominated sequence implies  $L^1$  convergence (see [3] and [8]). The proof is given in [11].

The relationship between different modes of *dominated* convergence is shown in Figure 5.10. Specifically these relationships are valid when there exists  $g \in L^1$  such that  $|f_n| \leq g$  for all  $n$ .

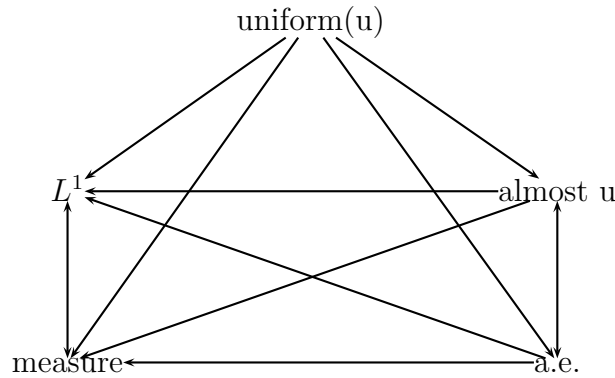


Figure 5.10: Dominated Convergence Relationships

In general, however, the relationships shown in Figure 5.11 are the ones that are valid. Here uniform convergence is shown as  $\text{uniform}(u)$  and almost uniform as  $\text{almost } u$ .

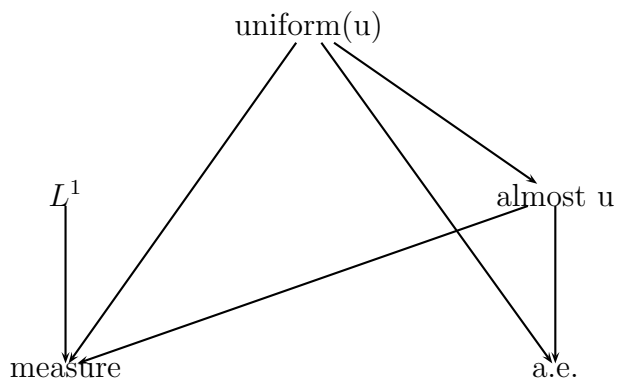


Figure 5.11: General Convergence Relationships

In case of finite measure space, the relationships shown in Figure 5.12 are the ones that are valid.

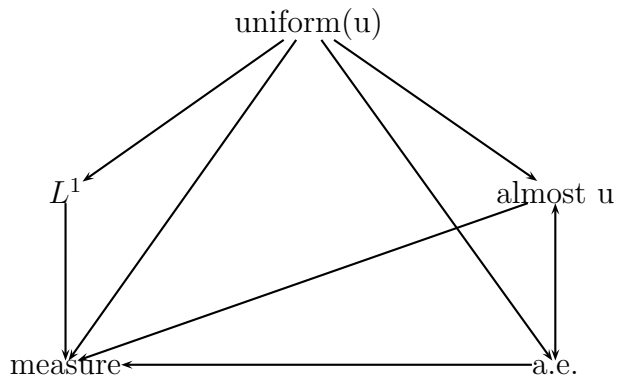


Figure 5.12: Finite Measure Space Convergence Relationships

One very important theorem that we need for convergence deals with the sequential compactness property of sequence of functions of bounded variations ( $BV$ ).

**Theorem 5.3.1. (Helly)** Consider a sequence of functions given by  $f_n : R \rightarrow R^n$  such that

$$\text{Total Variation}\{f_n\} \leq C, \quad |f_n(x)| \leq M \text{ for all } n, x \quad (5.35)$$

for constants  $C, M$ . Then, there exists a function  $f$  and a subsequence  $f_{n_k}$  such that

$$\lim_{n_k \rightarrow \infty} f_{n_k}(x) = f(x) \text{ for every } x \in R \quad (5.36)$$

$$\text{Total Variation}\{f\} \leq C, \quad |f(x)| \leq M \text{ for all } x \quad (5.37)$$

## 5.4 Scalar Riemann Problem

Scalar Riemann problem is the Cauchy problem for the scalar conservation law where the initial data is a piecewise constant function with only two values. In both cases there will be two different values on both sides of  $x = 0$  at time  $t = 0$ . In one case the left hand side value will be lower and in the other it will be higher than the right hand side value.

### 5.4.1 Shock Solution

Let us consider the following scalar Riemann problem for the traffic problem.

$$\frac{\partial}{\partial t} \rho(t, x) + \frac{\partial}{\partial x} v_f \rho \left(1 - \frac{\rho}{\rho_m}\right) = 0 \quad (5.38)$$

with data  $\rho(0, x) = \rho_\ell$  for  $x < 0$  and  $\rho(0, x) = \rho_r$  for  $x \geq 0$ , such that  $\rho_\ell < \rho_r$ . The characteristic speed for  $t = 0$  and  $x < 0$  is

$$\lambda(\rho_\ell) = f'(\rho_\ell) = v_f \left(1 - 2 \frac{\rho_\ell}{\rho_m}\right) \quad (5.39)$$

The characteristic speed for  $t = 0$  and  $x \geq 0$  is

$$\lambda(\rho_r) = f'(\rho_r) = v_f \left(1 - 2 \frac{\rho_r}{\rho_m}\right) \quad (5.40)$$

We see that the characteristic speed on the left is higher than that on the right and therefore the characteristic curves (straight lines) catch up with those on the right. This produces a shock curve with speed  $\lambda$ . This speed is given by *Rankine-Hugoniot* condition (see [78]). The shock wave is shown in Figure 5.13.

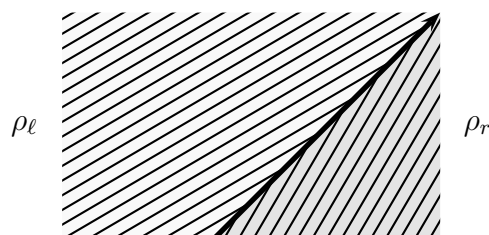


Figure 5.13: Shockwave Solution to Riemann Problem

The speed of the shockwave will satisfy the following Rankine-Hugoniot condition.

$$\lambda(\rho_r - \rho_\ell) = f(\rho_r) - f(\rho_\ell) \quad (5.41)$$

For derivation, consider Figure 5.14.

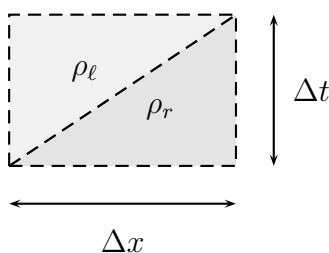


Figure 5.14: Shockwave Speed Derivation

We see that in time  $\Delta t$  the region of length  $\Delta x$  has changed its density completely from  $\rho_r$  to  $\rho_\ell$ . Therefore, the mass conservation principle enforces that the change in mass should be equal to the change through the flux at the boundaries during the same time. Hence

$$\Delta x(\rho_r - \rho_\ell) = \Delta t[f(\rho_r) - f(\rho_\ell)] \quad (5.42)$$

Dividing both sides by  $\Delta t$  and then taking limits produces equation (5.41).

### 5.4.2 Rarefaction Solution

Let us consider the scalar Riemann problem of equation (5.38) with data  $\rho(0, x) = \rho_\ell$  for  $x < 0$  and  $\rho(0, x) = \rho_r$  for  $x \geq 0$ , such that  $\rho_\ell > \rho_r$ .

We see that the characteristic speed on the left is lower than that on the right and this produces a gap in the characteristic lines that needs to be filled with some solution. This condition is shown in Figure 5.15.

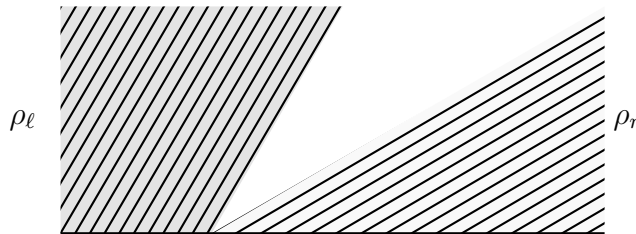


Figure 5.15: Blank Region in  $x - t$  Space

There are many solutions possible that will fill up the gap and also be weak solutions. One possible solution is shown in Figure 5.16. However, we reject this solution since it is not stable to perturbation to initial data. In this rejected solution characteristics come out of

the proposed shock line. In the correct shock solutions, characteristics can only impinge on the shock curve, not emanate from it.

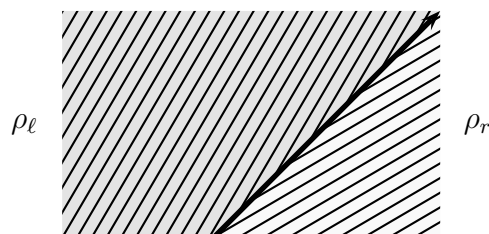


Figure 5.16: Entropy Violating (Rejected) Solution

There are many other solutions possible. We need to pick a solution that is stable. To accomplish this, many admissibility conditions have been proposed such as entropy, viscosity, and Lax condition. The correct solution which will also satisfy these conditions is a symmetry solution shown in Figure 5.17.

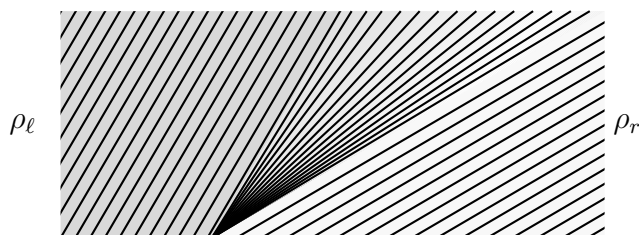


Figure 5.17: Rarefaction Solution

The symmetry rarefaction wave solution is given by

$$\rho(t, x) = \begin{cases} \rho_\ell & \text{if } \frac{x}{t} \leq \lambda(\rho_\ell) \\ \omega\left(\frac{x}{t}\right) & \text{if } \lambda(\rho_\ell) \leq \frac{x}{t} \leq \lambda(\rho_r) \\ \rho_r & \text{if } \frac{x}{t} \geq \lambda(\rho_r) \end{cases} \quad (5.43)$$

where

$$\omega\left(\frac{x}{t}\right) = \frac{\lambda_r - \lambda_\ell}{\rho_r - \rho_\ell}(x/t) \quad (5.44)$$

## 5.5 Admissibility Conditions

There are three admissibility conditions that help choose the physically relevant and stable solution out of the multiple ones possible. These are stated in this section.

### 5.5.1 Vanishing Viscosity Solution

This enables *viscous regularization* of the conservation law of equation (5.26). There is a large body of work related to this technique. For a brief overview of this technique, please see [32]. A weak solution  $u$  of (5.26) is admissible if there exists a sequence of smooth solutions  $u^\epsilon$  to the following viscous conservation law such that  $\lim_{\epsilon \rightarrow 0} \|u^\epsilon - u\|_{L^1_{loc}} = 0$ .

$$u_t^\epsilon + f(u^\epsilon)_x = \epsilon u_{xx}^\epsilon \quad (5.45)$$

### 5.5.2 Entropy Admissible Solution

A weak solution  $u$  of (5.26) is entropy admissible if for all non-negative smooth functions  $\phi$  with compact support

$$\iint [\eta(u)\phi_t + q(u)\phi_x] dx dt \geq 0 \quad (5.46)$$

$\forall(\eta, q)$  where  $\eta$ , an *entropy function* is a convex continuously differentiable function  $\eta : R^n \rightarrow R$  with *entropy flux*, such that<sup>1</sup>

$$D\eta(u) \cdot Df(u) = Dq(u) \quad u \in R^n \quad (5.47)$$

The integral entropy condition (5.46) can be equivalently written in a differential form where the solution is implied in the distributional sense of

$$\eta(u)_t + q(u)_x \leq 0 \quad (5.48)$$

To understand the relationship of the entropy condition with the viscosity solution, consider the scalar conservation law

$$u_t + f(u)_x = 0 \quad (5.49)$$

We have seen that there can be multiple solutions to this PDE. Hence we need to add some constraints such that only one solution remains. One way to do this is to add another variable that should satisfy a conservation law of its own. Let us take the new variable to be  $\eta(u)$  and its corresponding flux to be  $q(u)$ . Hence, the conservation law for this additional variable is (see [33])

$$n_t + q(u)_x = 0 \quad (5.50)$$

Let us assume smooth  $\eta(u)$ ,  $q(u)$  as well as smooth solution to (5.49). Then, multiplying (5.49) with  $\eta'(u)$  gives

$$\eta'(u)u_t + \eta'(u)f(u)_x = 0 \quad (5.51)$$

---

<sup>1</sup>In fact, it suffices to require  $\eta$  and  $q$  to be only Locally Lipschitz such that equation (5.47) is satisfied a.e.

Using the chain rule changes this equation to

$$\frac{\partial \eta(u)}{\partial t} + \eta'(u) f'(u) \frac{\partial u}{\partial x} = 0 \quad (5.52)$$

Comparing this equation with (5.50) we see that the following compatibility condition should be satisfied.

$$\eta'(u) f'(u) = q'(u) \quad (5.53)$$

Now, let us relax our assumption on  $u$  so that we allow piecewise  $C^1$  solution to (5.49) in the weak sense. Now according to the Rankine-Hugoniot condition, the speed of shock wave for  $u$  will be

$$\lambda = \frac{[f(\rho)]}{[\rho(u)]} \quad (5.54)$$

where

$$[f(\rho)] = f(\rho_r) - f(\rho_\ell) \text{ and } [\rho(u)] = \rho_r - \rho_\ell \quad (5.55)$$

The same shock speed must also satisfy

$$\lambda = \frac{[q(\rho)]}{[\eta(u)]} \quad (5.56)$$

Satisfying (5.54) and (5.56) simultaneously is generally too restrictive as is clear from applying this to the Cauchy problem for non-viscous Burger's equation.

$$\begin{aligned} \frac{\partial u}{\partial t} + \frac{\partial}{\partial x} \left( \frac{u^2}{2} \right) &= 0 \\ u(0, x) &= \begin{cases} u_\ell, & x < 0 \\ u_r, & x > 0 \end{cases} \end{aligned} \quad (5.57)$$

We can use the following entropy pair for this problem.

$$\eta(u) = u^k \text{ and } q(u) = \frac{k}{k+1} u^{k+1} \text{ for } k \neq 1 \quad (5.58)$$

Then

$$\lambda = \frac{[f(\rho)]}{[\rho(u)]} = \frac{1}{2} \quad (5.59)$$

However

$$\lambda = \frac{[q(\rho)]}{[\eta(u)]} = \frac{k}{k+1} \quad (5.60)$$

This shows that the entropy equality condition is too restrictive. However, if we use the inequality, then it is just right. To see this, let us consider the viscous perturbation of (5.49)

$$u_t^\epsilon + f(u^\epsilon)_x = \epsilon \Delta u^\epsilon \quad (5.61)$$

Multiplying (5.61) with  $\eta'(u^\epsilon)$  gives

$$\eta'(u^\epsilon)u_t^\epsilon + \eta'(u^\epsilon)f(u^\epsilon)_x = \epsilon \eta'(u^\epsilon)\Delta u^\epsilon \quad (5.62)$$

Using the chain rule changes this equation to

$$\frac{\partial \eta(u^\epsilon)}{\partial t} + \eta'(u^\epsilon) f'(u^\epsilon) \frac{\partial u^\epsilon}{\partial x} = \epsilon \eta'(u^\epsilon) \Delta u^\epsilon \quad (5.63)$$

Using the compatibility condition

$$\eta'(u^\epsilon) f'(u^\epsilon) = q'(u^\epsilon) \quad (5.64)$$

we obtain

$$\frac{\partial \eta(u^\epsilon)}{\partial t} + \frac{\partial q(u^\epsilon)}{\partial x} = \epsilon \Delta \eta(u^\epsilon) - \epsilon \eta''(u^\epsilon) |\nabla u^\epsilon|^2 \quad (5.65)$$

Taking a convex  $\eta$ , we obtain the inequality

$$\frac{\partial \eta(u^\epsilon)}{\partial t} + \frac{\partial q(u^\epsilon)}{\partial x} \leq \epsilon \Delta \eta(u^\epsilon) \quad (5.66)$$

This equation can be viewed as the viscous perturbation of the inequality

$$\frac{\partial \eta(u^\epsilon)}{\partial t} + \frac{\partial q(u^\epsilon)}{\partial x} \leq 0 \quad (5.67)$$

and it can be shown that equation (5.66) converges to (5.67) (see [33]).

### 5.5.3 Lax Admissibility Condition

A weak solution  $u$  of 5.26 is Lax admissible if at every point of approximate discontinuity, the left state  $u_\ell$ , the right state  $u_r$  and the shock speed  $\lambda$  are related as

$$\lambda(u_\ell) \geq \lambda \geq \lambda(u_r) \quad (5.68)$$

## 5.6 Kruzkov's Entropy Function

For a scalar balance law

$$u_t + f(x, t, u)_x = g(x, t, u) \quad (5.69)$$

with initial condition

$$u(x, 0) = u_0(x). \quad (5.70)$$

To obtain entropy enabled generalized solution to the problem (5.69) with (5.70) we can use entropy function proposed by Kruzkov ([41]).

Let  $\Pi_T = R \times [0, T]$ . Let  $u_0(x)$  be a bounded measurable function satisfying  $|u_0(x)| \leq M_0 \forall x \in R$  on  $R$ .

**Definition 5.6.1.** A bounded measurable function  $u(x, t)$  is called a generalized solution of problem (5.69) and (5.70)  $\Pi_T$  if:

i) for any constant  $k$  and any smooth function  $\phi(x, t) \geq 0$  finite in  $\Pi_T$  ( $\text{supp}(\phi) \subset \Pi_T$  strictly), if the following inequality holds,

$$\begin{aligned} & \int \int_{\Pi_T} \{ |u(x, t) - k| \phi_t + \text{sign}(u(x, t) - k) [f(x, t, u(x, t)) - f(x, t, k)] \phi_x - \\ & - \text{sign}(u(x, t) - k) [f_x(x, t, u(x, t)) - g(x, t, u(x, t))] \} dx dt \geq 0 \end{aligned} \quad (5.71)$$

ii) there exists a set  $E$  of zero measure on  $[0, T]$ , such that for  $t \in [0, T] \setminus E$ , the function  $u(x, t)$  is defined almost everywhere in  $R$ , and for any ball  $K_r = \{|x| \leq r\}$

$$\lim_{t \rightarrow 0} \int_{K_r} |u(x, t) - u_0(x)| dx = 0.$$

Inequality (5.82) is equivalent to condition  $E$  in [60], if  $(u_-, u_+)$  is a discontinuity of  $u$  and  $v$  is any number between  $u_-$  and  $u_+$ , then

$$\frac{f(x, t, v) - f(x, t, u_-)}{v - u_-} \geq \frac{f(x, t, u_+) - f(x, t, u_-)}{u_+ - u_-} \quad (5.72)$$

The Kruzkov condition comes from using the following entropy flux pair.

$$\eta(u) = |u - k| \quad \text{and} \quad q(u) = \text{sign}(u - k) \cdot (f(u) - f(k)) \quad (5.73)$$

## 5.7 Well-posedness

There are many methods to prove well-posedness of conservation laws (one and multi-dimensional Cauchy scalar case, one dimensional Cauchy systems case, boundary-initial value problems ([11] and [61]), for balance laws, and relaxation systems). These methods include vanishing viscosity method ([42]), Glimm scheme ([27]), front tracking method ([21], [10], [32]) and evolutionary integral equation regularization ([5]).

### 5.7.1 Solution Properties for Scalar Cauchy Problem

Here we summarize the properties of the solution to the scalar conservation law from [32].

**Theorem 5.7.1.** *Given the initial data  $u_0 \in BV \cap L^1$  and the corresponding flux  $f(u) \in C_{Lip}$ , then the unique weak entropy solution  $u(t, x)$  to the Cauchy problem*

$$u_t + f(u)_x = 0, \quad u(0, x) = u_0(x) \quad (5.74)$$

*satisfies the following properties for  $t \in \mathbb{R}^+$ :*

1. Maximum Principle:

$$\|u(t, \cdot)\|_\infty \leq \|u_0\|_\infty$$

2. Total variation diminishing:

$$TV(u(t, \cdot)) \leq TV(u_0)$$

3.  $L^1$  Contractive: If  $v_0$  and  $v(t, x)$  is another pair of admissible initial data and the corresponding solution, then

$$\|u(t, \cdot) - v(t, \cdot)\| \leq \|u_0 - v_0\|$$

4. Monotonicity Preserving:

$$u_0 \text{ monotone} \Rightarrow u(t, \cdot) \text{ monotone}$$

5. Monotonicity: If  $v_0$  and  $v(t, x)$  is another pair of admissible initial data and the corresponding solution, then

$$u_0 \leq v_0 \Rightarrow u(t, \cdot) \leq v(t, \cdot)$$

6. Lipschitz Continuity in time:

$$\|u(t, \cdot) - u(s, \cdot)\|_1 \leq \|f\|_{Lip} TV(u_0) |t - s|$$

$$\forall s, t \in R^+$$

## 5.8 Oleinik Entropy Condition

We present here an alternate definition of the entropy admissible solution ([23]) that uses Oleinik entropy condition ([60]).

**Definition 5.8.1.** A function  $u \in L^\infty(R \times (0, \infty))$  is an (Oleinik) entropy solution of the Cauchy problem

$$\begin{cases} u_t + f(u)_x = 0 & \text{in } R \times (0, \infty) \\ u = u_0 & \text{on } R \times \{t = 0\} \end{cases} \quad (5.75)$$

if for all test functions  $\phi : R \times [0, \infty) \rightarrow R$  with compact support

$$\int_0^\infty \int_{-\infty}^\infty u\phi_t + f(u)\phi_x dx dt + \int_{-\infty}^\infty u_0\phi dx |_{t=0} = 0 \quad (5.76)$$

and or some constant  $C \geq 0$  and a.e.  $x, z \in R, t > 0$ , and  $z > 0$  the following Oleinik entropy condition is satisfied.

$$u(x+z, t) - u(x, t) \leq C \left(1 + \frac{1}{t}\right) z \quad (5.77)$$

### 5.8.1 Sup-norm Decay of the Solution

Assume that flux  $f$  is smooth, uniformly convex, satisfies  $f(0) = 0$  and that the initial data  $u_0$  is bounded and summable (integrable with a finite integral), then

**Theorem 5.8.1.** *The solution of  $u(t, x)$  satisfies the following bound*

$$|u(t, x)| \leq \frac{C}{t^{1/2}} \quad (5.78)$$

$\forall x \in R, t > 0$ .

This theorem shows that the  $L^\infty$  norm of the solution  $u$  goes to zero as  $t \rightarrow \infty$ . It can be shown that ([23]) the solution converges in the  $L^1$  norm to an  $N$ -wave.

## 5.9 Scalar Initial-Boundary Problem

For a scalar conservation law

$$u_t + f(t, x, u)_x = 0 \quad (5.79)$$

with initial condition

$$u(0, x) = u_0(x), \quad (5.80)$$

and boundary conditions

$$u(t, a) = u_a(t) \text{ and } u(t, b) = u_b(t), \tag{5.81}$$

the definition of the generalized solutions of problem (5.79) with (5.80) is presented here. The boundary conditions cannot be prescribed point-wise, since characteristics from inside the domain might be traveling outside at the boundary. If there are any data at the boundary for that time, that has to be discarded. Moreover, the data also must satisfy entropy condition at the boundary so as to render the problem well-posed. This is shown in Figure 5.18 where for some time boundary data on the left can be prescribed when characteristics from the boundary can be *pushed in* (see [80]). However when the characteristics are coming from inside, the boundary data can not be prescribed.

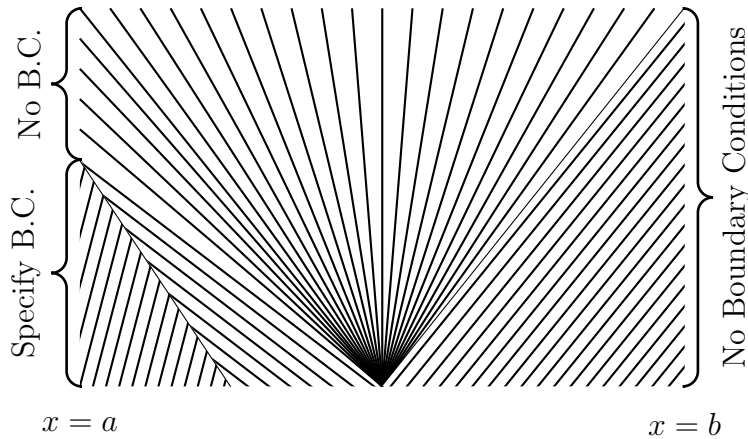


Figure 5.18: Boundary Data

Let  $\Pi_T = [0, T] \times [a, b]$ . Let  $u_0(x)$  be a bounded measurable function satisfying  $|u_0(x)| \leq M_0 \forall x \in [a, b]$  on  $R$ .

**Definition** A bounded measurable function  $u(t, x)$  is called a generalized solution of problem (5.79) with (5.80) in  $\Pi_T$  if:

i) for any constant  $k$  and any smooth function  $\phi(t, x) \geq 0$  finite in  $\Pi_T$  ( $\text{supp}(\phi) \subset \Pi_T$  strictly), if the following inequality holds,

$$\begin{aligned} & \int \int_{\Pi_T} \{ |u(t, x) - k| \phi_t + \text{sign}(u(t, x) - k) [f(t, x, u(t, x)) - f(t, x, k)] \phi_x - \\ & - \text{sign}(u(t, x) - k) f_x(t, x, u(t, x)) \} dx dt \geq 0; \end{aligned} \quad (5.82)$$

ii) there exists sets  $E, E_\ell$  and  $E_r$  of zero measure on  $[0, T]$ , such that for  $t \in [0, T] \setminus E$ , the function  $u(t, x)$  is defined almost everywhere in  $[a, b]$ , and for any ball  $K_r = \{|x| \leq r\}$

$$\lim_{t \rightarrow 0} \int_{K_r} |u(t, x) - u_0(x)| dx = 0.$$

$$\lim_{x \rightarrow a, x \notin E_\ell} \int_0^T L(u(t, x), u_a(t)) \phi(t) dt = 0.$$

$$\lim_{x \rightarrow b, x \notin E_r} \int_0^T R(u(t, x), u_b(t)) \phi(t) dt = 0.$$

where

$$L(x, y) = \sup_{k \in I(x, y)} (\text{sign}(x - y)(f(x) - f(k)))$$

$$R(x, y) = \inf_{k \in I(x, y)} (\text{sign}(x - y)(f(x) - f(k)))$$

and

$$I(x, y) = [\inf(x, y), \sup(x, y)]$$

# Chapter 6

## Traffic Control

In this chapter we study the question of existence of optimal controllers for time-optimal and cost-optimal problems. We start by presenting the existence theorems. We then present dynamics in a semigroup operator formulation from and to appropriate spaces, and then study the general conditions for existence of optimal control laws. After that, the results are applied to a traffic control problem.

### 6.1 Scalar Conservation Law Solution

This section is adapted from [10]. Consider the following scalar conservation law with flux  $f : R \rightarrow R$  locally Lipschitz continuous function and the initial data  $u_0 \in L^1_{loc}$ .

$$u_t + f(u)_x = 0 \quad -\infty < x < +\infty \quad (6.1)$$

with initial condition

$$u(0, x) = u_0(x) \quad (6.2)$$

The entropy solution of (6.1) with (6.2) is a continuous map  $u : R^+ \rightarrow L^1_{loc}(R)$  that satisfies the initial condition (6.2) and also

$$\iint_{R^+ \times R} \{|u(t, x) - k| \phi_t + \text{sign}(u - k)[f(u) - f(k)] \phi_x\} dx dt \geq 0 \quad (6.3)$$

$\forall k \in R$  and non-negative  $\phi \in C^1_c(R^2)$ . The integral inequality (6.3) for entropy function  $\eta(u) = |u - k|$  and its corresponding flux  $q(u) = (f(u) - f(k)) \text{sign}(u - k)$  implies

$$\eta(u)_t + q(u)_x \leq 0 \quad (6.4)$$

For bounded  $u$  and  $k < \inf u(t, x) \forall \phi \geq 0$  in the half plane  $t > 0$ , we get

$$\iint \{u \phi_t + f(u) \phi_x\} dx dt \geq 0 \quad (6.5)$$

Similarly, for bounded  $u$  and  $k > \sup u(t, x) \forall \phi \geq 0$  in the half plane  $t > 0$ , we get

$$\iint \{u \phi_t + f(u) \phi_x\} dx dt \leq 0 \quad (6.6)$$

Combining inequalities (6.5) and (6.6) shows that  $u$  is the weak solution since

$$\iint \{u \phi_t + f(u) \phi_x\} dx dt = 0 \quad (6.7)$$

The following two theorems state the existence and uniqueness results for scalar conservation laws (see [10]).

**Theorem 6.1.1.** *The Cauchy problem (6.1) for locally Lipschitz continuous flux and initial data  $u_0 \in L^1$  having bounded variation has an entropy admissible weak solution that satisfies  $\forall t \in R^+$*

$$\begin{aligned} TV(u(t, \cdot)) &\leq TV(u_0) \\ \|u(t, \cdot)\|_{L^\infty} &\leq \|u_0\|_{L^\infty} \end{aligned} \quad (6.8)$$

**Theorem 6.1.2.** *For locally Lipschitz continuous flux if  $u$  and  $v$  are two bounded entropy solutions of (6.1) then  $\forall t > 0$*

$$\|u(0, \cdot) - v(0, \cdot)\|_{L^1} < \infty \Rightarrow \int_{-\infty}^{+\infty} |u(t, x) - v(t, x)| dx \leq \int_{-\infty}^{+\infty} |u(0, x) - v(0, x)| dx \quad (6.9)$$

Moreover,  $\forall u_0 \in L^\infty$  the Cauchy problem (6.1) has at most one bounded entropy admissible weak solution.

## 6.2 Optimal Flux Control for Scalar Conservation Law

Consider the following scalar traffic control system.

$$\frac{\partial}{\partial t} \rho + \frac{\partial}{\partial x} \left[ v_f(t, x, \rho(t, x)) \rho \left( 1 - \frac{\rho}{\rho_m} \right) \right] = 0 \quad (6.10)$$

The control variable in this model is  $v_f(t, x, \rho)$ . If we design the control such that  $v_f(t, x, \rho)$  is independent of  $\rho$  then the control is an open-loop control. On the other hand, if the control variable is  $\rho$  dependent, then we obtain a feedback control law. In general we assume that  $v_f(t, x, \rho)$  is locally Lipschitz in  $\rho$  and smooth in  $(t, x)$ .

In two dimensions, the corresponding (pedestrian) traffic control problem is

$$\frac{\partial}{\partial t} \rho + \frac{\partial}{\partial x} v_{f_1}(t, x, y, \rho) \rho \left( 1 - \frac{\rho}{\rho_m} \right) + \frac{\partial}{\partial y} v_{f_2}(t, x, y, \rho) \rho \left( 1 - \frac{\rho}{\rho_m} \right) = 0 \quad (6.11)$$

Now, we would like to use  $u$  as the control variable as is traditional in control literature. Hence we will use the variable  $y$  as the scalar conserved variable, and  $f$  for flux. This also puts us in the same notation as [82]. We will also use  $x$  for the  $n$ -dimensional space and we have, in general,  $r$  control variables. For the two-dimensional traffic problem,  $n = 2$  and  $r = 2$ . We can make the control more general and include the initial data as a component in the control vector.

The optimal control problem is to minimize some cost  $J$  that depends on the control variable and the solution of the conservation law. As an example the cost could measure how different is the actual traffic density from some desired traffic density. The cost could also put weight on the value of the control variable. The control belongs to some appropriate space  $\mathcal{U}_{ad}$ .

$$\text{minimize } J(y, u) \text{ subject to } u \in \mathcal{U}_{ad} \quad (6.12)$$

where  $u$  is control and  $y = y(u)$  is the entropy solution to the nonlinear scalar conservation law. The cost  $J(y, u)$  is a functional that maps the state  $y$  and cost  $u$  to  $\mathbb{R}^+$ .

$$\begin{aligned} y_t + \operatorname{div} f(y, u) &= 0, \quad (t, x) \in (0, T) \times \mathbb{R}^n =: \Omega_T \\ y(0, x) &= u_0(x), \quad x \in \mathbb{R}^n \end{aligned} \quad (6.13)$$

We work in the control space  $\mathcal{U} = L^\infty(\Omega_T)^r$  and assume that

**(A1)** : The flux  $f : \mathbb{R} \times \mathbb{R}^r \rightarrow \mathbb{R}^n$  is locally Lipschitz.

**(A2)** : The admissible set  $\mathcal{U}_{ad}$  is bounded in  $\mathcal{U}$  and closed in  $L^1_{loc}(\Omega_T)^r$

A function  $y \in L^\infty(\Omega_T)$  is an entropy solution of (6.13) if  $\forall k \in \mathbb{R}$ ,  $\eta(\lambda) := |\lambda - k|$ ,  $q(\lambda) := \operatorname{sgn}(\lambda - k)(f(\lambda, u) - f(k, u))$  in the distributional sense

$$\eta(y)_t + \operatorname{div} q(y) \leq 0 \quad (6.14)$$

and if the initial data  $y_0 \in L^\infty(\mathbb{R}^n)$  satisfies

$$\lim_{t \rightarrow 0^+} \frac{1}{t} \int_0^t \|y(\tau, \cdot) - y_0\|_{1,K} d\tau = 0 \quad \forall K \subset\subset R^n \quad (6.15)$$

We present here the uniqueness result which is derived easily from [41] for this specific control case here.

**Theorem 6.2.1.** *Let  $\mathcal{U} = L^\infty(\Omega_T)^r$  and let (A1) and (A2) hold. Then for any  $u \in \mathcal{U}_{ad}$  there is at most one entropy solution  $y = y(u) \in L^\infty(\Omega_T)$  satisfying (6.14) and (6.15). Let  $y = y(u_0, u_1) \in L^\infty(\Omega_T)$  with initial condition  $u_0$ ,  $\hat{y} = y(\hat{u}_0, u_1) \in L^\infty(\Omega_T)$  with initial condition  $\hat{u}_0$  be entropy solutions with  $\|y\|_\infty, \|\hat{y}\|_\infty \leq M$ . For  $(\bar{t}, \bar{x}) \in \Omega_T$  and  $R > 0$  the propagation cone*

$$K(\bar{t}, \bar{x}, R) := (\tau, x); 0 \leq \tau \leq \bar{t}, \|x - \bar{x}\|_2 \leq R + M_{f'}(\bar{t} - \tau) \quad (6.16)$$

with  $M_{f'} = \text{ess sup}_{|\lambda| \leq M} \|\nabla f\|_2$  and denote by  $S_2$  the cross-section of the cone  $K(\bar{t}, \bar{x}, R)$  at  $\tau = t$ . Then  $\forall t \in [0, \bar{t}]$

$$\|y(t) - \hat{y}(t)\|_{1,S_t} \leq \|u_0 - \hat{u}_0\|_{1,S_0} \quad (6.17)$$

## 6.2.1 Optimal Control in Space of Constant Controls

We will study the existence of optimal controls for the scalar traffic model in the case of taking controls in the space of constant values. The control enters multiplicatively through flux.

**Theorem 6.2.2.** *Consider the model*

$$\frac{\partial}{\partial t} \rho + \frac{\partial}{\partial x} v_f \rho \left(1 - \frac{\rho}{\rho_m}\right) = 0 \quad (6.18)$$

where the control  $v_f$  belongs to a set of constant functions and  $-v_M \leq v_f \leq v_M$ . The optimal time control problem has a solution, and for a lower(upper) semicontinuous cost functional, the minimizing(maximizing) cost control solution exists.

*Proof.* The mapping from  $[0, v_M]$  to set of constant functions  $v_f$  taking values in  $[0, v_M]$  is an isomorphism. For given initial data  $\rho_0 \in L^1$  a measurable function of bounded variation that is essentially bounded, each constant control  $v_f$  generates a unique entropy admissible solution. Moreover, the set  $[0, v_M]$  is compact in the usual topology. Following lemma 6.2.1 given below we can show that the set of admissible controls is strongly compact, i.e. there exists a convergent subsequence given any sequence of solutions obtained by applying a sequence of controls. The optimal time control has a solution, and for a lower(upper) semicontinuous cost functional, the minimizing(maximizing) cost control solution exists. The proof depends on the lemma 6.2.1 which is presented as theorem 2.4 in [10] and which is a consequence of sequential compactness of functions of bounded variations as presented in Helly's theorem.

Given a sequence of control  $v_{f_k}$  applied to the scalar traffic model with initial condition  $\rho_0 \in L^1$  a function of bounded variations and in  $L^\infty$ , then by theorem 5.7.1 for each solution  $\rho_k$ , we have

1. *Maximum Principle:*

$$\|\rho_k(t, \cdot)\|_\infty \leq \|\rho_0\|_\infty$$

2. *Total variation diminishing:*

$$TV(\rho_k(t, \cdot)) \leq TV(\rho_0)$$

3. *Lipschitz Continuity in time:*

$$\|\rho_k(t, \cdot) - \rho_k(s, \cdot)\|_1 \leq v_M \|f\|_{Lip} TV(\rho_0) |t - s|$$

$\forall s, t \in R^+$  where we have taken  $f$  to be the flux when  $v_f = 1$ . From the sequence we take a subsequence for which  $v_{f_k} \rightarrow v_{\bar{f}}$ . This is possible because of the compactness of the control values, i.e.  $v_{f_k} \in [0, \rho_m]$ . This subsequence satisfies the conditions for lemma 6.2.1 given below and therefore a further convergent subsequence exists that converges to some function

$\rho$ . Since all  $\rho_k$  take values in a compact set  $[0, \rho_m]$  and also that  $v_f \in [0, v_M]$ , then we see that  $v_{f_k} f(\rho_k)$  is bounded by  $LM$ , and also that  $v_{f_k} f(\rho_k) - v_{\bar{f}} f(\rho)$  is bounded by  $2LM$ . Now, using the dominated convergence theorem of Lebesgue, we get  $v_{f_k} f(\rho_k) \rightarrow v_{\bar{f}} f(\rho)$  in  $L^1_{loc}$ .  $\square$

**Lemma 6.2.1.** *Given a sequence of functions  $u_k : \mathbb{R}^+ \times \mathbb{R} \mapsto \mathbb{R}^n$  such that*

$$\text{Total Variation } u_k(t, \cdot) \leq C \quad |u_k(t, x)| \leq M \quad \forall t, x \quad (6.19)$$

and

$$\int_{-\infty}^{+\infty} |u_k(t, x) - u_k(s, x)| dx \leq L |t - s| \quad \forall t, s \geq 0 \quad (6.20)$$

for given constants  $C$ ,  $M$ , and  $L$ . Then there exists a subsequence  $u_j$  converging to  $u$  in  $L^1_{loc}$  that satisfies

$$\int_{-\infty}^{+\infty} |u(t, x) - u(s, x)| dx \leq L |t - s| \quad \forall t, s \geq 0 \quad (6.21)$$

We require for the limit function  $u(t, x) = \lim_{y \rightarrow x^+} u(t, y)$  for all  $t, x$ . The limit function  $u$  also satisfies the bounds

$$\text{Total Variation } u(t, \cdot) \leq C \quad |u(t, x)| \leq M \quad \forall t, x \quad (6.22)$$

### 6.3 Feedback Control for Scalar Law

We can design feedback control in an attempt to make the traffic density follow some specific traffic density profile. In the design of these feedback control laws, we are not trying to achieve any optimal solution or any quantitative properties. The aim here is to achieve some qualitative behavior for the traffic motion using ad hoc methods. The desired traffic

behavior will involve advective and diffusive flows. We will also ignore implementation issues. For instance, in the actual implementation of controlling traffic, a feedback control design produces the control variable as a function of the state. However, in implementation sensors are used to measure the state and then the control value is computed and then implemented. This implementation involves time delays as well as time and space discretizations. For our purpose here, we leave aside implementation issues and explore the theoretical closed-loop profiles of interest. We will design controllers specifically for traffic models. The traffic model for one dimensional case we will use is:

$$\frac{\partial}{\partial t}\rho + \frac{\partial}{\partial x}v_f(\rho)\rho\left(1 - \frac{\rho}{\rho_m}\right) = 0 \quad (6.23)$$

The control variable in this model is  $v_f(\rho)$ . In two dimensions, the corresponding (pedestrian) traffic control problem is

$$\frac{\partial}{\partial t}\rho + \frac{\partial}{\partial x}v_{f_1}(\rho)\rho\left(1 - \frac{\rho}{\rho_m}\right) + \frac{\partial}{\partial y}v_{f_2}(\rho)\rho\left(1 - \frac{\rho}{\rho_m}\right) = 0 \quad (6.24)$$

### 6.3.1 Advection Control

In this section we will design the feedback control to make the initial density profile move in some specific direction at fixed speed. We will study both types of controls: unbounded and bounded.

#### Unbounded Control

We will study controls for one-dimensional and two dimensional cases separately.

**One Dimensional Case** We would like the initial traffic profile to move to either right or left with a constant desired speed as shown in Figure 6.1.

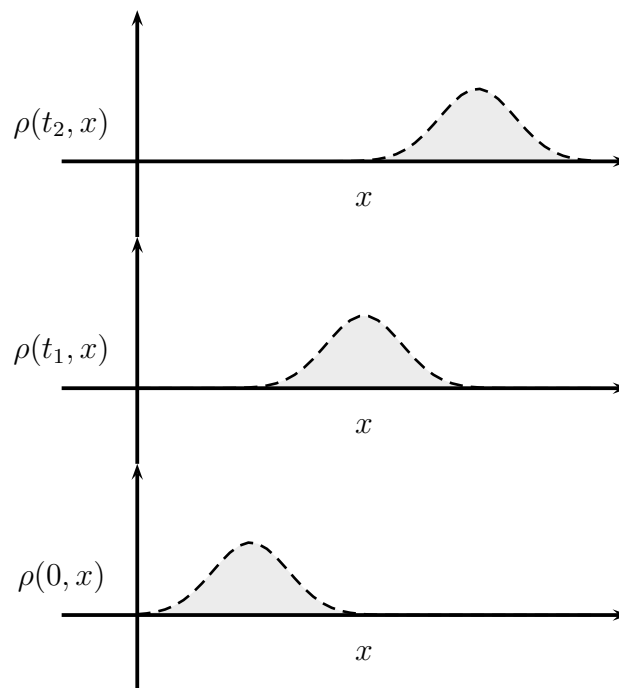


Figure 6.1: Advection Control in 1D

We can obtain this desired constant advection by using the following feedback control law, given that  $\forall x \in R \rho(0, x) \leq \rho_m$ . We write  $\rho(0, x)$  as  $\rho_0$ .

$$v_f = a \left[ \left( 1 - \frac{\rho}{\rho_m} \right) \right]^{-1} \quad (6.25)$$

Substituting (6.25) in (6.23) gives us the constant advection equation.

$$\frac{\partial \rho}{\partial t} + a \frac{\partial \rho}{\partial x} = 0 \quad (6.26)$$

Solution of this equation is  $\rho(t, x) = \rho_0(x - at)$ .

**Two Dimensional Case** In this case we would like the initial traffic profile to move at some constant speed  $a$  and at some fixed angle  $\theta$  from the  $x$ -axis as shown in Figure 6.2.

We can obtain this desired constant advection by using the following feedback control law, given that  $\forall x \in R \rho(0, x, y) \leq \rho_m$ . We write  $\rho(0, x, y)$  as  $\rho_0$ .

$$v_{f_1} = a \cos \theta \left[ \left( 1 - \frac{\rho}{\rho_m} \right) \right]^{-1} \quad (6.27)$$

$$v_{f_2} = a \sin \theta \left[ \left( 1 - \frac{\rho}{\rho_m} \right) \right]^{-1} \quad (6.28)$$

Substituting (6.27) and (6.28) in (6.24) gives us the constant advection equation for the two dimensional case.

$$\frac{\partial \rho}{\partial t} + a \cos \theta \frac{\partial \rho}{\partial x} + a \sin \theta \frac{\partial \rho}{\partial y} = 0 \quad (6.29)$$

Solution of this equation is  $\rho(t, x, y) = \rho_0(x - a \cos \theta t, y - a \sin \theta t)$ .

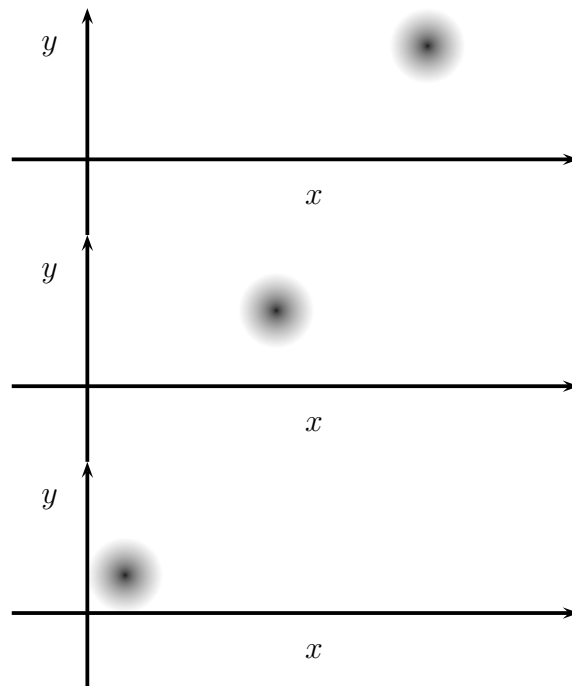


Figure 6.2: Advection Control in 2D

## Bounded Control

Now let us assume that the control is bounded. We will study this case separately for one and two dimensional cases.

**One Dimensional Case** We would like the initial traffic profile to move to either right or left with a constant speed. However the constant desired speed is dictated by the initial traffic density profile and also the bounds on the control. Let us assume that  $|v_f| \leq v_M \in R$ .

Let us assume that the initial density has compact support and is bounded away from  $\rho_m$  i.e. ,  $max\rho_0 = \rho_M < \rho_m$ . Then the maximum speed that this density can move with is given by

$$a = v_M \left[ \left( 1 - \frac{\rho_M}{\rho_m} \right) \right] \quad (6.30)$$

Using this constant advection speed given by (6.30), we can apply control (6.25) and obtain closed loop behavior (6.26).

**Two Dimensional Case** For the two dimensional case, we again assume initial density with compact support and choose the advection speed by (6.30). Using this speed we can achieve the closed loop dynamics of (6.29) by applying (6.27) and (6.28).

### 6.3.2 Diffusion Control

In this section we will design the feedback control to make the initial density profile diffuse out at some specified rate. We will study both types of controls: unbounded and bounded.

## Unbounded Control

We will study controls for one-dimensional and two dimensional cases separately.

**One Dimensional Case** We would like the initial traffic profile to diffuse out as shown in Figure 6.3.

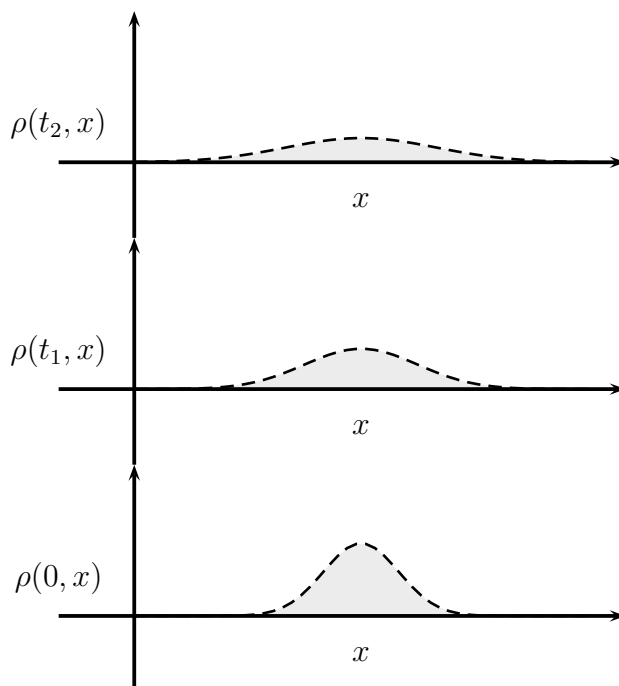


Figure 6.3: Diffusion Control in 1D

We can obtain this desired constant rate of diffusion by using the following feedback control law, given that  $\forall x \in R, \rho(0, x) \leq \rho_m$ .

$$v_f = -\mu \left[ \rho \left( 1 - \frac{\rho}{\rho_m} \right) \right]^{-1} \frac{\partial \rho}{\partial x} \quad (6.31)$$

Substituting (6.31) in (6.23) gives us the constant diffusion equation.

$$\frac{\partial \rho}{\partial t} - \mu \frac{\partial^2 \rho}{\partial x^2} = 0 \quad (6.32)$$

Solution of this equation is

$$\rho(t, x) = \frac{1}{\sqrt{4\pi\mu t}} \int_{-\infty}^{\infty} \exp\left(\frac{-(x-y)^2}{4\mu t}\right) \rho_0(y) dy \quad (6.33)$$

This equation can also be written as follows:

$$\rho(t, x) = \int_{-\infty}^{\infty} k(t, x, y) \rho_0(y) dy \quad (6.34)$$

where the one dimensional diffusion kernel is

$$k(t, x, y) = \frac{1}{\sqrt{4\pi\mu t}} \exp\left(\frac{-(x-y)^2}{4\mu t}\right) \quad (6.35)$$

From the solution it can be easily seen that if the initial condition is  $\delta(x)$ , then the solution is given by:

$$\rho(t, x) = \frac{1}{\sqrt{4\pi\mu t}} \exp\left(\frac{-x^2}{4\mu t}\right) \quad (6.36)$$

We can also observe two properties of the diffusion equation:

1. **Conservation:** The total traffic is conserved as can be shown by

$$\frac{d}{dt} \int_{-\infty}^{\infty} \rho(t, x) dx = \int_{-\infty}^{\infty} \mu \rho_{xx} dx = [\mu \rho_x(t, x)]_{x=-\infty}^{\infty} = 0 \quad (6.37)$$

2. **Energy Dissipation:** The *energy* is dissipated over time as shown by

$$\frac{d}{dt} \int_{-\infty}^{\infty} \frac{1}{2} \rho^2 dx = \int_{-\infty}^{\infty} \mu \rho \rho_{xx} dx = - \int_{-\infty}^{\infty} \mu (\rho_x)^2 dx \leq 0 \quad (6.38)$$

It is interesting to note that the feedback control laws for diffusion require the computation of the gradient of density. In control implementation, in general, derivative terms can be problematic. This is especially true for derivatives involving time, because numerical differentiation is noisy and also involves causality issues. However, in the pedestrian traffic control, one way to measure this gradient could be through image processing which at a given sample time involves computing density as a function of spatial variables. Then the gradient can be computed. Proper filters can also be used for smoothing out the data to reduce noise. For the purpose of the present work, we are ignoring the implementation details. The effect of discrete approximations of these controls could be a topic of future research.

**Two Dimensional Case** In this case we would like the initial traffic profile to diffuse at some constant rate  $a$  in all directions as shown in Figure 6.4.

We can obtain this desired constant advection by using the following feedback control law, given that  $\forall x \in R \rho(0, x, y) \leq \rho_m$ . We write  $\rho(0, x, y)$  as  $\rho_0$ .

$$v_{f_1} = -\mu \left[ \rho \left( 1 - \frac{\rho}{\rho_m} \right) \right]^{-1} \frac{\partial \rho}{\partial x} \quad (6.39)$$

$$v_{f_2} = -\mu \left[ \rho \left( 1 - \frac{\rho}{\rho_m} \right) \right]^{-1} \frac{\partial \rho}{\partial y} \quad (6.40)$$

Substituting (6.39) and (6.40) in (6.24) gives us the following diffusion equation for the two dimensional case.

$$\frac{\partial}{\partial t} \rho - \mu \Delta \rho = 0 \quad (6.41)$$

For the two dimensional case, the kernel is given by:

$$k(t, x, y) = \frac{1}{\sqrt{4\pi\mu t}} \exp\left(\frac{-|x - y|^2}{4\mu t}\right) \quad (6.42)$$

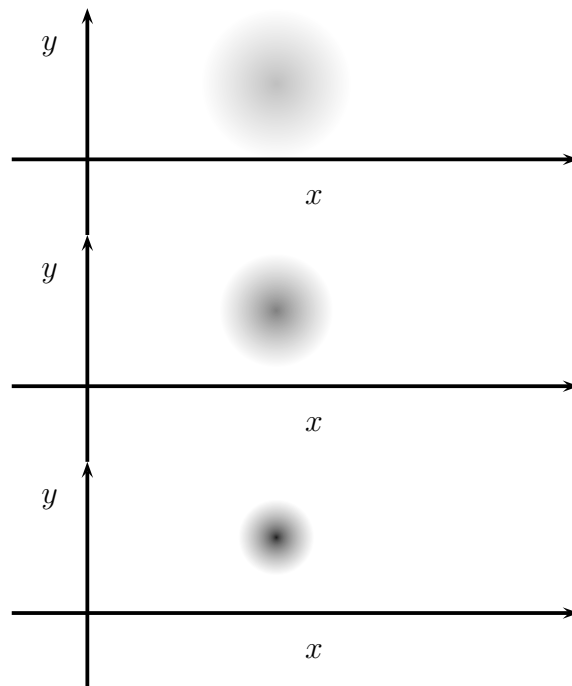


Figure 6.4: Diffusion Control in 2D

and the solution by:

$$\rho(t, x, y) = \left( \frac{1}{\sqrt{4\pi\mu t}} \right)^2 \int_{-\infty}^{\infty} \int_{-\infty}^{\infty} \exp\left(\frac{-(x-m)^2}{4\mu t}\right) \exp\left(\frac{-(y-n)^2}{4\mu t}\right) \rho_0(m, n) dm dn \quad (6.43)$$

### Bounded Control

Now let us assume that the control is bounded. We will study this case separately for one and two dimensional cases.

**One Dimensional Case** We would like the initial traffic profile to diffuse with a constant rate  $\mu$ . However the constant desired rate is dictated by the initial traffic density profile and also the bounds on the control. Let us assume that  $|v_f| \leq v_M \in R$ .

The rate of diffusion that this density can achieve using the feedback control design we have chosen will satisfy the following inequality. More analysis is needed to figure out how long this can be maintained for a given class of initial conditions.

$$\mu \leq \left| v_M \left[ \rho \left( 1 - \frac{\rho}{\rho_m} \right) \right] \left[ \frac{\partial \rho}{\partial x} \right]^{-1} \right| \quad (6.44)$$

**Two Dimensional Case** For the two dimensional case, the inequality (6.44) gets replaced by

$$\mu \leq \min \left( \left| v_M \left[ \rho \left( 1 - \frac{\rho}{\rho_m} \right) \right] \left[ \frac{\partial \rho}{\partial x} \right]^{-1} \right|, \left| v_M \left[ \rho \left( 1 - \frac{\rho}{\rho_m} \right) \right] \left[ \frac{\partial \rho}{\partial y} \right]^{-1} \right| \right) \quad (6.45)$$

### 6.3.3 Advective-Diffusion Control

In this section we will design the feedback control to make the initial density profile diffuse out at some specified rate and at the same time advect in some specified direction.

#### One Dimensional Case

We would like the initial traffic profile to move to either right or left with a constant desired speed  $a$  and at the same time a constant diffusion rate  $\mu$  as shown in Figure 6.5.

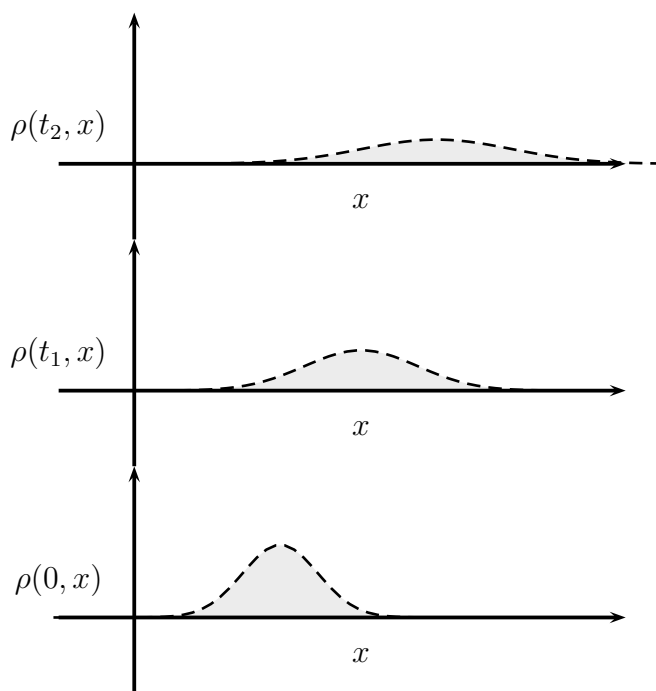


Figure 6.5: Advective-Diffusion Control in 1D

We can obtain this desired constant advective diffusion by using the following feedback control law.

$$v_f = \left[ \rho \left( 1 - \frac{\rho}{\rho_m} \right) \right]^{-1} \left[ a\rho - \mu \frac{\partial \rho}{\partial x} \right] \quad (6.46)$$

Substituting (6.46) in (6.23) gives us the desired closed loop behavior as

$$\frac{\partial \rho}{\partial t} + a \frac{\partial \rho}{\partial x} - \mu \frac{\partial^2 \rho}{\partial x^2} = 0 \quad (6.47)$$

In the case of bounded control, the control law becomes:

$$v_f = \min \left( v_M, \left[ \rho \left( 1 - \frac{\rho}{\rho_m} \right) \right]^{-1} \left[ a\rho - \mu \frac{\partial \rho}{\partial x} \right] \right) \quad (6.48)$$

## Two Dimensional Case

We would like the initial traffic profile to move to in some specified direction with a constant desired speed  $a$  and at the same time a constant diffusion rate  $\mu$  as shown in Figure 6.6.

We can obtain this desired advective diffusion by using the following feedback control law.

$$v_{f_1} = \left[ \rho \left( 1 - \frac{\rho}{\rho_m} \right) \right]^{-1} \left[ a \cos \theta \rho - \mu \frac{\partial \rho}{\partial x} \right] \quad (6.49)$$

$$v_{f_2} = \left[ \rho \left( 1 - \frac{\rho}{\rho_m} \right) \right]^{-1} \left[ a \sin \theta \rho - \mu \frac{\partial \rho}{\partial y} \right] \quad (6.50)$$

Substituting (6.49) and (6.50) in (6.24) gives us the advective diffusion equation for the two dimensional case.

$$\frac{\partial \rho}{\partial t} + a \cos \theta \frac{\partial \rho}{\partial x} + a \sin \theta \frac{\partial \rho}{\partial y} - \mu \Delta \rho = 0 \quad (6.51)$$

In the case of bounded controls, the control laws become

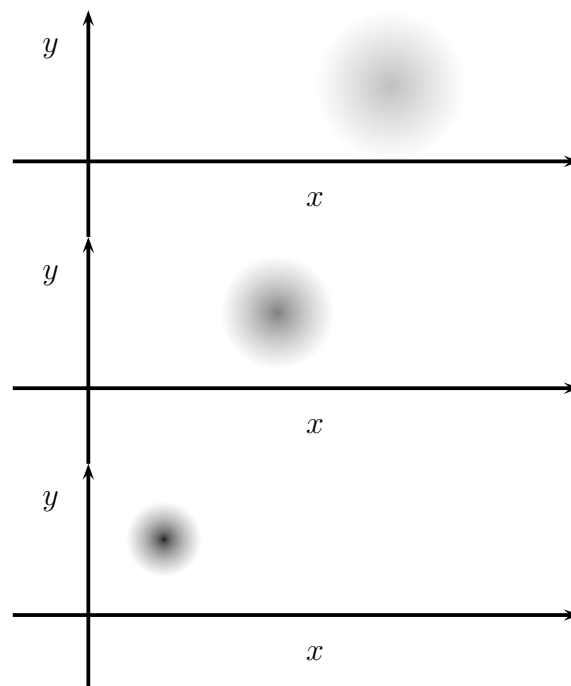


Figure 6.6: Advective-Diffusion Control in 2D

$$v_{f_1} = \min \left( v_M, \left[ \rho \left( 1 - \frac{\rho}{\rho_m} \right) \right]^{-1} \left[ a \cos \theta \rho - \mu \frac{\partial \rho}{\partial x} \right] \right) \quad (6.52)$$

$$v_{f_2} = \min \left( v_M, \left[ \rho \left( 1 - \frac{\rho}{\rho_m} \right) \right]^{-1} \left[ a \sin \theta \rho - \mu \frac{\partial \rho}{\partial y} \right] \right) \quad (6.53)$$

## 6.4 Advective Feedback Control for Relaxation Systems

The systems of PDEs that have been used as traffic models in this work are relaxation models (see [36] and [48]). In the relaxation schemes, we still use the free flow speed as the control variable, and because of the convergence of the models to equilibrium conditions, we still propose to use the same form of the feedback control laws that have been used for scalar conservation laws. To illustrate this concept, we will use a general example.

Following [48] consider the relaxation system

$$\rho_t + (\rho v)_x = 0 \quad (6.54)$$

$$v_t + \left( \frac{1}{2} v^2 + g(\rho) \right)_x = \frac{v_e(\rho) - v}{\tau} \quad (6.55)$$

with initial data

$$(\rho(0, x), v(0, x)) = (\rho_0(x), v_0(x)). \quad (6.56)$$

In this model  $g$  is the anticipation factor satisfying

$$g'(\rho) = \rho (v_e'(\rho))^2. \quad (6.57)$$

and  $\tau > 0$  is the relaxation time.

Let us define the function  $h$  as

$$h(\rho, v) = \frac{v_e(\rho) - v}{\tau}. \quad (6.58)$$

The equilibrium condition for system (6.54) and (6.55) is given by

$$\rho_t + (\rho v_e(\rho))_x = 0 \quad (6.59)$$

We assume that the equilibrium velocity  $v_e(\rho)$  is a linear function of  $\rho$ , which is the case in Greenshield's model.

$$v_e(\rho) = -a\rho + b, \quad a, b > 0 \quad (6.60)$$

Let us take

$$g(\rho) = \frac{a^2}{2}\rho^2 \quad (6.61)$$

and

$$q(\rho) = \rho v_e(\rho) = -a\rho^2 + b\rho \quad (6.62)$$

We can diagonalize the system to obtain

$$(-v_e(\rho) - v)_t + \lambda_1(-v_e(\rho) - v)_x = -h(\rho, v) \quad (6.63)$$

$$(-v_e(\rho) + v)_t + \lambda_2(-v_e(\rho) + v)_x = h(\rho, v) \quad (6.64)$$

In terms of the Riemann invariants  $r$  and  $s$

$$r(\rho, v) = -v_e(\rho) - v \quad (6.65)$$

$$s(\rho, v) = -v_e(\rho) + v. \quad (6.66)$$

we get (see [48])

$$r_t - \left( \frac{1}{2}r^2 + br \right)_x = \frac{s}{\tau} \quad (6.67)$$

$$s_t + \left( \frac{1}{2}s^2 + bs \right)_x = -\frac{s}{\tau}. \quad (6.68)$$

The initial conditions are

$$r(x, 0) = r_0(x) \quad (6.69)$$

$$s(x, 0) = s_0(x). \quad (6.70)$$

For advection control, we get the equilibrium speed as the desired speed  $b$ .

$$v_e(\rho) = b \quad (6.71)$$

Now, we can compare (6.68) to the scalar balance law studied by Kruzkov (see [41]).

$$u_t + f(x, t, u)_x = g(x, t, u) \quad (6.72)$$

with initial data

$$u(x, 0) = u_0(x), \quad (6.73)$$

We present here the theorem from Kruzkov ([41]) which is also used in [48].

For any  $R > 0$  and  $M > 0$ , we set

$$N_M(R) = \max_{K_R \times [0, T] \times [-M, M]} |f_u(x, t, u)|$$

and let  $\kappa$  be the cone  $\{(x, t) : |x| \leq R - Nt, 0 \leq t \leq T_0 = \min\{T, RN^{-1}\}\}$ . Let  $S_\tau$  designate the cross-section of the cone  $\kappa$  by the plane  $t = \tau$ ,  $\tau \in [0, T_0]$ .

**Theorem 6.4.1.** (*Kruzkov*) Assume that: *i*)  $f(t, x, u)$  and  $g(t, x, u)$  are continuously differentiable in the region  $\{(x, t) \in \Pi_T, -\infty < u < +\infty\}$ ; *ii*)  $f_x(t, x, u)$  and  $f_t(t, x, u)$  satisfy Lipschitz condition in  $u$ . Let  $u(x, t)$  and  $v(x, t)$  be generalized solutions of problem (6.72) (6.73) with bounded measurable initial data  $u_0(x)$  and  $v_0(x)$ , respectively, where  $|u(x, t)| \leq M$  and  $|v(x, t)| \leq M$  almost everywhere in  $K_R \times [0, T]$ . Let  $\gamma = \max g_u(t, x, u)$  in the region  $(t, x) \in \kappa$  and  $|u| \leq M$ . Then for almost all  $t \in [0, T_0]$

$$\int_{S_t} |u(t, x) - v(t, x)| dx \leq e^{\gamma t} \int_{S_0} |u_0(x) - v_0(x)| dx. \quad (6.74)$$

Direct application of this in (6.68), as shown in [48] gives

**Theorem 6.4.2.** If  $s_1(t, x)$  and  $s_2(t, x)$  are generalized solutions of problem (6.68) (6.70) with bounded measurable initial data  $s_{10}(x)$  and  $s_{20}(x)$  such that  $s_{10} - s_{20} \in L^1$ . Then for almost all  $t > 0$

$$\int_{S_t} |s_1(t, x) - s_2(t, x)| dx \leq e^{-\frac{t}{\tau}} \int_{S_0} |s_{10}(x) - s_{20}(x)| dx \quad (6.75)$$

Another theorem from [48] is directly applicable for the advection feedback control law for systems. Hence, we reproduce that here.

**Theorem 6.4.3.** If  $r_1(t, x)$  and  $r_2(t, x)$  are generalized solutions of problem (6.67) (6.69) with bounded measurable initial data  $r_{10}(x)$  and  $r_{20}(x)$  such that  $r_{10} - r_{20} \in L^1$ . Then for almost all  $t > 0$

$$\begin{aligned} \int_{S_t} |r_1(t, x) - r_2(t, x)| dx &\leq \int_{S_0} |r_{10}(x) - r_{20}(x)| dx + \\ &+ (1 - e^{-\frac{t}{\tau}}) \int_{S_0} |s_{10}(x) - s_{20}(x)| dx. \end{aligned} \quad (6.76)$$

### 6.4.1 Unbounded Advection for Relaxation Systems

For traffic relaxation models the control variable is the free flow speed that shows up in the equilibrium speed term. As an example, consider the relaxation traffic model

$$\rho_t + (\rho v)_x = 0 \quad (6.77)$$

$$v_t + \left(\frac{1}{2}v^2 + g(\rho)\right)_x = \frac{v_e(\rho) - v}{\tau} \quad (6.78)$$

with initial data

$$(\rho(0, x), v(0, x)) = (\rho_0(x), v_0(x)) \quad (6.79)$$

Following Greenshield model, the equilibrium speed term  $v_e(\rho)$  can be taken as

$$v_e(\rho) = v_f \left(1 - \frac{\rho}{\rho_m}\right) \quad (6.80)$$

For advection control, we use the following feedback control

$$v_f = b \left[ \left(1 - \frac{\rho}{\rho_m}\right) \right]^{-1} \quad (6.81)$$

Hence, in the case of unbounded control, the equilibrium speed becomes constant and we get

$$v_e(\rho) = b \quad (6.82)$$

Let us take

$$s_1(t, x) = v(t, x) - b \quad (6.83)$$

and

$$s_2(t, x) = 0 \quad (6.84)$$

Notice that  $s_1(t, x)$  and  $s_2(t, x)$  as in 6.83 and 6.84 are generalized solutions of problem (6.68) (6.70) with bounded measurable initial data  $s_{10}(x)$  and  $s_{20}(x)$  such that  $s_{10} - s_{20} \in L^1$ . We obtain the following corollary for the unbounded advection control for relaxation systems.

**Corollary 6.4.1.** *Given  $s_1(t, x)$  and  $s_2(t, x)$  as in 6.83 and 6.84 the unbounded advection feedback control 6.81 for relaxation system 6.78 provides the following result for almost all  $t > 0$*

$$\int_{S_t} |v(t, x) - b| dx \leq e^{-\frac{t}{\tau}} \int_{S_0} |v(0, x) - b| dx \quad (6.85)$$

This shows that the actual speed of traffic exponentially in time decays in  $L_1$  norm to the desired constant speed. We can also conclude some behavior for the density profile. If we assume that the system speed is actually following the equilibrium speed then the conservation law for the traffic density would simply be the following advection equation.

$$\rho_t + b\rho_x = 0 \quad (6.86)$$

with given initial data

$$\rho(0, x) = \rho_0(x) \quad (6.87)$$

The solution of this equation is

$$\rho(t, x) = \rho_0(x - bt) \quad (6.88)$$

Let us take  $\rho^\tau$  and  $v^\tau$  to be the solution of the relaxation model (6.78), then, as is shown in [47], for  $\phi \in C_0^1$ , we get

$$\int_0^{+\infty} \int_{\mathbb{R}} (\rho^\tau \phi_t + \rho^\tau v_t \phi_x) dx dt = 0 \quad (6.89)$$

and

$$\int_0^{+\infty} \int_{\mathbb{R}} \left( v^\tau \phi_t + \left( \frac{1}{2} (v^\tau)^2 + g(\rho^\tau) \right) \phi_x + \frac{v_e(\rho^\tau) - v^\tau}{\tau} \phi \right) dx dt = 0 \quad (6.90)$$

After multiplying (6.90) by  $\tau$  and then taking  $\tau \rightarrow 0$  we get

$$\int_0^{+\infty} \int_{\mathbb{R}} (v_e(\rho) - v) \phi dx dt = 0 \quad (6.91)$$

which leads to

$$v = v_e(\rho) \text{ a.e.} \quad (6.92)$$

We can apply the result in Theorem 5.1 in [48] for the unbounded advection control case to get for  $\tau \rightarrow 0$  the following.

$$\|\rho^\tau(t, \cdot) - \rho_s(\cdot)\|_{L^1} \rightarrow 0 \quad (6.93)$$

where  $\rho_s(x) = \rho_0(x - bt)$ . This result implies that for small  $\tau$  the density profile of the relaxation feedback control system is close to the pure advection profile.

## 6.4.2 Bounded Advection for Relaxation Systems

For bounded advection case, we apply the following control law

$$v_f = \min \left( v_M, b \left[ \left( 1 - \frac{\rho}{\rho_m} \right) \right]^{-1} \right) \quad (6.94)$$

Applying this control law results in the following equilibrium speed function.

$$v_e(\rho) = \begin{cases} b & \text{if } \rho \leq \left[ 1 - \frac{b}{v_M} \right] \rho_m, \\ v_M \left( 1 - \frac{\rho}{\rho_m} \right) & \text{otherwise} \end{cases} \quad (6.95)$$

This makes the equilibrium speed function piecewise affine. Using this expression gives a corresponding equation for variable  $s$  in (6.68) where the flux for  $s$  is still Lipschitz. Hence the results provided by Theorems (6.4.2) and (6.4.3) are still valid. The corresponding result to (6.4.1) that we obtain for the bounded case then is

$$\int_{S_t} |v(t, x) - v_e(t, x)| dx \leq e^{-\frac{t}{\tau}} \int_{S_0} |v(0, x) - v_e(0, x)| dx \quad (6.96)$$

where  $v_e(t, x)$  is given by (6.95). Similar to the unbounded case as  $\tau \rightarrow 0$  the system behavior converges to the equilibrium behavior, but not to pure advection but to a bounded advection equilibrium density profile.

## 6.5 Wellposedness for Bounded Advection Control

We consider the dynamics

$$\frac{\partial}{\partial t} \rho + \frac{\partial}{\partial x} v_f(t, x, \rho) \rho \left( 1 - \frac{\rho}{\rho_m} \right) = 0 \quad (6.97)$$

We analyze the case where the advection speed  $a$  is taken to be

$$a > v_M \left[ \left( 1 - \frac{\rho_M}{\rho_m} \right) \right] \quad (6.98)$$

The advection control law with the constraint becomes

$$v_f = \min \left( v_M, a \left[ \left( 1 - \frac{\rho}{\rho_m} \right) \right]^{-1} \right) \quad (6.99)$$

The closed loop dynamics are given by

$$\begin{cases} \rho_t + a\rho_x = 0 & \text{if } \rho \leq \rho_a, \\ \rho_t + \left( v_M \rho \left( 1 - \frac{\rho}{\rho_m} \right) \right)_x = 0 & \text{otherwise} \end{cases} \quad (6.100)$$

where

$$\rho_a = \rho_m \left[ 1 - \frac{a}{v_M} \right] \quad (6.101)$$

The bounded advection feedback control modifies the flux to be a piecewise smooth function given by:

$$f(\rho) = \begin{cases} a\rho & \text{if } \rho \leq \rho_a, \\ v_M \rho \left( 1 - \frac{\rho}{\rho_m} \right) & \text{otherwise} \end{cases} \quad (6.102)$$

The plot of this feedback flux is shown in Figure 6.7.

The following theorem presents the conditions for the weak entropy solutions for Riemann problems. This theorem is covered in many sources such as [10] and [32]. The proof is also given in those references. Here we reproduce the theorem since it will be used to prove the existence and wellposedness of the closed-loop solution of the bounded advection control.

**Theorem 6.5.1.** *The following piecewise constant function*

$$\rho(t, x) = \begin{cases} u^r & \text{if } x > st, \\ u^\ell & \text{if } x < st \end{cases} \quad (6.103)$$

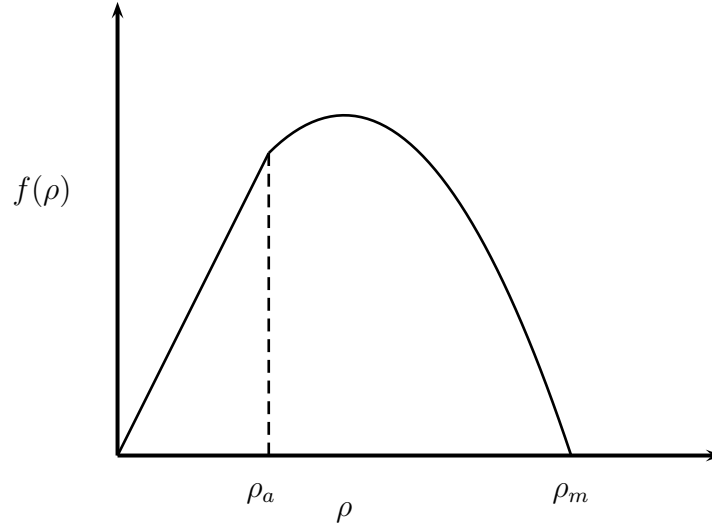


Figure 6.7: Feedback Bounded Advective Flux

is a weak entropy solution of

$$\rho_t + f(\rho)_x = 0 \quad (6.104)$$

if and only if the following Rankine-Hugoniot equation is satisfied

$$s(u^r - u^\ell) = f(u^r) - f(u^\ell) \quad (6.105)$$

and for every  $\alpha \in [0, 1]$  the following are satisfied.

$$\begin{cases} f(\alpha u^r + (1 - \alpha)u^\ell) \geq \alpha f(u^r) + (1 - \alpha)f(u^\ell) & \text{if } u^\ell < u^r, \\ f(\alpha u^r + (1 - \alpha)u^\ell) \leq \alpha f(u^r) + (1 - \alpha)f(u^\ell) & \text{if } u^\ell > u^r \end{cases} \quad (6.106)$$

The following lemma (see [10]) is also needed for the wellposedness proof for bounded advection solution. This lemma provides the result for approximation of functions of bounded variation by piecewise constant functions.

**Lemma 6.5.1.** *For any right continuous function of bounded variation  $\rho : \mathbb{R} \rightarrow \mathbb{R}$  and any  $\epsilon > 0$  there exists a piecewise constant function  $\bar{\rho}$  such that*

$$\text{Total Variation } \bar{\rho} \leq \text{Total Variation } \rho \quad (6.107)$$

and

$$\|\rho - \bar{\rho}\|_{L^\infty} \leq \epsilon \quad (6.108)$$

Moreover, if the function  $\rho$  also satisfies

$$\int_{-\infty}^0 |\rho(x) - \rho(-\infty)| dx + \int_0^{\infty} |\rho(x) - \rho(\infty)| dx < \infty \quad (6.109)$$

then a piecewise constant function can be obtained with the following additional property

$$\|\rho - \bar{\rho}\|_{L^1} \leq \epsilon \quad (6.110)$$

### 6.5.1 Riemann Problems

Riemann problem is the Cauchy problem with initial data given by

$$\rho = \begin{cases} \rho_\ell & \text{if } x \leq 0 \\ \rho_r & \text{if } x > 0 \end{cases} \quad (6.111)$$

We consider all possible Riemann problems as shown in Table 6.1.

#### Case 1

In Case 1, since  $\rho_\ell$  and  $\rho_r$  are both less than  $\rho_a$ , the dynamics reduce to the case of simple advection for all future time.

$$\rho_t + a\rho_x = 0 \quad (6.112)$$

Case	Condition
1	$\rho_a > \rho_r > \rho_\ell$
2	$\rho_r > \rho_a > \rho_\ell$
3	$\rho_r > \rho_\ell > \rho_a$
4	$\rho_a > \rho_\ell > \rho_r$
5	$\rho_\ell > \rho_a > \rho_r$
6	$\rho_\ell > \rho_r > \rho_a$

Table 6.1: Riemann Problems for Bounded Advective Control

This case is shown in the fundamental diagram in Figure 6.8.

Hence, the initial profile is simply shifted at the speed given by  $a$ . This is shown in Figure 6.9

### Case 2

Case 2 has the density on the right  $\rho_r$  greater than  $\rho_a$  which is in turn greater than the density on the left  $\rho_\ell$ .

This case is shown in the fundamental diagram in Figure 6.10.

The solution of Case 2 is a shock wave traveling with a speed given by

$$s = \frac{v_M \rho_r \left(1 - \frac{\rho_r}{\rho_m}\right) - a \rho_\ell}{\rho_r - \rho_\ell} \quad (6.113)$$

### Case 3

Case 3 also has the density on the right  $\rho_r$  greater than the density on the left  $\rho_\ell$ . However, in this case both these density values are greater than  $\rho_a$ . Hence, both values lie on the same smooth section of the piecewise smooth curve.

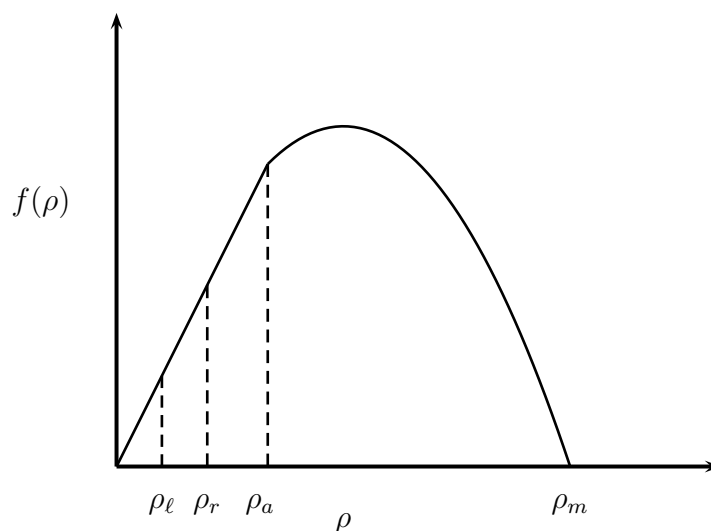


Figure 6.8: Case 1: Fundamental Diagram

This case is shown in the fundamental diagram in Figure 6.12.

The solution of Case 3 is a shock wave traveling with a speed given by

$$s = \frac{v_M \rho_r \left(1 - \frac{\rho_r}{\rho_m}\right) - v_M \rho_\ell \left(1 - \frac{\rho_\ell}{\rho_m}\right)}{\rho_r - \rho_\ell} \quad (6.114)$$

Case 2 and Case 3 characteristics are shown in Figure 6.11.

#### Case 4

Case 4 has the density on the right  $\rho_r$  less than the density on the left  $\rho_\ell$ . Moreover, in this case both these density values are smaller than  $\rho_a$ . Hence, both values lie on the straight line section of the piecewise smooth curve.

This case is shown in the fundamental diagram in Figure 6.13. The solution of Case 4 is a

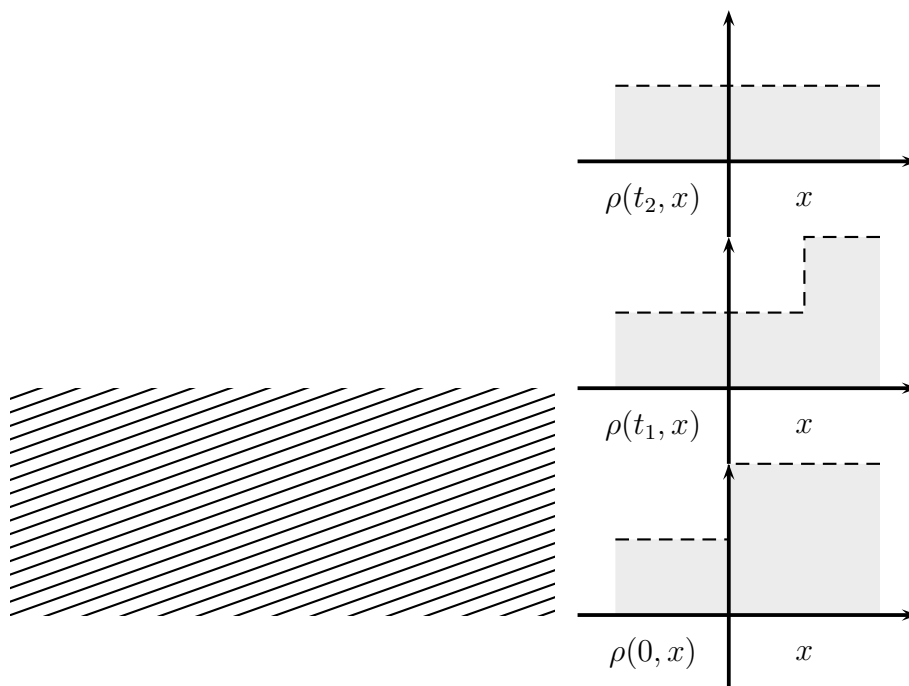


Figure 6.9: Case 1 Characteristics

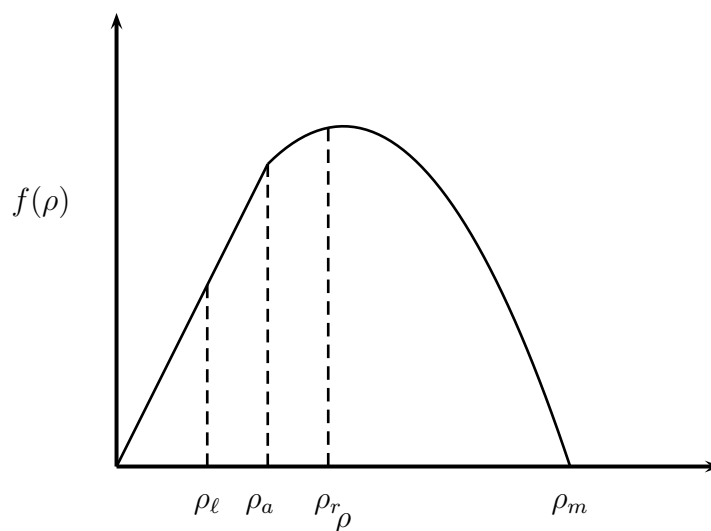


Figure 6.10: Case 2: Fundamental Diagram

pure advection since both densities are smaller than  $\rho_a$ . Case 4 characteristics are shown in Figure 6.14.

### Case 5

Case 5 has the density on the right  $\rho_r$  smaller than  $\rho_a$  which is in turn smaller than the density on the left  $\rho_\ell$ .

This case is shown in the fundamental diagram in Figure 6.15.

The solution of Case 5 is a rarefaction wave and a contact wave.

$$\rho = \begin{cases} \rho_\ell & \text{if } x \leq f'(\rho_\ell)t \\ v(x/t) & \text{if } f'(\rho_\ell)t \leq x \leq at \\ \rho_r & \text{if } x > at \end{cases} \quad (6.115)$$

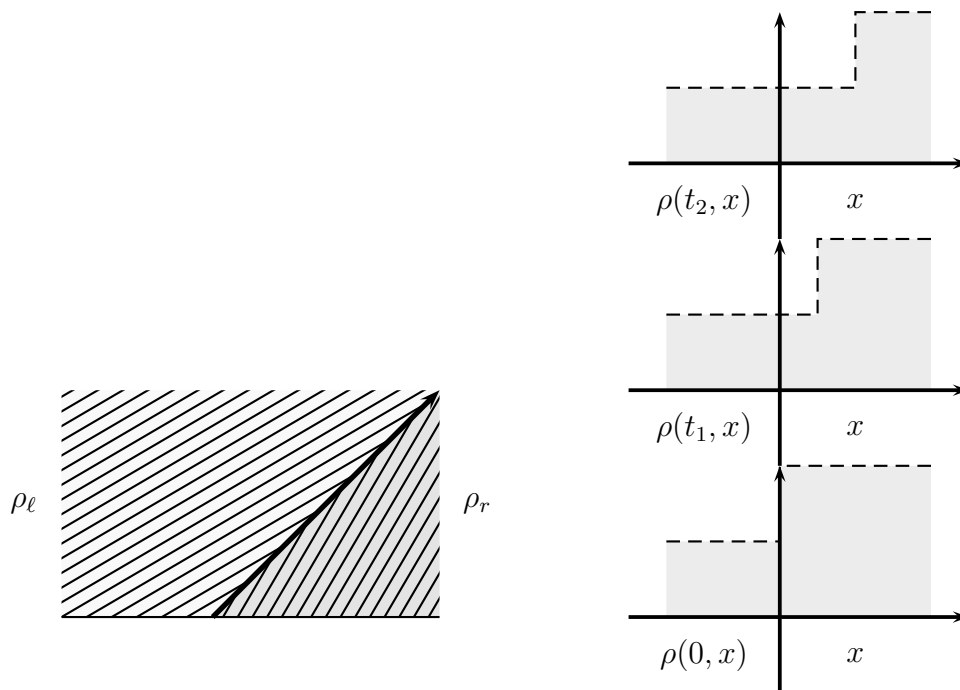


Figure 6.11: Case 2 and Case 3 Characteristics

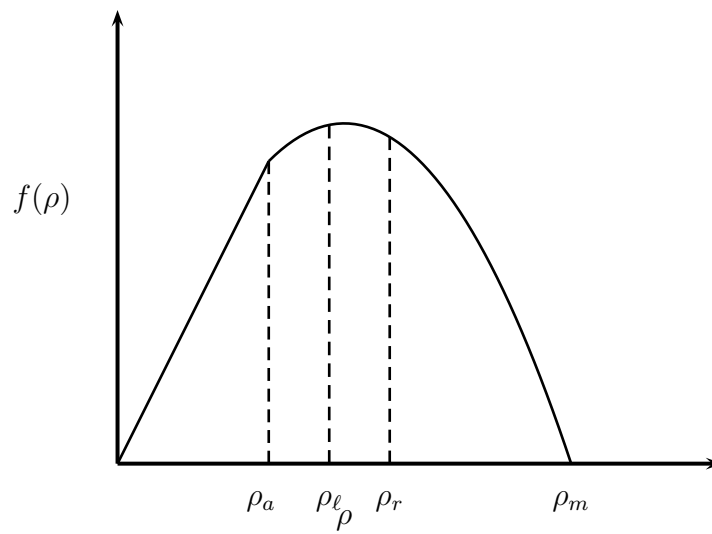


Figure 6.12: Case 3: Fundamental Diagram

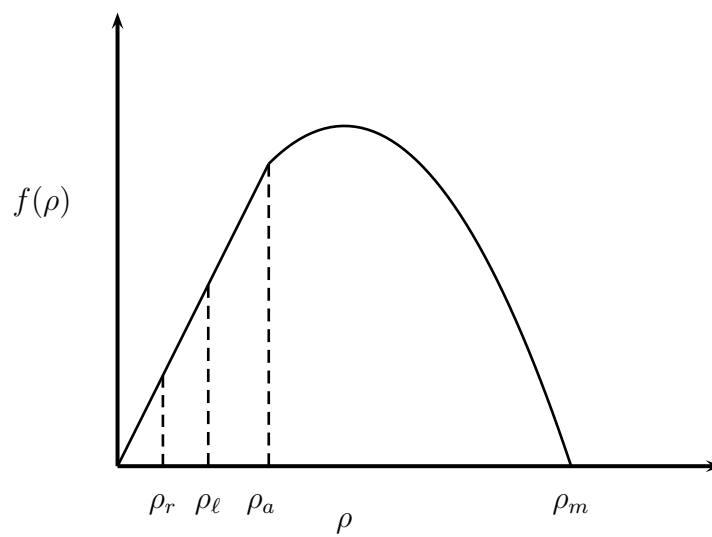


Figure 6.13: Case 4: Fundamental Diagram

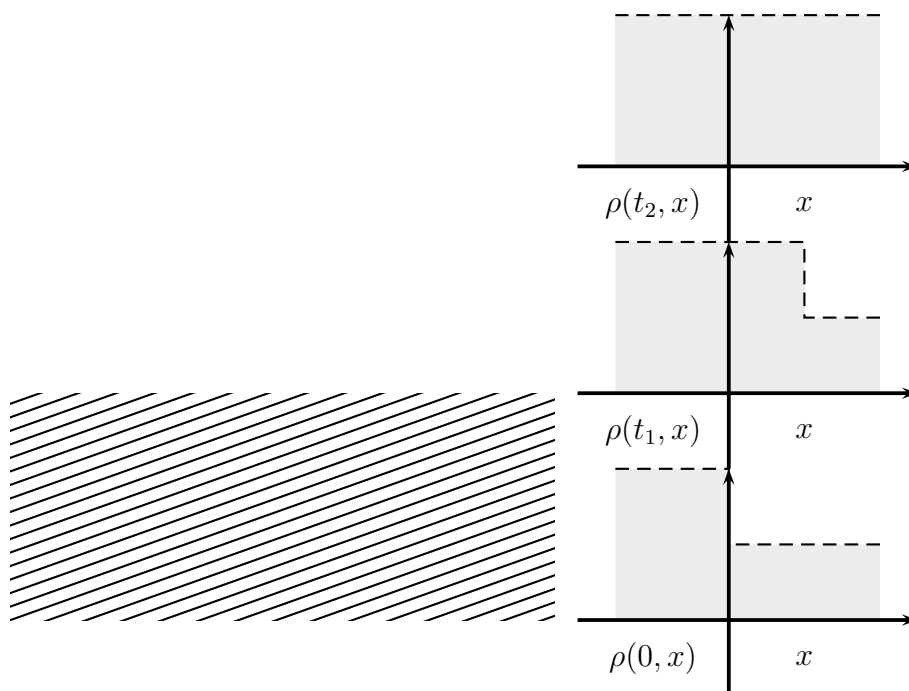


Figure 6.14: Case 4 Characteristics

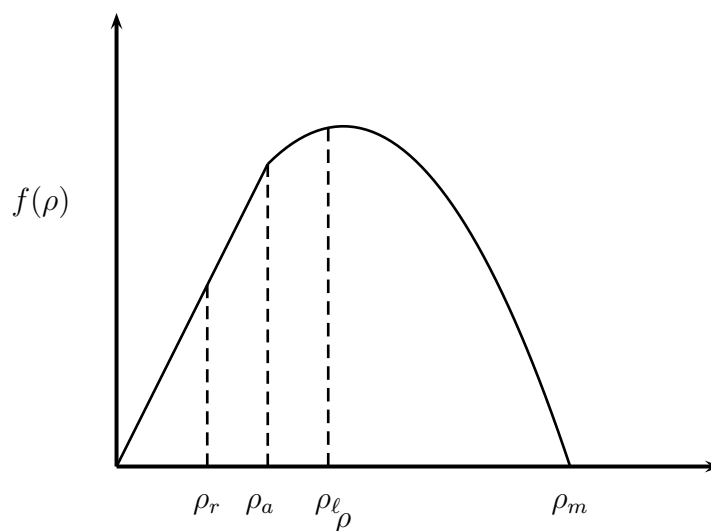


Figure 6.15: Case 5: Fundamental Diagram

where  $v(\xi)$  is the solution to  $f'(v(\xi)) = \xi$ .

**Case 6**

Case 6 has the density  $\rho_a$  smaller than the density on the right  $\rho_r$  which is in turn smaller than the density on the left  $\rho_\ell$ .

This case is shown in the fundamental diagram in Figure 6.17.

The solution of Case 6 is a rarefaction wave. Compared to Case 5 there is no contact wave.

$$\rho = \begin{cases} \rho_\ell & \text{if } x \leq f'(\rho_\ell)t \\ v(x/t) & \text{if } f'(\rho_\ell)t \leq x \leq f'(\rho_r)t \\ \rho_r & \text{if } x > f'(\rho_r)t \end{cases} \tag{6.116}$$

where  $v(\xi)$  is the solution to  $f'(v(\xi)) = \xi$ .

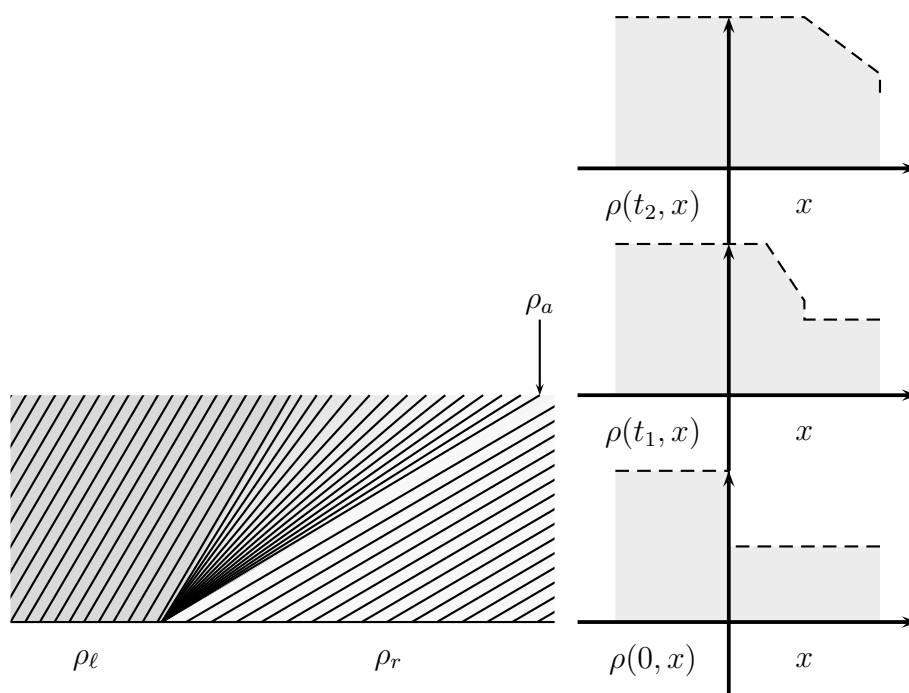


Figure 6.16: Case 5 Characteristics

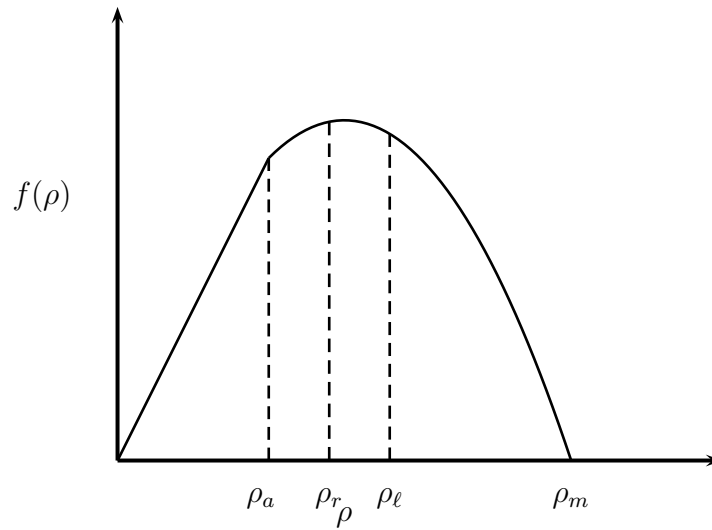


Figure 6.17: Case 6: Fundamental Diagram

### 6.5.2 Existence of Solution

We present the existence theorem for the closed-loop solution for the bounded advection control problem. The proof first involves substituting the feedback control law into the dynamics to obtain the closed-loop solution. The solution can be viewed as a scalar conservation law with a specific flux function, which is Lipschitz. The standard results would follow for existence. We, however, would like to add the result of invariance of density in  $[0, \rho_m]$ . In order to obtain this result we go through the steps of existence theorem using front tracking method, and show that this invariance condition is satisfied at every step.

**Theorem 6.5.2.** *Consider the following initial condition*

$$\rho(0, x) = \rho_0(x) \tag{6.117}$$

where  $\rho_0 \in L^1$  has a bounded variation and also  $0 \leq \rho_0 \leq \rho_m$ , for the dynamics

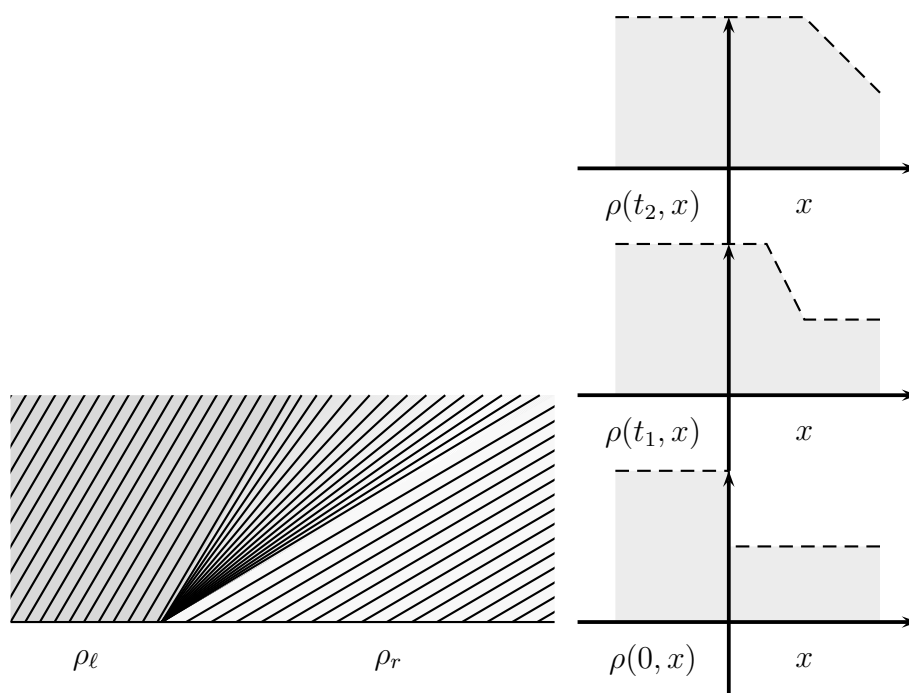


Figure 6.18: Case 6 Characteristics

$$\rho_t + \left( v_f(\rho) \rho \left( 1 - \frac{\rho}{\rho_m} \right) \right)_x = 0 \quad (6.118)$$

The bounded advective control law

$$v_f(\rho) = \min \left( a \left[ 1 - \frac{\rho}{\rho_m} \right]^{-1}, v_M \right) \quad (6.119)$$

where  $a$  and  $v_M$  are two non-negative constants, produces a closed loop dynamics that admits an entropy weak solution  $\rho(t, x)$  for all  $t \geq 0$  such that

$$\text{Total Variation } \rho(t, \cdot) \leq \text{Total Variation } \rho_0 \text{ for all } t \geq 0 \quad (6.120)$$

$$\|\rho(t, \cdot)\|_{L^\infty} \leq \|\rho_0\|_{L^\infty} \text{ for all } t \geq 0 \quad (6.121)$$

and

$$0 \leq \rho(t, x) \leq \rho_m \text{ for all } t \geq 0 \text{ and } x \in \mathbb{R} \quad (6.122)$$

The proof of this theorem relies on using piecewise approximation of functions of bounded variation shown in lemma 6.5.1. The weak entropy solution when the initial data uses this approximation relies on theorem 6.5.1. There are many methods for obtaining the solution for this approximation. One of the methods is the front-tracking method. This method was introduced by Dafermos (see [14]), further developed by Holden (see [31], [32]) and Risebro (see [71]). This method is also used by Bressan (see [10]). The existence is obtained by using the sequential compactness property of functions of bounded variations shown in Helly's theorem 5.3.1.

*Proof.* 1. When  $\min(a, v_M) = 0$  then clearly  $v_f(\rho) = 0$ . This implies that  $\rho_t = 0$ . Hence

$\rho(t, x) = \rho_0(x)$  for all  $t \geq 0$ . In this case then we see that conditions 6.120, 6.121 and 6.122 are satisfied.

2. Now we consider the case when  $a$  and  $v_M$  are both greater than zero. By applying control law 6.119 on the system 6.118 we get the closed loop dynamics that can be expressed as

$$\rho_t + f(\rho)_x = 0 \quad (6.123)$$

The flux is given by

$$f(\rho) = \begin{cases} a\rho & \text{if } \rho \leq \rho_a, \\ v_M \rho \left(1 - \frac{\rho}{\rho_m}\right) & \text{otherwise} \end{cases} \quad (6.124)$$

where

$$\rho_a = \rho_m \left[1 - \frac{a}{v_M}\right] \quad (6.125)$$

The proof will follow in steps as presented next.

**Step 1: Construction of Piecewise Constant Approximations:** Given a positive integer  $k$ , we approximate the flux  $f$  as a piecewise affine function which coincides with  $f$  at  $\{s = 2^{-k}j | j \in \mathbb{Z}\} \cap \{s | 0 \leq s \leq \rho_m\}$ .

The piecewise affine approximation  $f_0$  of the flux  $f$  is shown in Figure 6.19.

The formula for the approximation is given by

$$f_k(s) = \frac{s - 2^{-k}j}{2^{-k}} f(2^{-k}(j+1)) + \frac{2^{-k}(j+1) - s}{2^{-k}} f(2^{-k}j) \quad (6.126)$$

where  $s \in [2^{-k}j, 2^{-k}(j+1)]$  for those  $js$  such that  $[2^{-k}j, 2^{-k}(j+1)] \subset [0, \rho_m]$

Following lemma 6.5.1 we can approximate the initial data  $\rho_0$  by  $\rho_{0_k}$  such that it takes values inside the discrete set  $2^{-k}\mathbb{Z} \cap [0, \rho_m]$  where  $2^{-k}\mathbb{Z} = \{2^{-k}j | j \text{ integer}\}$ .

Now we consider the Cauchy problem

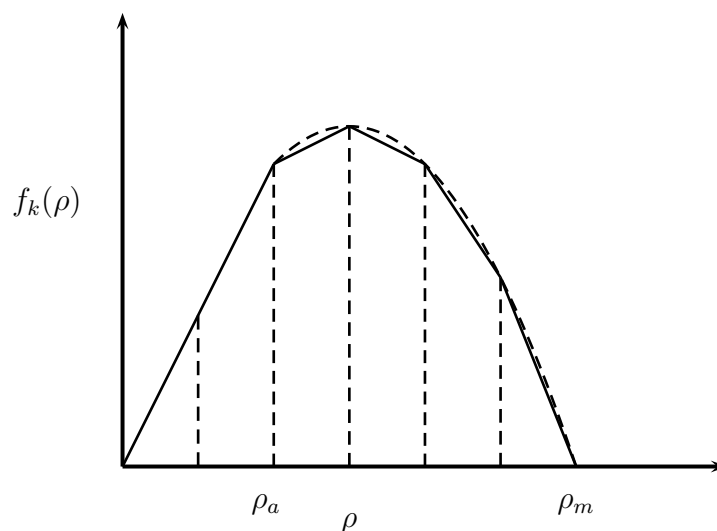


Figure 6.19: Piecewise Affine Flux Approximation

$$\rho_t + f_k(\rho)_x = 0 \quad (6.127)$$

with

$$\rho(0, x) = \rho_{0_k} \quad (6.128)$$

In order to obtain the solution for this problem, we first solve the Riemann problem for the approximation (6.127) and data

$$\rho(0, x) = \begin{cases} \rho^\ell & \text{if } x < 0, \\ \rho^r & \text{if } x > 0 \end{cases} \quad (6.129)$$

where  $\rho^\ell$  and  $\rho^r \in 2^{-k}\mathbb{Z} \cap [0, \rho_m]$ .

*Case 1:*  $\rho^\ell < \rho^r$ : In this case, the solution is obtained by applying the Rankine-Hugoniot condition. The solution is

$$\rho(t, x) = \begin{cases} \rho^\ell & \text{if } x < \lambda t, \\ \rho^r & \text{if } x > \lambda t \end{cases} \quad (6.130)$$

where the shock speed  $\lambda$  is obtained from

$$\lambda = \frac{f_k(\rho^\ell) - f_k(\rho^r)}{\rho^\ell - \rho^r} \quad (6.131)$$

An example of this shock is shown in Figure 6.20.

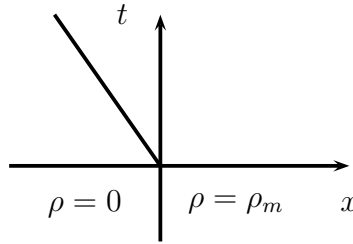


Figure 6.20: Case 1 Shock

*Case 2:*  $\rho^\ell > \rho^r$ : The derivative of  $f_k$  is piecewise constant, non-increasing function, with jumps at points  $\rho^r < m_1 < \dots < m_{q-1} < \rho^\ell$ . Let the shock speeds be given by

$$\lambda_p = \frac{f_k(m_p) - f_k(m_{p-1})}{m_p - m_{p-1}} \quad p = 1, \dots, q. \quad (6.132)$$

Then the following provides a weak, entropy-admissible solution of the Riemann problem.

$$\rho(t, x) = \begin{cases} \rho^\ell & \text{if } x < \lambda_q t, \\ m_p & \text{if } \lambda_{p+1} t < x < \lambda_p t, \quad 1 \leq p \leq q-1 \\ \rho^r & \text{if } x > \lambda_1 t \end{cases} \quad (6.133)$$

Notice that all values again lie in  $2^{-k}\mathbb{Z} \cap [0, \rho_m]$ . An example of this shock is shown in Figure 6.21.

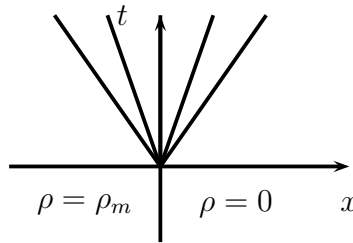


Figure 6.21: Case 2 Shocks

Now, we can consider the Cauchy problem (6.127) with initial data  $\rho_{0_k}$  taking values inside  $2^{-k}\mathbb{Z} \cap [0, \rho_m]$ . Then the solution can be prolonged by using the solution of the Riemann problems just shown, and the solution can be extended until the first time any shock lines intersect. Since the values of the solution still remain inside  $2^{-k}\mathbb{Z} \cap \{0, \rho_m\}$ , new Riemann problems can be solved to generate a new solution that is again extended till there is another time when some shock lines intersect. An example wave front propagation is shown in Figure 6.22.

When multiple discontinuities intersect at a time  $t$ , and if all jumps from left to right across all those discontinuities have the same sign, then all those discontinuities are replaced by a single shock traveling with speed given by

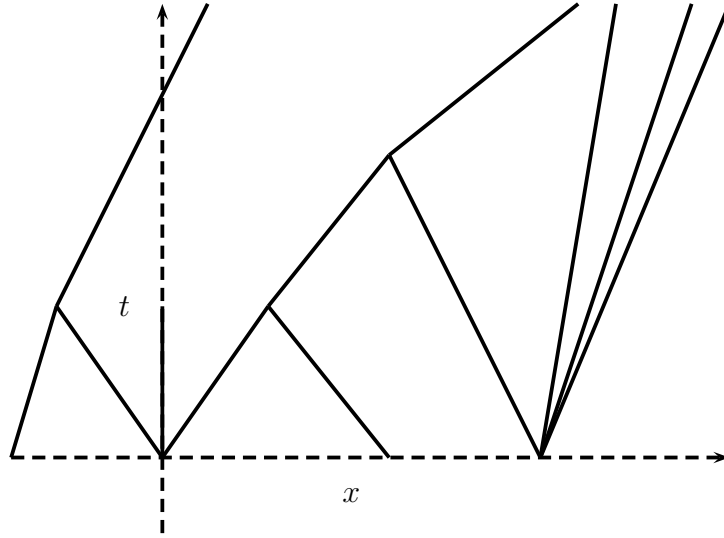


Figure 6.22: Wave Front Tracking

$$s = \frac{f_k(\rho_r) - f_k(\rho_\ell)}{\rho_r - \rho_\ell} \tag{6.134}$$

where  $\rho_r$  and  $\rho_\ell$  are the right most and the leftmost densities of the interacting discontinuities. The total variation of the solution does not change due to this interaction and the number of discontinuity lines decreases. On the other hand if there is a change in sign between the jumps that interact at a point, the total strength of the outgoing wave front is  $|u_r - u_\ell|$  and the total variation of the solution at that point decreases by at least  $2^{1-k}$ . This proves that the total variation is non-increasing over time, and therefore, the total number of interactions are finite. Moreover the solution remains between 0 and  $\rho_m$  for all times.

**Step 2: Obtaining Converging Subsequence:** Using lemma 6.5.1 we can obtain a sequence of approximated piecewise constant initial data such that

- (a)  $\rho_{0_k}(x) \in \{2^{-k}\mathbb{Z}\} \cap [0, \rho_m]$  for all  $x$

$$(b) \|\rho_{0_k}\|_{L^\infty} \leq \rho_m$$

$$(c) \text{Total Variation } \rho_{0_k} \leq \text{Total Variation } \rho_0$$

$$(d) \|\rho_{0_k} - \rho_0\|_{L^1} \rightarrow 0$$

By applying the front tracking algorithm we obtain solution  $\rho_k$  for each initial condition  $\rho_{0_k}$ . We obtain for all  $t, x$  and  $k$

$$\text{Total Variation } \rho_k(t, \cdot) \leq \text{Total Variation } \rho_0 \quad (6.135)$$

and also

$$|\rho_k(t, x)| \leq \rho_m \quad (6.136)$$

and

$$\rho_k(t, x) \in (0, \rho_m) \quad (6.137)$$

Since the flux is Lipschitz continuous, we get

$$|f(m_1) - f(m_2)| \leq L |m_1 - m_2| \quad (6.138)$$

for all  $m_1$  and  $m_2 \in [0, \rho_m]$ . Since the Lipschitz constant  $L$  is also the same for all  $f_k$ s, we obtain for all  $t_1, t_2 \geq 0$

$$\|\rho_k(t_1, \cdot) - \rho_k(t_2, \cdot)\|_{L^1} \leq L |t_1 - t_2| \cdot \text{Total Variation } \rho_0 \quad (6.139)$$

This condition allows us to use theorem 2.4 in [10] as is used in theorem 6.1 in [10] to show that there exists a subsequence which converges to the solution.

□

# Chapter 7

## Simulations for Advective Control

In this chapter we perform numerical simulations to verify the performance of feedback advective control for scalar traffic problems for unbounded and bounded control. There are many good references for numerical methods for hyperbolic systems such as [28], [40], [45], [46] and [81]. We briefly present the basics of Godunov's method adapted from [45], describe the software implementation and then present simulation results for unbounded and bounded feedback advection control.

### 7.1 Godunov's Method

For Godunov's method for scalar conservation laws for variable  $u$  with flux function  $f$ , consider piecewise constant data  $u^n(x, t_n)$  at time  $t_n$  that is constant in each cell  $x_{j-\frac{1}{2}} < x < x_{j+\frac{1}{2}}$ .

One can solve the exact Riemann problem at each discontinuity (see Figure 7.1) and then average over the cells to get piecewise constant approximation at time  $t_2$ . We define the averaged variable as follows.

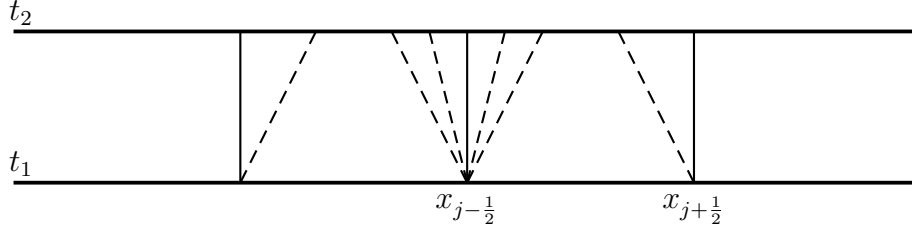


Figure 7.1: Characteristics for Computing Flux

$$U_j^{n+1} = \frac{1}{h} \int_{x_{j-\frac{1}{2}}}^{x_{j+\frac{1}{2}}} u^n(x, t_{n+1}) dx \quad (7.1)$$

We use the integral form of the conservation law in the cell to obtain

$$\begin{aligned} \int_{x_{j-\frac{1}{2}}}^{x_{j+\frac{1}{2}}} u^n(x, t_{n+1}) dx &= \int_{x_{j-\frac{1}{2}}}^{x_{j+\frac{1}{2}}} u^n(x, t_n) dt + \int_{t_n}^{t_{n+1}} f(u^n(x_{j-\frac{1}{2}}, t)) dt \\ &\quad - \int_{t_n}^{t_{n+1}} f(u^n(x_{j+\frac{1}{2}}, t)) dx \end{aligned} \quad (7.2)$$

Defining

$$F(U_j^n, U_{j+1}^n) = \frac{1}{k} \int_{t_n}^{t_{n+1}} f(u^n(x_{j+\frac{1}{2}}, t)) dt \quad (7.3)$$

and using in equation (7.2), we get

$$U_j^{n+1} = U_j^n - \frac{k}{h} F(U_j^n, U_{j+1}^n) - F(U_{j-1}^n, U_j^n) \quad (7.4)$$

As can be seen in Figure 7.1, the solution to the Riemann problem is constant on the vertical line at  $x_{j+\frac{1}{2}}$  from time  $t_n$  to  $t_{n+1}$  and also at all other cell intersection points from  $t_n$  to  $t_{n+1}$ .

The constant value of  $u^n$  only depends on  $U_j^n$  and  $U_{j+1}^n$ . We use the notation  $u^*(U_j^n, U_{j+1}^n)$  for this value. Using this notation, we get the following for Godunov's method.

$$U_j^{n+1} = U_j^n - \frac{k}{h} f(u^*(U_j^n, U_{j+1}^n)) - f(u^*(U_{j-1}^n, U_j^n)) \quad (7.5)$$

The CFL (Courant, Friedrichs and Lewy) condition for the scheme requires

$$\left| \frac{k}{h} \lambda_p(U_j^n) \right| \leq 1 \quad (7.6)$$

for all eigenvalues  $\lambda_p$ .

For a scalar conservation law, given Riemann data on the left and right as  $\rho_\ell$  and  $\rho_r$  respectively, the flux function takes a very simple form as given below. (see [45] for details)

$$F(\rho_\ell, \rho_r) = \begin{cases} \min_{\rho_\ell \leq \rho \leq \rho_r} f(\rho) & \text{if } \rho_\ell \leq \rho_r, \\ \max_{\rho_\ell \leq \rho \leq \rho_r} f(\rho) & \text{if } \rho_\ell > \rho_r \end{cases} \quad (7.7)$$

### 7.1.1 Matlab Code

The Matlab code for the simulations is written in three files. The main file is *Godunov.m* that has the Godunov algorithm coded. That file uses file *initial.m* for the initial data, and uses *flux.m* for the formula for the flux function. The file dependencies are shown in Figure 7.2.

#### Main File

```
a = -20; b = 20; T = 4; M = 500; rhom = 0.2;
n = 100; drho = rhom/n; rho = 0:drho:rhom;
frho = flux(rho);
```

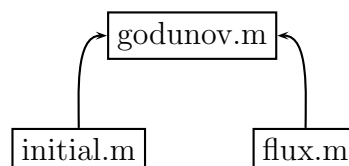


Figure 7.2: File Dependencies for Matlab Simulation Code

```
[qmax,s] = max(frho);  
rhostar = rho(s);  
% CFL Condition  
lambda = max(abs(frho(2:n)-frho(1:n-1)))/drho;  
h = (b-a) / M;  
ka = 0.5 * h / lambda;  
N = ceil(T/ka);  
k = T / N;  
% Initialise:  
xticks = transpose(a+h/2:h:b-h/2);  
U = zeros(M,N+1);  
U(:,1) = initial(xticks);  
% Algorithm  
for j=1:N  
    rhol = U(1:M-1,j);  
    rhor = U(2:M,j);  
    qval = flux(U(:,j));  
    ql = qval(1:M-1);  
    qr = qval(2:M);  
    case1 = rhol <= rhor;
```

```
case2 = rho1 > rhostar & rhostar > rhor;
case3 = not(case1 | case2);
Q = case1 .* min(ql,qr) + case2 * qmax + case3 .* max(ql,qr);
% Specifying Boundary Flows
Q = [flux(initial(a)); Q; qval(M)];
U(:,j+1)=U(:,j) + (k/h) * (Q(1:M) - Q(2:M+1));
% Plotting
if floor(j/20)==j/20
plot(xticks,U(:,j+1),'k','LineWidth',2)
axis([a b 0 0.5*rhom])
ylabel('density')
xlabel('x')
pause
end
end
```

### Initial Data File

```
function init=initial(x)
init=0.09 * exp(-x.^2/50);
```

### Flux File

```
function fl=flux(rho)
vf = 15;
rhom = 0.2;
fl = vf*(1-rho/rhomax).*rho;
```

## Output Plots

For this sample set of files the control variable, the free flow speed, is kept at a constant. The simulation plots for this example are shown in Figure 7.3. The plots clearly show how shocks are formed in finite time even when the initial density profile is smooth.

The model that we are simulating is

$$\rho_t + \left[ v_f \rho \left( 1 - \frac{\rho}{\rho_m} \right) \right]_x = 0 \quad (7.8)$$

The initial density function in the simulation is

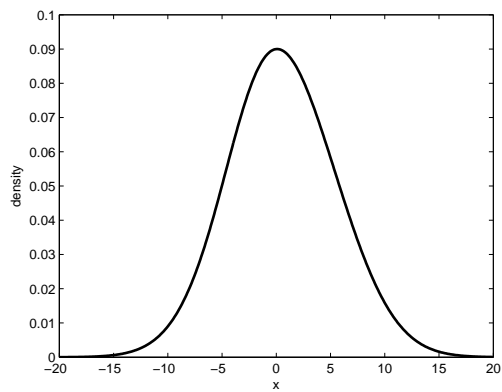
$$\rho_0 = 0.09 \exp\left(\frac{-x^2}{50}\right) \quad (7.9)$$

The simulation parameters are given in Table 7.1.

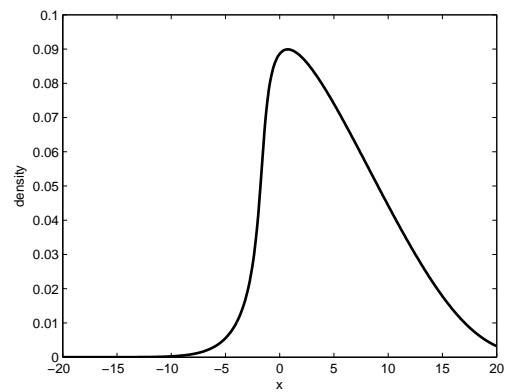
Parameter	Value
$v_f$	15
$\rho_m$	0.2
Cells	500
Left Boundary	$x = -20$
Right Boundary	$x = 20$

Table 7.1: Simulation Parameters for Constant Free Flow Speed

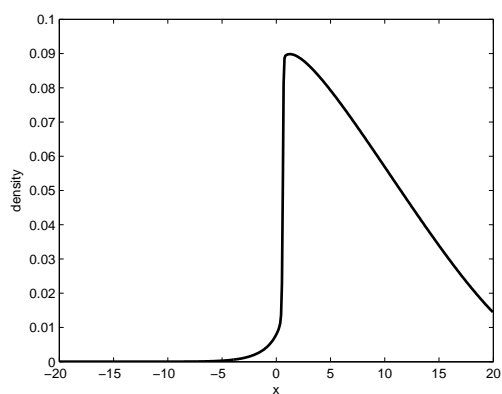
Lower density initially on the left side travels faster than the higher density in front creating a shock wave.



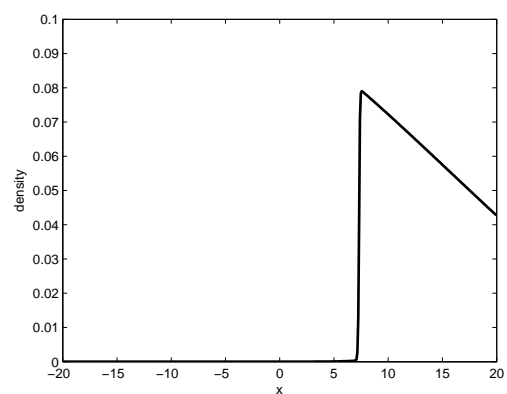
(a) Time 1



(b) Time 2



(c) Time 3



(d) Time 4

Figure 7.3: Traffic Flow with Constant Free Flow Speed

## 7.2 Simulation Results for Advective Control

Simulations are performed for the model given by (7.8) using the Godunov scheme for advective feedback unbounded and bounded controls.

### 7.2.1 Unbounded Control Results

The unbounded control produces pure advection of desired speed. The unbounded control is given by

$$v_f = a \left[ \left( 1 - \frac{\rho}{\rho_m} \right) \right]^{-1} \quad (7.10)$$

For the simulation performed here, we take  $a = 11.25$ . The resulting plots are shown in Figure 7.4. The initial data is the same as in (7.9). The flux file is changed to the following.

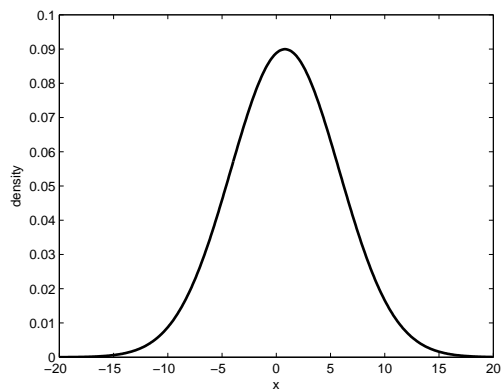
```
function fl=flux(rho)
fl = 11.25.*rho;
```

### 7.2.2 Bounded Control Results

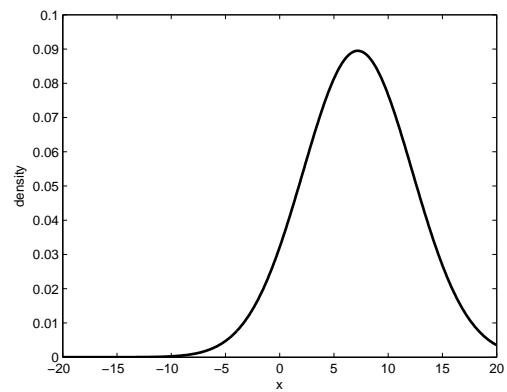
The bounded advective control is given by

$$v_f = \min \left( v_M, b \left[ \left( 1 - \frac{\rho}{\rho_m} \right) \right]^{-1} \right) \quad (7.11)$$

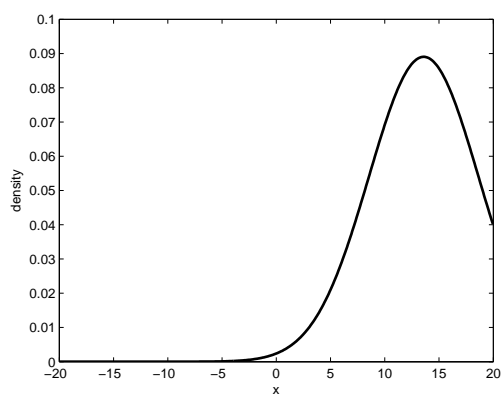
For the simulation performed here, we take  $v_M = 11.25$ . This results in  $\rho_a = 0.05$  which is the density at which  $f'(\rho^+) \neq f'(\rho^-)$ . The resulting plots are shown in Figure 7.5. The initial data is the same as in (7.9). The flux file is changed to the following.



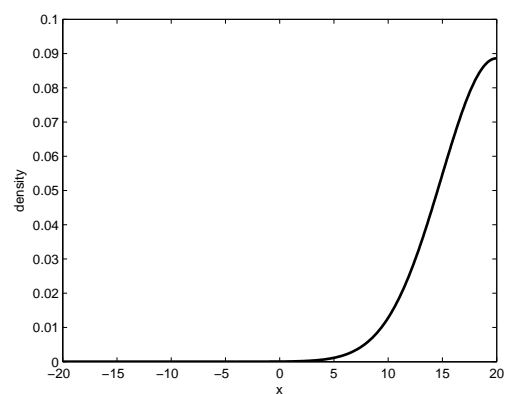
(a) Time 1



(b) Time 2



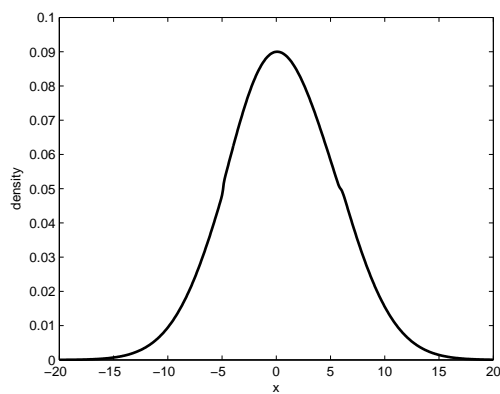
(c) Time 3



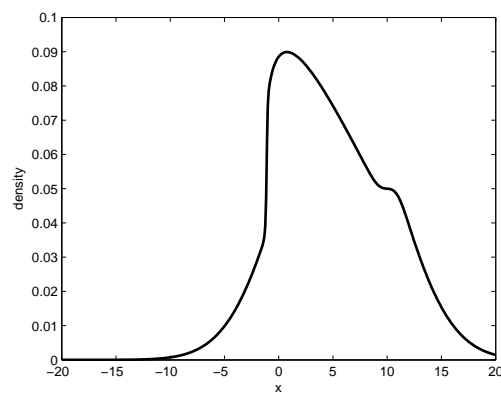
(d) Time 4

Figure 7.4: Unbounded Feedback Advective Control

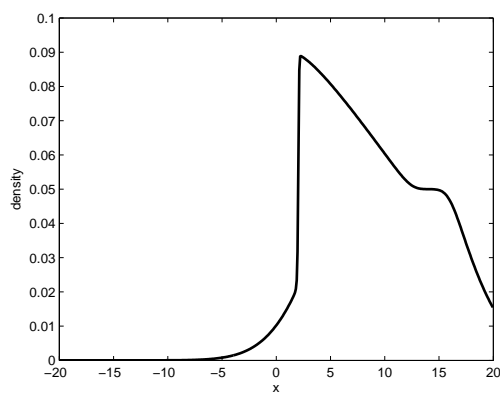
```
function fl=flux(rho)
vf = 15;
rhom = 0.2;
rhoa = 0.05;
fa = vf*(1-rhoa/rhom);
case1 = rho <= rhoa;
case2 = rho > rhoa;
fl = case1 .* fa.*rho + case2 .* vf.*(1-rho/rhom).*rho;
```



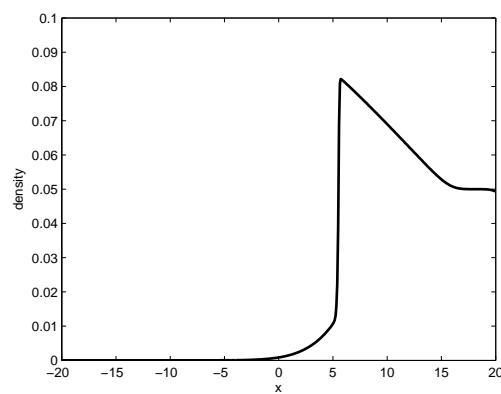
(a) Time 1



(b) Time 2



(c) Time 3



(d) Time 4

Figure 7.5: Bounded Feedback Advective Control

It is interesting to observe the behavior of the density profile where density is equal to  $\rho_a$  which is equal to 0.05 in this simulation. To get a better understanding and also for validation we will perform simulations for the six different Riemann problems for bounded feedback advective control.

### Simulation of Riemann Problems for Bounded Feedback Advective Control

We consider all types of possible Riemann problems as shown in Table 7.2.

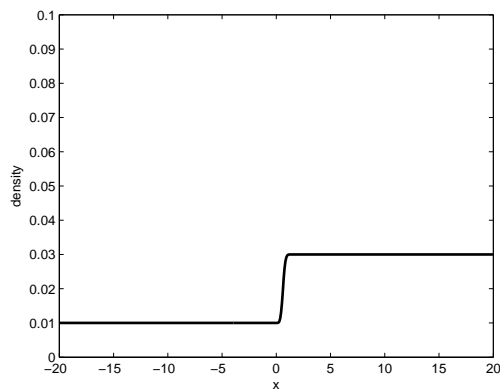
Case	Condition
1	$\rho_a = 0.05 > \rho_r = 0.03 > \rho_\ell = 0.01$
2	$\rho_r = 0.07 > \rho_a = 0.05 > \rho_\ell = 0.03$
3	$\rho_r = 0.09 > \rho_\ell = 0.07 > \rho_a = 0.05$
4	$\rho_a = 0.05 > \rho_\ell = 0.03 > \rho_r = 0.01$
5	$\rho_\ell = 0.07 > \rho_a = 0.05 > \rho_r = 0.03$
6	$\rho_\ell = 0.09 > \rho_r = 0.07 > \rho_a = 0.05$

Table 7.2: Riemann Problems for Bounded Advective Control Simulations

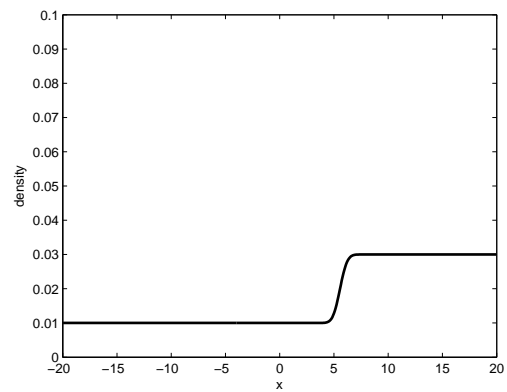
**Case 1** The initial data file used in the simulation for this case is

```
function init=initial(x)
case1 = x<=0;
case2 = x>0;
init = case1 .* 0.01 + case2 .* 0.03;
```

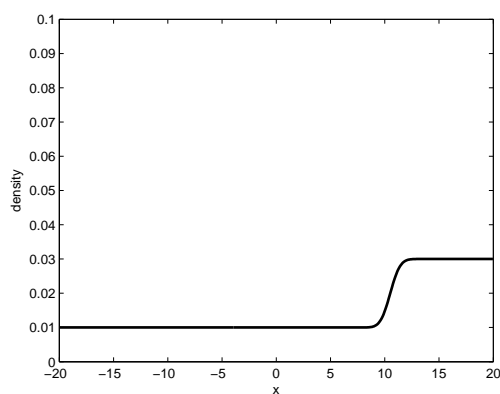
Since both densities in this case are below  $\rho_a$ , the behavior of the closed loop system is pure advection. The simulation results are shown in Figure 7.6.



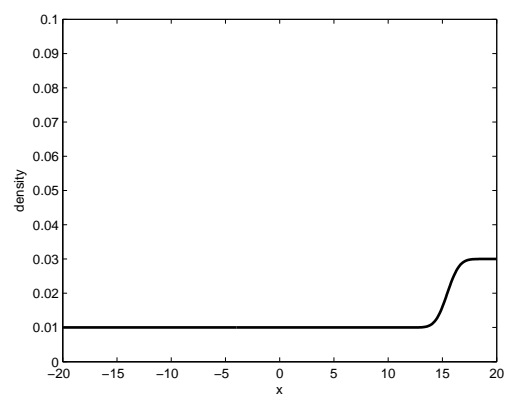
(a) Time 1



(b) Time 2



(c) Time 3



(d) Time 4

Figure 7.6: Bounded Feedback Advective Control: Case1

**Case 2** The initial data file used in the simulation for this case is

```
function init=initial(x)
case1 = x<=0;
case2 = x>0;
init = case1 .* 0.03 + case2 .* 0.07;
```

Since the density on the left is below  $\rho_a$  and the density on the right is above  $\rho_a$ , the behavior of the closed loop system is a shock wave traveling with the corresponding shock speed given by

$$s = \frac{v_M \rho_r \left(1 - \frac{\rho_r}{\rho_m}\right) - a \rho_\ell}{\rho_r - \rho_\ell} \quad (7.12)$$

The simulation results are shown in Figure 7.7.

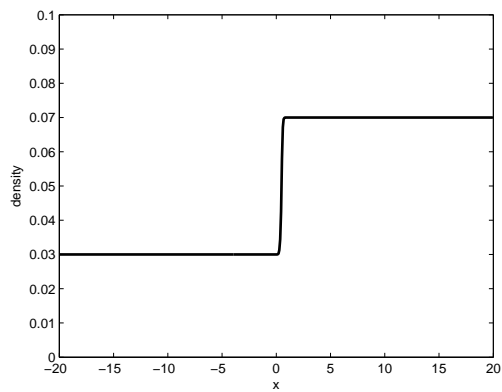
**Case 3** The initial data file used in the simulation for this case is

```
function init=initial(x)
case1 = x<=0;
case2 = x>0;
init = case1 .* 0.07 + case2 .* 0.09;
```

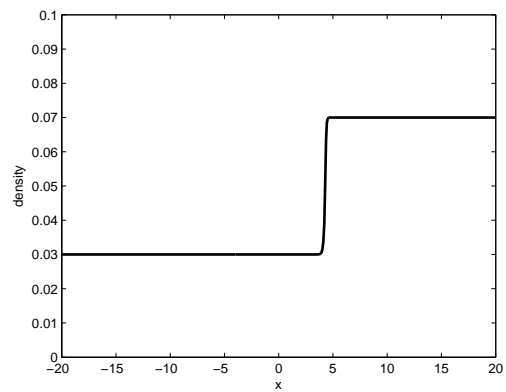
Since the density on the left is less than the density on the right, the behavior of the closed loop system is again a shock wave traveling with the corresponding shock speed given by

$$s = \frac{v_M \rho_r \left(1 - \frac{\rho_r}{\rho_m}\right) - v_M \rho_\ell \left(1 - \frac{\rho_\ell}{\rho_m}\right)}{\rho_r - \rho_\ell} \quad (7.13)$$

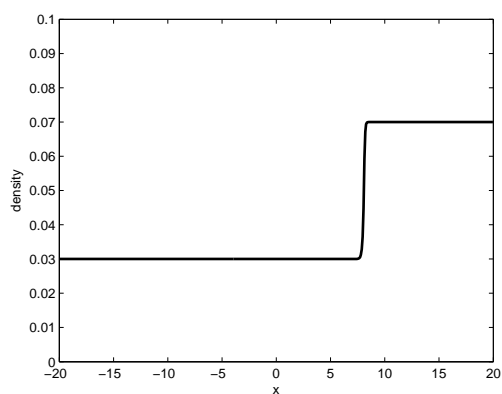
The simulation results are shown in Figure 7.8.



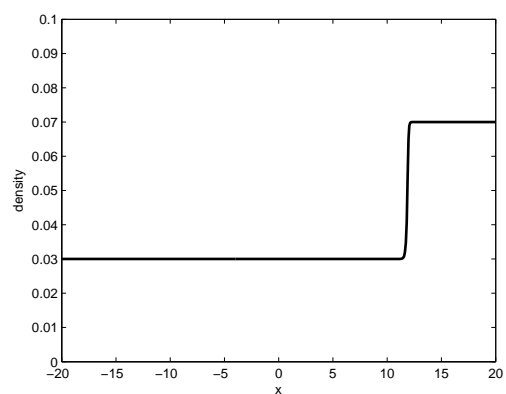
(a) Time 1



(b) Time 2

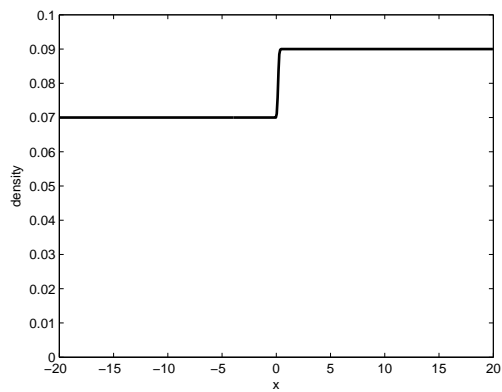


(c) Time 3

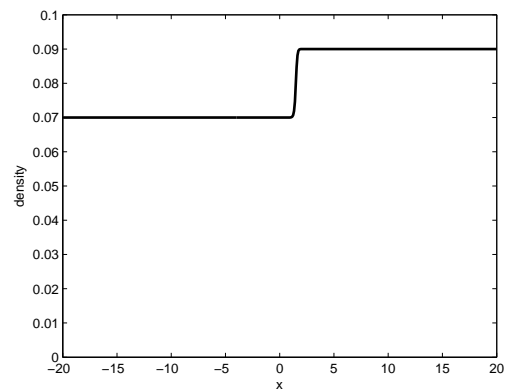


(d) Time 4

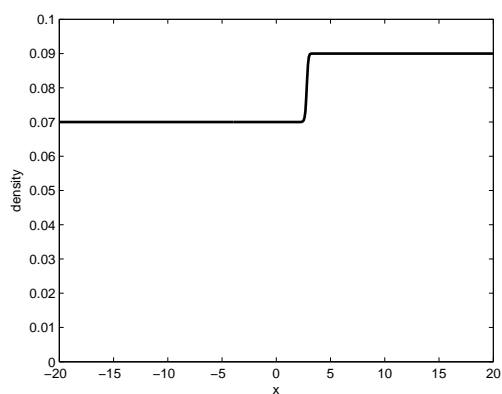
Figure 7.7: Bounded Feedback Advective Control: Case2



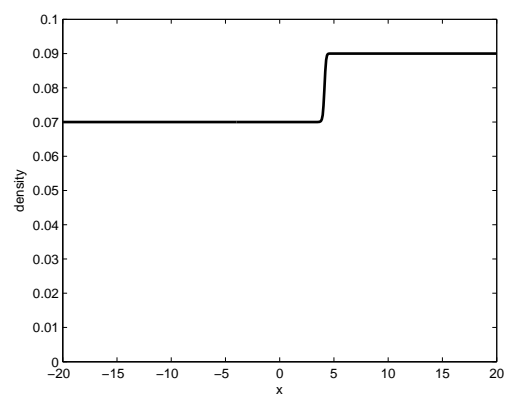
(a) Time 1



(b) Time 2



(c) Time 3



(d) Time 4

Figure 7.8: Bounded Feedback Advective Control: Case3

**Case 4** The initial data file used in the simulation for this case is

```
function init=initial(x)
case1 = x<=0;
case2 = x>0;
init = case1 .* 0.03 + case2 .* 0.01;
```

Since both densities are less than  $\rho_a$ , the initial density profile moves with pure advection in this case.

The simulation results are shown in Figure 7.9.

**Case 5** The initial data file used in the simulation for this case is

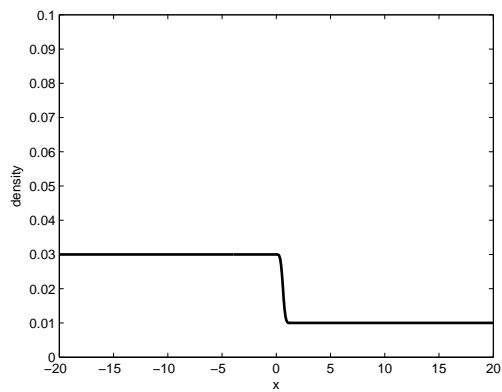
```
function init=initial(x)
case1 = x<=0;
case2 = x>0;
init = case1 .* 0.07 + case2 .* 0.03;
```

Case 5 has the density on the right  $\rho_r$  smaller than  $\rho_a$  which is in turn smaller than the density on the left  $\rho_\ell$ . The solution of Case 5 is a rarefaction wave and a contact wave.

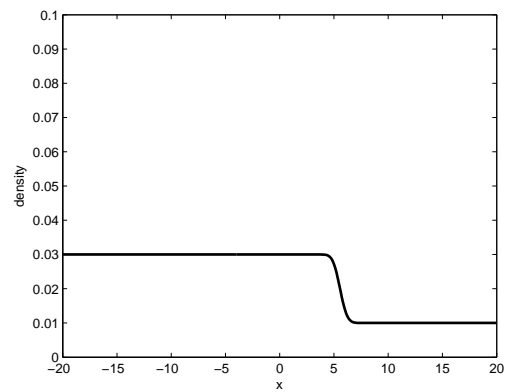
The simulation results are shown in Figure 7.10.

**Case 6** The initial data file used in the simulation for this case is

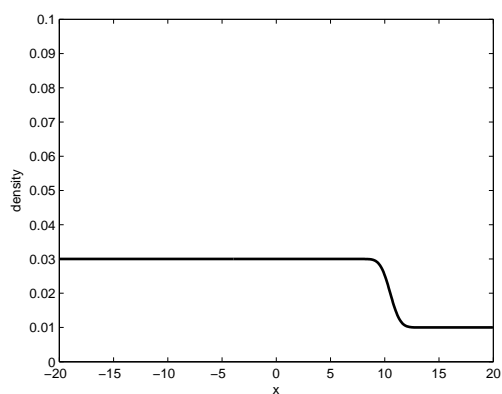
```
function init=initial(x)
case1 = x<=0;
case2 = x>0;
init = case1 .* 0.09 + case2 .* 0.07;
```



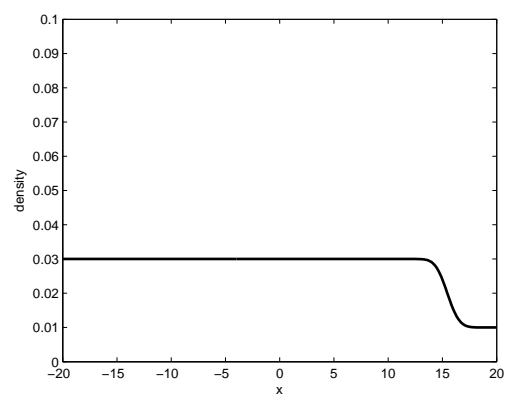
(a) Time 1



(b) Time 2

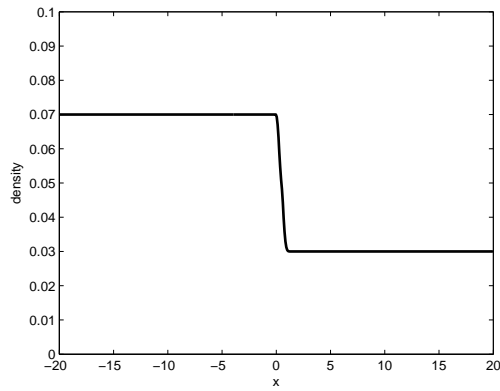


(c) Time 3

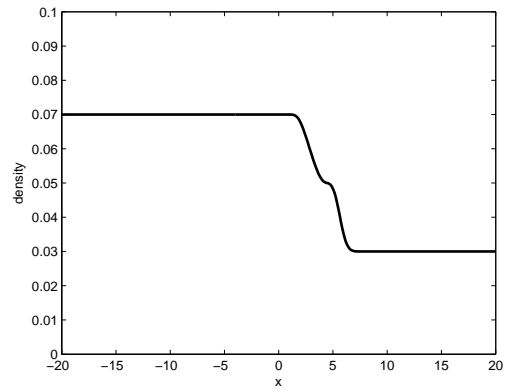


(d) Time 4

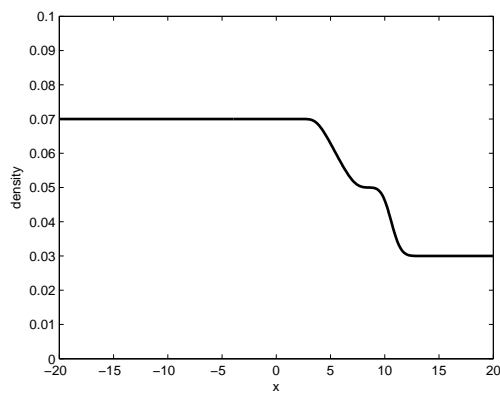
Figure 7.9: Bounded Feedback Advective Control: Case4



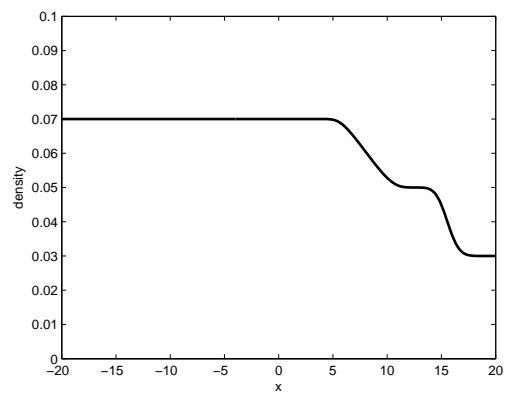
(a) Time 1



(b) Time 2



(c) Time 3

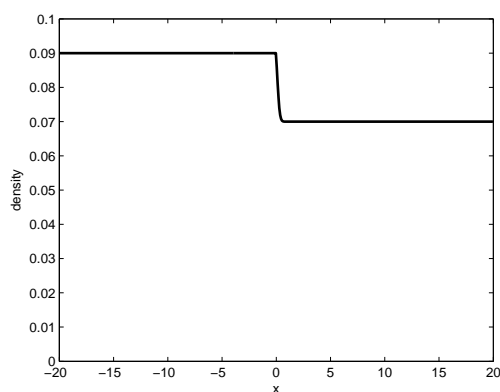


(d) Time 4

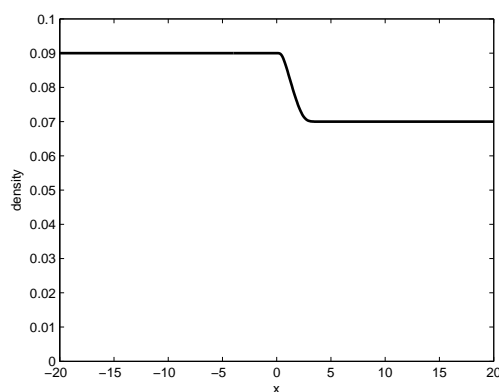
Figure 7.10: Bounded Feedback Advective Control: Case5

Case 6 has the density on the right smaller than the density on the left and moreover these are both greater than  $\rho_a$ . The solution of Case 6 is a rarefaction wave.

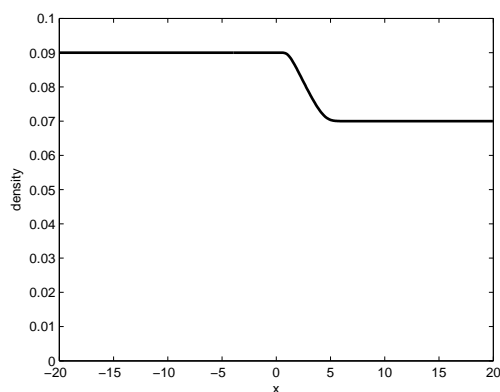
The simulation results are shown in Figure 7.11.



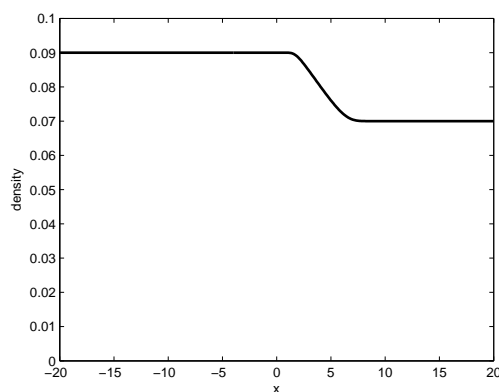
(a) Time 1



(b) Time 2



(c) Time 3



(d) Time 4

Figure 7.11: Bounded Feedback Advective Control: Case6

# Chapter 8

## Conclusions

### 8.1 Summary

This dissertation presented the derivation of conservation laws for scalar case as well as vector models. Then more details based on physics and traffic behavior were provided for specific model for gas dynamics and traffic dynamics. The reason for that was that traffic models are developed following the compressible gas behavior. Pedestrian models were developed by extending the one-dimensional traffic models to two dimensions and also by adding multi-directional motion. The system of PDE models for traffic were developed using relaxation models, which in the limit of the relaxation parameter going to zero turn into the corresponding scalar traffic models.

Analysis of the traffic models was provided. The meaning of solutions in terms of distributional and weak solutions was presented. The review of wellposedness was presented for the scalar conservation models based on entropy admissible solutions.

Existence of optimal control for scalar traffic models were developed. Feedback control laws were designed that obtained various closed loop controlled traffic behavior. These were: unbounded and bounded versions of advective, diffusive, and advective-diffusive controllers.

Wellposedness of the unbounded closed loop systems was simple, since the closed-loop dynamics for those cases became linear. The bounded advective case was studied rigorously. Its existence was proved using the front tracking method. Six different Riemann problems were analyzed. Moreover, qualitative properties of the closed loop behavior of the relaxation model with bounded advective control was also developed.

Godunov scheme for numerical simulation was presented, coded and then used for performing simulations for unbounded and bounded feedback advective controls. The simulation results confirm the analysis results for the controllers.

## 8.2 Contributions

The contributions of this dissertation work are listed below.

1. The two dimensional traffic models that use magnitude and angle vector fields to for multi-directional pedestrian movement have been proposed and their analysis has been presented in Chapter 4.
2. Chapter 6 presented the  $L^1$  contraction property of the solution with respect to the controls, existence results for optimal control in the space of constant controls.
3. Chapter 6 also presented feedback control for scalar conservation law, specifically for unbounded and bounded case, and also one and two-dimensional problems, we presented the following:
  - (a) feedback advection control
  - (b) feedback diffusion control
  - (c) feedback advective-diffusion control
  - (d) advective feedback control for relaxation systems

Wellposedness for bounded advection control using front tracking method and Riemann problems for bounded feedback advective control were also presented.

4. Chapter 7 used Godunov scheme for numerical simulation and presented the results for unbounded and bounded feedback advective control that provided validation for the analysis of the controllers.

### 8.3 Future Work

There are many areas of this dissertation that can be enhanced by further research. These are listed below.

1. Wellposedness analysis needs to be performed for bounded advective control in two dimensions, as well as for all bounded diffusion and advective-diffusion control. Wellposedness analysis also needs to be performed for system versions of these feedback laws.
2. Although existence results for optimal control are provided, the specific controllers can be designed.
3. Numerical simulations need to be developed for all various controllers proposed such as bounded diffusion, bounded advective-diffusion and relaxation versions of these.
4. Analysis and design of discretized controls and their convergence results for these controllers would be very useful for practical implementation. Study of other implementation issues would also be very useful. These effects could include delays and noise.

# Bibliography

- [1] S. Al-nasur. *New Models for Crowd Dynamics and Control*. PhD thesis, Virginia Tech, 2006.
- [2] S. Al-nasur and P. Kachroo. A microscopic-to-macroscopic crowd dynamic model. In *9th International IEEE Conference on ITSC*, pages 606–611, 2006.
- [3] Judith B. Bruckner Andrew M. Bruckner and Brian S. Thomson. *Real Analysis*. Prentice Hall, 1996.
- [4] A. Aw and M. Rascle. Reconstruction of ‘second order’ models of traffic flow. *SIMA J. Appl. Math.*, 60:916–938, 2000.
- [5] G. Gripenberg B. Cockburn and S-O. Londen. On convergence to entropy solutions of a single conservation law. *J. Differential Equations*, (128):206–251, 1996.
- [6] Joseph Ball, Marty Day, and Pushkin Kachroo. Robust feedback control of a single server queueing system. *Mathematics of Control, Signal, and Systems*, 12(2):307–345, 1999.
- [7] M. Bando. Dynamical model of traffic congestion and numerical simulation. *Phy. Rev. E*, 51:1035–1042, 1995.
- [8] Robert G. Bartle. *The Elements of Integration and Lebesgue Measure*. Wiley, 1995.

- [9] Sylvie Benzoni-Gavage and Denis Serre. *Multi-dimensional Hyperbolic Partial Differential Equations: First-order Systems and Applications*. Oxford Mathematical Monographs, 2006.
- [10] Alberto Bressan. *Hyperbolic Systems of Conservation Laws: The One-Dimensional Cauchy Problem*. Oxford University Press, 2005.
- [11] A.Y. Leroux C. Bardos and J.C. Nedelec. First order quasilinear equations with boundary conditions. *Comm. Partial Diff. Eqs.*, 4:1017–1034, 1979.
- [12] R. E. Chandler, R. Herman, and E. W. Montroll. Traffic dynamics; studies in car following. *Operations Research*, (6):165–184, 1958.
- [13] Richard Courant and K.O. Friedrichs. *Supersonic Flow and Shock Waves*. Springer, 1999.
- [14] C. M. Dafermos. Polygonal approximations of solutions of the initial value problem for a conservation law. *J. Math. Anal. Appl.*, 38:33–41, 1972.
- [15] Constantine M. Dafermos. *Hyperbolic Conservation Laws in Continuum Physics*. Springer, 2005.
- [16] C. Daganzo. Requiem for second-order fluid approximation to traffic flow. *Transp. Res. B*, 29B(4):277–286, 1995.
- [17] Robert Resnick David Halliday and Jearl Walker. *Fundamentals of Physics*. Wiley, 2004.
- [18] Robert Herman Denos C. Gazis and Renfrey B. Potts. Car-following theory of steady-state traffic flow. *Operations Research*, 7(4).
- [19] Robert Herman Denos C. Gazis and Richard W. Rothery. Nonlinear follow-the-leader models of traffic flow. *Operations Research*, 9(4).
- [20] Emmanuele DiBenedetto. *Real Analysis*. Birkhauser, 2005.

- [21] R.J. DiPerna. Global existence of solutions to nonlinear systems of conservation laws. *J. Diff. Eqns.*, 20:187–212, 1976.
- [22] Donald R. Drew. *Traffic Flow Theory and Control*. McGraw Hill, 1968.
- [23] Lawrence. C. Evans. *Partial Differential Equations*. American Mathematical Society, 1998.
- [24] Hector O. Fattorini. *Infinite Dimensional Optimization and Control Theory*. Cambridge University Press, 1999.
- [25] A. V. Fursikov. *Optimal control of distributed systems. Theory and applications*. American Mathematical Society, Providence, RI, 2000.
- [26] Denos C. Gazis. The origins of traffic theory. *Operations Research*, 50(1).
- [27] James Glimm. Solutions in the large for nonlinear hyperbolic systems of equations. *Comm. Pure Appl. Math.*, 18:697–715, 1965.
- [28] Edwige Godlewski and Pierre-Arnaud Raviart. *Numerical Approximation of Hyperbolic Systems of Conservation Laws*. Springer, 1996.
- [29] H. Greenberg. An analysis of traffic flow. *Operationa Research*, 7:78–85, 1959.
- [30] B. D. Greenshields. A study in highway capacity. *Highway Research Board*, 14:458, 1935.
- [31] L. Holden H. Holden and R. Hegh-Krohn. A numerical method for first order nonlinear scalar conservation laws in one dimension. *Comput. Math. Applic.*, 15:595–602, 1988.
- [32] Helge Holden and Nils H. Risebro. *Front Tracking for Hyperbolic Conservation Laws*. Springer-Verlag, 2002.
- [33] M. Rokyta J. Malek, J. Necas and M. Ruzicka. *Weak and Measure-Valued Solutions to Evolutionary PDEs*. CRC, 1996.

- [34] J. L. Schofer J. S. Drake and A. D. May. A statistical analysis of speed density hypothesis. In *Third Symposium on the Theory of Traffic Flow Proceedings*, New York. Elsevier, North Holland Inc.
- [35] Yingjie Liu James Glimm, Xiao Lin Li and Ning Zhao. Conservative front tracking and level set algorithms. *PNAS*, 98(25):14198–14201, 2001.
- [36] S. Jin and Z. Xin. The relaxation schemes for systems of conservation laws in arbitrary space dimensions. *Comm. Pure Appl. Math.*, 48:235–276, 1995.
- [37] P. Kachroo and K. Ozaby. *Feedback Control Theory for Ramp Metering in Intelligent Transportation Systems*. Kulwer, 2004.
- [38] Pushkin Kachroo and Kaan Ozbay. *Feedback Control Theory For Dynamic Traffic Assignment*. Springer-Verlag, 1999.
- [39] Axel Klar and Raimund Wegener. Kinetic derivation of macroscopic anticipation models for vehicular traffic. *SIAM Journal on Applied Mathematics*, 60(5):1749–1766, 2000.
- [40] D. Kröner. *Numerical Schemes for Conservation Laws*. Wiley, Teubner, 1997.
- [41] S. N. Kruzkov. First order quasi-linear equations in several independent variables. *Math. USSR Sbornik*, 10:217–243, 1970.
- [42] P.D Lax. Hyperbolic systems of conservation laws and mathematical theory of shock waves. In *SIMA Regional Conf. Series in Appl. Math*, number 11, 1972.
- [43] P.D Lax. *Linear Algebra*. Wiley, 1996.
- [44] P.D Lax. *Hyperbolic Partial Differential Equations*. AMS, 2006.
- [45] R. J. Leveque. *Numerical Methods for Conservation Laws*. Birkhauser, 1992.
- [46] R. J. Leveque. *Finite Volume Methods for Hyperbolic Problems*. Cambridge University Press, UK, 2002.

- [47] Tong Li. Global solutions and zero relaxation limit for a traffic flow model. *SIAM Journal on Applied Mathematics*, 61(3):1042–1061, 2000.
- [48] Tong Li. L1 stability of conservation laws for a traffic flow model. *Electronic Journal of Differential Equations*, ISSN: 1072-6691, 2001(14):1–18, 2001.
- [49] M. J. Lighthill and G. B. Whitham. On kinematic waves. i:flow movement in long rivers. ii:a theory of traffic on long crowded roads. In *Proc. Royal Soc.*, number A229, pages 281–345, 1955.
- [50] Jacques Louis Lions. *Optimal Control of Systems Governed by Partial Differential Equations*. Springer, 1971.
- [51] Jerrold E. Marsden and Anthony Tromba. *Vector Calculus*. W. H. Freeman, 5th edition, 2003.
- [52] A. C. May. *Traffic Flow Fundamental*. Prentice Hall, New Jersey, 1990.
- [53] J.V. Morgan. *Numerical Methods for Macroscopic Traffic Models*. PhD thesis, University of Reading, 2002.
- [54] K. Nagel. Partical hopping models and traffic flow theory. *Phy. Rev. E*, (53):4655–4672, 1996.
- [55] K. Nagel and M. Shreckenberg. A cellular automaton model for freeway traffic. *J. Phisique I*, 2(12).
- [56] I. P. Natanson. *Theory of functions of a real variable*. F. Ungar, 1955.
- [57] Hermann Knoflach, Nathalie Waldau, Peter Gattermann and Michael Schreckenberg. *Pedestrian and Evacuation Dynamics 2005*. Springer, 2007.
- [58] Lucien W Neustadt. *Optimization: A theory of necessary conditions*. Princeton University Press, 1976.

- [59] G. F. Newell. Nonlinear effects in the dynamics of car following. *Operations Research*, 9(2).
- [60] O.A. Oleinik. Uniqueness and stability of the generalized solution of the cauchy problem for a quasi-linear equation. *English transl., Amer. Math. Soc. Transl.*, 2(33):165–170, 1963.
- [61] Felix Otto. Initial-boundary value problem for a scalar conservation law. *C. R. Acad. Sci. Paris Sér. I Math.*, 322(8):729–734, 1996.
- [62] M. Papageorgiou. *Applications of Automatic Control Concepts to Traffic Flow Modelling and Control*. Springer-Verlag, 1983.
- [63] H. J. Payne. Models of freeway traffic and control. In *Math. Models Publ. Sys. Simul. Council Proc.*, number 28, pages 51–61, 1971.
- [64] M. Perrowitz and O. Etzioni. An operational analysis of traffic dynamics. *Journal of Applied Physics*, 24:271–281, 1953.
- [65] Benedetto Piccoli and Mauro Garavello. *Traffic Flow on Networks*. American Institute of Mathematical Sciences, 2006.
- [66] I. Prigogine. *Kinetic theory of vehicular traffic*. American Elsevier Pub. Co, 1971.
- [67] Sungkwon Kang Pushkin Kachroo, Kaan zbay and John A. Burns. System dynamics and feedback control formulations for real time dynamic traffic routing. *Mathl. Comput. Modelling*, 27(9-11):27–49, 1998.
- [68] M. Rascle. An improved macroscopic model of traffic flow: Derivation and links with the lighthill-whitham model. *Math. and Computer Modelling*, (35):581–590, 2002.
- [69] M. Renardy and R. Rogers. *Introduction to Partial differential equation*. Springer, NY., 2ed edition edition, 2004.
- [70] P. I. Richards. Shockwaves on the highway. *Operationa Research*, 4:42–51, 1956.

- [71] N. H. Risebro. A front tracking alternative to the random choice method. In *Proc. of the Amer. Math.*, volume 117, pages 1125–1139, 1933.
- [72] Renfrey B. Potts Robert Herman, Elliott W. Montroll and Richard W. Rothery. Traffic dynamics: Analysis of stability in car following. *Operations Research*, 7(1):86–106, 1959.
- [73] Halsey Royden. *Real Analysis*. Prentice Hall, third edition, 1988.
- [74] Walter Rudin. *Principles of Mathematical Analysis*. McGraw Hill, third edition, 1976.
- [75] Michael Schreckenberg and Som Deo Sharma. *Pedestrian and Evacuation Dynamics*. Springer, 2001.
- [76] Denis Serre and I. N. Sneddon. *Systems of Conservation Laws 1: Hyperbolicity, Entropies, Shock Waves*. Cambridge University Press, 1999.
- [77] Denis Serre and I. N. Sneddon. *Systems of Conservation Laws 2: Geometric Structures, Oscillations, and Initial-Boundary*. Cambridge University Press, 2000.
- [78] Joel Smoller. *Shock Waves and Reaction-Diffusion Equations*. Springer-Verlag, second edition, 1994.
- [79] Arnold J. Insel Stephen H. Friedberg and Lawrence E. Spence. *Linear Algebra*. Prentice Hall, 2002.
- [80] Issam Strub and Alexandre Bayen. Weak formulation of boundary conditions for scalar conservation laws: an application to highway modeling. *International Journal on Robust and Nonlinear Control*, 16:733–748, 2006.
- [81] E. F. Toro. *Riemann Solvers and Numerical Methods for Fluid Dynamics*. Springer, Germany, second edition, 1999.
- [82] S. Ulbrich. The existence and approximation of solutions for the optimal control of nonlinear hyperbolic conservation laws; [citeseer.ist.psu.edu/ulbrich98existence.html](http://citeseer.ist.psu.edu/ulbrich98existence.html).

- [83] S. Ulbrich. *Optimal Control of Nonlinear Hyperbolic Conservation Laws with Source Terms*. PhD thesis, Technische Universitat Munchen, 2001.
- [84] S. Ulbrich. Adjoint-based derivative computations for the optimal control of discontinuous solutions of hyperbolic conservation laws. *Systems and Control Letters*, 48(3-4):309–324, 2003.
- [85] R. T. Underwood. Speed, volume, and density relationships: Quality and theory of traffic flow. *Yale Bureau of Highway Traffic*, pages 141–188, 1961.
- [86] Sabiha Wadoo. *Evacuation Distributed Feedback Control and Abstraction*. PhD thesis, Virginia Tech, 2007.
- [87] Sabiha Wadoo and Pushkin Kachroo. Feedback control design and stability analysis of one dimensional evacuation system. In *Proceedings of the IEEE Intelligent Transportation Systems Conference*, pages 618–623, Canada, 2006.
- [88] Sabiha Wadoo and Pushkin Kachroo. Feedback control design and stability analysis of two dimensional evacuation system. In *Proceedings of the IEEE Intelligent Transportation Systems Conference*, pages 1108–1113, Canada, 2006.
- [89] J. Was. Cellular automata model of pedestrian dynamics for normal and evacuation conditions. In *5th IEEE Conference on ISDA*, pages 145–159, 2005.
- [90] J.M. Watts. Computer models for evacuation analysis. *Fire and Safety Journal*, 12:1237–245, 1987.
- [91] G. B. Whitham. *Linear and Nonlinear Waves*. John Wiley, NY., 1974.
- [92] H.M. Zhang. A theory of nonequilibrium traffic flow. *Transportation Research B*, 32:485–498, 1998.
- [93] H.M. Zhang. A non-equilibrium traffic model deviod of gas-like behaviour. *Transpn. Res.B*, 36B:275–290, 2002.

# Vita

Pushkin Kachroo received his Ph.D. in Mechanical Engineering from University of California at Berkeley in 1993, his M.S. in Mechanical Engineering from Rice University in 1990, and his B.Tech. in Civil Engineering from I.I.T Bombay in 1988. He obtained the P.E. license from the State of Ohio in Electrical Engineering 1995. He obtained M.S. in Mathematics from Virginia Tech. in 2004 and defended the final exam for Ph.D. in Mathematics from Virginia Tech on May 10th, 2007. He is currently an Associate Professor in the Bradley Department of Electrical & Computer Engineering at Virginia Tech. He was a research engineer in the Robotics R&D Laboratory of the Lincoln Electric Co. from 1992 to 1994, after which he was a research scientist at the Center for Transportation Research at Virginia Tech for about three years. He has four published books (Feedback Control Theory for Dynamic Traffic Assignment, Springer-Verlag, 1999, Incident Management in Intelligent Transportation Systems, Artech House, 1999, Feedback Control Theory for Ramp Metering in Intelligent Transportation Systems, Kluwer, 2003, and Mobile Robotics Car Design, McGraw Hill, (August 2004)), three edited volumes and overall more than eighty publications including journal papers. He is currently writing two more books on which there are contracts with publishers (Springer and CRC); one on robotics and one on evacuation control of pedestrians. He has been the chairman of ITS and Mobile Robotics sessions of SPIE conference multiple times. He received the award of “The Most Outstanding New Professor” from the College of Engineering at Virginia tech. in 2001, and Deans Teaching Award in 2005.